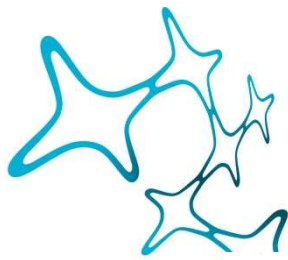


---

# NEURONAL DYNAMICS IN HEALTH AND ALZHEIMER'S DISEASE

---

Elena Itzcovich



Graduate School of  
Systemic Neurosciences

LMU Munich



Dissertation at the  
Graduate School of Systemic Neurosciences  
Ludwig-Maximilians-Universität München

October, 2020

Supervisor  
Prof. Dr. Anton Sirota  
Chair for Cognition and Neural Plasticity  
Ludwig-Maximilians Universität München

First Reviewer:	Prof. Dr. Anton Sirota
Second Reviewer:	Prof. Dr. Laura Busse
External Reviewer	Prof. Dr. Tatiana Korotkova

Date of Submission:	20.10.2020
Date of Defense:	02.02.2021

## Table of Contents

Abbreviations.....	6
Acknowledgements.....	7
Abstract.....	8
1. Introduction.....	10
1.1 The hippocampal formation.....	11
1.2 Brain States.....	12
1.3 Single Unit activity in the Hippocampal formation.....	13
1.4 Oscillatory dynamics in the hippocampus.....	13
1.4.1 Sharp wave-ripple complexes.....	14
1.4.2 Theta oscillations.....	14
1.4.3 Gamma oscillations.....	15
1.4.4 Respiration.....	16
1.5 Alzheimer’s Disease.....	16
1.5.1 Animal Models of AD.....	19
1.5.1.1 Behaviour.....	19
1.5.2 Oscillatory dynamics in AD.....	21
1.5.2.1 Oscillatory dynamics in AD patients.....	22
1.5.2.2 Oscillatory dynamics in animal models of AD.....	22
1.5.3 Unit activity in AD.....	23
2. Materials and Methods.....	24
2.1 Brain recordings and Electrophysiology.....	24
2.2 Surgeries and Data Collection.....	25
2.2.1 Subjects and surgery.....	25

2.2.2 Recordings.....	26
2.3 Preprocessing.....	27
2.3.1 Spike sorting and cell type attribution.....	27
2.3.2 Speed.....	27
2.3.3 Pupil size.....	28
2.4 Analytical Methods.....	28
2.4.1 Spectral Analysis.....	28
2.4.2 Phase Extraction.....	29
2.4.3 Pairwise Phase Consistency (PPC).....	30
2.4.4 Gamma bursts detection.....	30
2.5 Statistical Methods.....	31
3. Results.....	32
3.1 Brain States.....	32
3.2 Anatomical localization.....	34
3.3 LFP Analysis.....	36
3.3.1 Theta.....	36
3.3.1.1 Theta in different layers.....	36
3.3.1.2 Theta and speed.....	37
3.3.1.3 Theta Power and average frequency.....	42
3.3.1.4 First Theta harmonic and asymmetry.....	44
3.3.2 Gamma.....	46
3.3.2.1 Gamma as gamma bursts.....	47
3.3.3 Resting state.....	55
3.3.3.1 Sharpwave Ripples.....	56
3.4 Unit activity.....	60
3.4.1 Firing rate and burstiness.....	60
3.4.2 Theta modulation of neurons.....	62
3.4.3 Respiration Modulation of neurons.....	65

4. Discussion.....	67
4.1 Theta.....	67
4.2 Gamma.....	68
4.3 Sharp-wave Ripples.....	69
4.4 Respiration.....	70
4.5 Single Units.....	70
4.6 Conclusions.....	71
Bibliography.....	73

## ABBREVIATIONS

---

<b>A<math>\beta</math></b>	-	Amyloid- $\beta$
<b>APP</b>	-	Amyloid Precursor Protein
<b>AD</b>	-	Alzheimer's Disease
<b>CA</b>	-	Cornus Ammonis
<b>CSD</b>	-	Current Source Density
<b>DG</b>	-	Dentate Gyrus
<b>EC</b>	-	Entorhinal Cortex
<b>MEC</b>	-	Medial Entorhinal Cortex
<b>LEC</b>	-	Lateral Entorhinal Cortex
<b>HCN</b>	-	Hyperpolarization-activated Cyclic Nucleotide-gated (channels)
<b>LFP</b>	-	Local Field Potential
<b>NFT</b>	-	Neurofibrillary Tangle
<b>PPC</b>	-	Pairwise Phase Consistency
<b>PSD</b>	-	Power Spectral Density
<b>REM</b>	-	Rapid Eye Movement
<b>SWR</b>	-	Sharp Wave Ripple complexes
<b>SWS</b>	-	Slow Wave Sleep
<b>WT</b>	-	Wild Type

## ACKNOWLEDGEMENTS

---

Approaching the conclusion of the journey that this PhD has been, there are many towards who I want to express my gratitude. I can only start by writing about how Anton has always been there, not only in his role as a PI, but also at a personal and human level.

This work would not have been possible without Kaichuan, Zagorka and Monchen, who collected the data and run the behavioural experiments. The data they collected makes analysis a pleasure. Kaichuan in particular has also guided me in the difficult process of translating exploratory analysis in hard statistics and clear figures.

The Cognition and Neural Plasticity Lab wouldn't be the same without Zhenja, who fights for us the demons of bureaucracy to allow experiments to happen and who has written uncountable valuable lines of code and of protocols. With his calming presence he's a rock in the most strenuous times, and I will sorely miss our coffees together.

Andreas has read an early version of this thesis and found ways to encourage me while pointing my shortcomings and had thus a role both in shaping this thesis and in helping me preserving my sanity while writing it.

Nikolas, Gerrit and Eduardo have been there when I needed help and made me grow into the scientist I am today. Together with Andrey, another Nikolas and Fabian they have provided the kind of stimulating conversations that are the backbone of any scientific environment while sharing some late night pizza or a beer.

On a more personal note, I have to thank Benni. Not only for reading this whole thesis in an effort to reduce the number of inevitable typos, but for always being at my side. I also thank his parents for providing a home away from home where I could both relax and study.

This section wouldn't be complete without mentioning my parents. When I travelled to Italy to take care of them during the lock-down, they are the ones who took care of me while I was working on this thesis. In all these years they have always supported me no matter how distant from home this would take me and have managed to be there for me despite this distance. Thanks mum, thanks dad.

## ABSTRACT

---

Neuroscience has been both investigating fundamental questions about the nature of cognitive processes and giving medical sciences an understanding of biological mechanism that can be used to prevent or cure diseases. While these two branches of research are commonly separated, in the present study we will try to answer questions about memory formation while studying Alzheimer's disease (AD) development.

It is by now well known that the hippocampal formation plays a fundamental role in the acquisition, consolidation and retrieval of episodic memory. These processes are currently hypothesized to be supported or at least reflected in the appearance and synchronization of oscillatory activity patterns within and across regions. However, it is still unclear how these functions emerge from the underlying processes.

Studying these phenomena through correlation alone is limited and does not allow to find causal effects. For this reason, scientists have resorted to various perturbations to better understand the causal links in the system. These perturbations of the normal brain activity range from the complete ablation of brain regions to more subtle manipulations like opto- or chemogenetics.

Neuropathology can be seen as a more naturalistic perturbation of the brain function and research on the mechanisms underlying cognitive deficits can also contribute to our understanding of the internal computation of the brain. In particular, we will focus on AD, a chronic neurodegenerative disease and the most common cause of dementia, recognized by the World Health Organization as a global public health priority. Notoriously, AD symptoms include disorientation and memory loss.

One of the first brain regions suffering from neuronal damage in AD, after the entorhinal cortex, is the hippocampus. Given this clear connection between symptoms and the affected brain region, investigating the development of AD in this area has medical relevance, since understanding the systemic origin of the functional deficits of AD would open the door for the development of new medical approaches, and improve early diagnoses.

Using a model of amyloid pathology, APP<sup>NL-G-F</sup> knock-in mice, in the present study we aim to answer to the following questions:

- Do APP<sup>NL-G-F</sup> mice present changes in the firing patterns of neurons in the hippocampal formation and in the cortical region above it?
- Are there different patterns of oscillatory activity in the hippocampus of APP<sup>NL-G-F</sup> mice compared to wild type animals?
- Is there a distinguishable progression of electrophysiological changes for mice of different ages?

Our findings show minimal changes on the system level during the active state, the most prominent of which is a significant decrease in the average frequency of theta. On the neuronal level, principal cells tend to have a later theta phase. Since the changes at the system level don't explain the behavioural deficit, further studies focusing on the active state could focus on the single cell contributions.

During the resting state we found multiple differences, the most interesting of which is the diminished occurrence rate of gamma bursts in CA1lm and DGml, reflecting a reduced input from the entorhinal cortices, i.e. the first areas affected by AD. Sharp wave-ripples had a significantly decreased frequency of the ripple itself. Moreover, the strength of respiratory modulation of sharp wave-ripples was diminished, while their occurrence rate did not significantly differ. This points at the possibility that the behavioural changes observed in APP<sup>NL-G-F</sup> knock-in mice are due to changes mainly happening during the resting state and not during activity.

## 1. INTRODUCTION

---

The limbic system is responsible for emotional states and memory formation (Papez 1936; MacLean 1949; Scoville and Milner 1957). The hippocampus in particular is needed for the encoding of new memories, as shown by the famous case of patient H.M., who in 1953 developed severe anterograde amnesia after surgical bilateral removal of the majority of the hippocampal formation (Scoville and Milner 1957).

Starting from the first recordings of the brain electro-encephalogram, it has become evident that the brain is host to multiple forms of oscillatory activity. It has since then been hypothesized that slow oscillations facilitate communication between different brain regions, while faster ones correlate with local activity (Buzsáki 2009). Faster oscillations are short-lived and are thought to emerge from the interaction of local populations of excitatory and inhibitory neurons. The magnitude of these fast oscillations is modulated by the slower ones (Buzsáki and Wang 2012).

In the context of episodic memory, it has been shown that oscillatory activity in the hippocampus correlates with memory formation and consolidation. In the present understanding, these oscillations constitute the substrate for the activity of cell assemblies of neurons providing the memory coding, coordinate information transfer between networks and neural plasticity.

At the level of spatial coding, the discoveries of place cells in the rodent hippocampus (O'Keefe and Dostrovsky 1971) and of grid cells in the medial entorhinal cortex (Hafting et al. 2005), point to a role of the hippocampal formation in the generation of a cognitive map that could provide context information to episodic memory. Communication between these two brain areas and encoding of spatial and memory content by neural ensembles is organized by theta oscillations (Mizuseki et al. 2009, Buzsáki 2009).

Of particular interest are in this context also the sharp-wave ripples (SWRs), bouts of fast oscillatory activity during which place cell sequences are re-activated and that have been connected to memory consolidation (Buzsáki 2015).

However, demonstration of a causal link between oscillations and cognitive function is an ongoing work. Attempts to do so have up to now involved abrupt perturbations of the system, potentially interfering with unknown mechanisms causing both the effects on observed oscillations and the effects on memory.

Examining oscillatory dynamics in a pathological model such as AD mice may help us form a better understanding of memory and the process of learning within the brain while providing insights into the cause of the cognitive deficits.

## 1.1 THE HIPPOCAMPAL FORMATION

The hippocampal formation is a group of highly interconnected limbic structures including the hippocampus proper, subiculum and medial and lateral entorhinal cortices (respectively medial entorhinal cortex, MEC, and lateral entorhinal cortex, LEC). The hippocampus is commonly subdivided into dentate gyrus (DG) and the cornu ammonis (CA), which in rodents is further subdivided in CA1 CA2 and CA3, presenting different internal connectivity (Andersen et al. 2009). Our study focuses on CA1 and the DG.

### CA regions

- Principal cells: pyramidal cells

Pyramidal cells in the hippocampus are found in a thin layer named pyramidal layer, from which they extend elaborate dendritic trees in both directions perpendicularly to said layer. The dendrites extending towards the centre of the hippocampus are longer and span two to three strata: stratum lucidum (present only in CA3), stratum radiatum and stratum lacunosum-moleculare. Stratum radiatum of CA1 receives input from CA3 through the Shaffer collaterals, while Stratum radiatum of CA3 receives input from dentate gyrus through the mossy fibres (Schaffer 1892; Ramon y Cajal 1904).

An important difference between the internal organization of CA1 and CA3 is the high degree of excitatory recurrent connectivity between CA3 pyramidal cells (Lorente de Nò 1934).

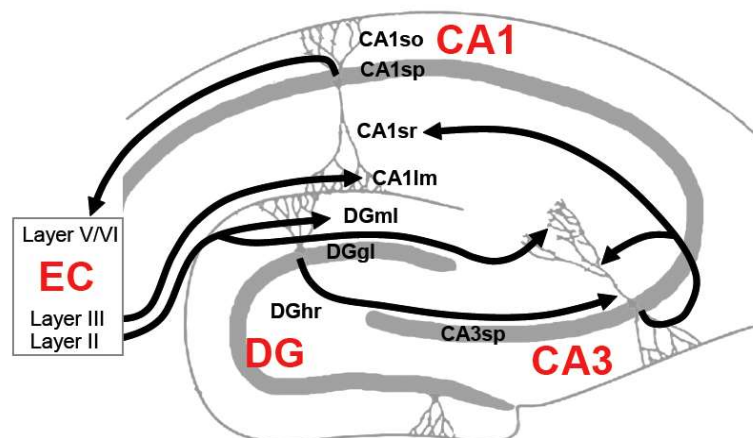


Figure 1: Connection schema in the Hippocampal Circuit  
Modified from (Petranonakis and Poirazi 2014). Figure published under [Creative Commons Attribution License](#), so present use is permitted.

## Dentate Gyrus

- Principal cells: granule cells

The dentate gyrus can be divided into three distinct layers: the molecular layer, the granule cell layer, and the polymorphic layer, also known as the hilus. The molecular layer can be further divided into outer, middle and inner molecular layer. Granule cells are densely packed granule cell layer enclosed by the mostly acellular molecular layer (DG mol) and the hilus. In the Dentate Gyrus, the perforant path fibres originating in LEC terminate in the outer molecular layer, while those originating from MEC terminate in the middle molecular layer. Inner molecular layer receives projections from the mossy cells, which are in turn targeted by CA3 projections (Amaral, Scharfman, and Lavenex 2007).

The entorhinal cortices (EC) are deeply interconnected with the Hippocampus, acting both as input source and as an output structure. Specifically layers V and VI of EC receive input from the hippocampal area CA1, which projects also to Subiculum, while layers II and III of EC project to DG and CA3 through the perforant path. Layer three also project to CA1 through the temporoammonic pathway (Ramon y Cajal 1901; Canto, Wouterlood, and Witter 2008).

The main subcortical structure projecting to the hippocampus is the medial septum. Through the septohippocampal pathway, cholinergic, glutamatergic and GABAergic neurons from the medial septum project to glutamatergic pyramidal neurons and to a different subset of GABAergic neurons in CA1 (Sun et al. 2014; Müller and Remy 2018).

---

## 1.2 BRAIN STATES

---

When in 1924 Hans Berger recorded for the first time in human history the electrical activity of the human brain with scalp electrodes, one of his first findings was that the EEG pattern changes dramatically with the behavioural state of the subject (Berger 1929).

This change of the neural dynamics reflects an effective change of the dynamical system caused by a switch in a host of neuromodulatory inputs ascending to cortical and hippocampal circuits from the brainstem and subcortical nuclei (Pace-Schott and Hobson 2002; Saper et al. 2010). Changes in the neuromodulation, most importantly that of acetylcholine, norepinephrine, serotonin, histamine and dopamine profoundly affect the intrinsic properties of neurons and synaptic transmission. These cellular changes are not only resulting in different network dynamics, but also affect processing of sensory inputs and motor activity. Thus at the level of motor activity, brain states broadly correlate with immobility and movement.

At the network dynamics level, immobile, quiescent and slow wave sleep states are associated with synchronous slow wave dynamics emerging in the thalamo-cortical

system and engaging the whole brain and with sharp-waves in the hippocampal circuits (Sirota and Buzsáki 2005). States of locomotion and REM sleep, in contrast, are associated with desynchronized network activity in the neocortex and synchronous theta oscillation engaging the whole limbic system.

Different network dynamics between brain states gives rise to their distinct functional role in learning and memory. While theta dynamics are implicated in acquisition of memory, synchronous dynamics associated with offline states are implicated in memory consolidation (G. Buzsáki 1989; Klinzing, Niethard, and Born 2019). Dissection of the origin of the cognitive deficit thus requires comprehensive characterization of oscillatory dynamics in each brain states.

---

### 1.3 SINGLE UNIT ACTIVITY IN THE HIPPOCAMPAL FORMATION

---

The hippocampal formation presents multiple spatially modulated cells, the most famous of which are indubitably the place cells in the hippocampus proper (O'Keefe and Dostrovsky 1971) and the grid cells in medial entorhinal cortex (MEC) (Fyhn et al. 2004).

Place cells are pyramidal neurons in CA1 pyramidal layer whose activity is spatially modulated so that a cell will only fire in a localized area (named place field). The ensemble activity of place cells encodes the position of the animal (Wilson and McNaughton 1993), forming a representation of space called a cognitive map (Tolman 1948; O'Keefe and Nadel 1978). Given that place cells contain information regarding the spatial context an event took place, they are thought to play an important role in episodic memory.

As we will see in the next few sections, oscillatory activity is deeply connected with place cell firing.

---

### 1.4 OSCILLATORY DYNAMICS IN THE HIPPOCAMPUS

---

Oscillations are a prominent feature of natural neural circuits, characterized by a mixture of continuous, usually slower, oscillations and bursts of faster activity. Slower oscillations are often generated by an external pacemaker and involve a large number of cells, while fast oscillation arise from the local interaction of inhibitory and excitatory cells. This leads to the hypothesis that slower oscillations facilitate long-range interactions between different brain regions.

A traditional way to distinguish between the different oscillatory bands is to classify them by letters of the Greek alphabet, in the order they were first discovered and described: delta (1–4 Hz), theta (4–8 Hz), beta (13–30 Hz) and gamma (30 Hz and above) (Steriade et al. 1990). Gamma is usually further divided in slow gamma and fast gamma (Başar et al. 2013).

---

#### 1.4.1 SHARP WAVE-RIPPLE COMPLEXES

---

One of the most recognizable patterns of hippocampal activity are the sharp waves-ripple complexes (SWR), appearing during slow wave sleep (SWS) periods and in quiet wakefulness (György Buzsáki et al. 1992). To the best of our knowledge, sharp wave ripples are generated when a bout of highly synchronous activity in CA3 leads to the strong depolarization of pyramidal cells projecting through the Shaffer collaterals to stratum radiatum of CA1 (showing as a “sharp wave” in the LFP of the region). This activates both interneurons and pyramidal cells in CA1, giving rise to fast oscillations (140-250 Hz), the so-called ripples (György Buzsáki 2015). SWRs have been observed in a multitude of species, including humans (Bragin et al. 1999; Van Quyen et al. 2010).

During SWRs, sequences of place cells that had been firing together during active behaviour are spontaneously reactivated, a phenomenon called replay. The sequences of place cells activated during a ripple are activated in a time-compressed manner. This reactivation is believed to be important for memory consolidation (Wilson and McNaughton 1994). In an attempt to corroborate this hypothesis, it has been shown that if hippocampal activity is disrupted selectively when SWRs occur, either during sleep (Girardeau et al. 2009) or during quiet wakefulness (Jadhav et al. 2012), resulting in an impairment of spatial memory.

---

#### 1.4.2 THETA OSCILLATIONS

---

One of the most distinct oscillation in the mammalian brain are theta oscillations, in the range of 4-10 Hz and associated with clear behavioural correlates, such as exploratory behaviour and locomotion. During sleep, they are associated with REM sleep. In the rodent, they are the most prominent oscillation and they span the whole hippocampal structure (György Buzsáki 2002).

Models suggest that theta oscillations have a role in the encoding of episodic memories and in their retrieval (Hasselmo 2005). In particular, it is by now well established that theta rhythmic currents recorded in the hippocampus reflect inputs from multiple interacting structures in the hippocampal-entorhinal system (Montgomery, Sirota, and Buzsáki 2008). This is shown by the fact that bilateral lesions of EC abolish the theta dipole between radiatum and deeper layers (Kamondi et al. 1998). However, the theta modulation of local activity is not identical across all regions and in all conditions: different compartments are entrained preferentially at different phases of theta (Mizuseki et al. 2009).

There are two different types of theta oscillation, namely:

- type 1 (atropine independent)
- type 2 (atropine dependent)

These can be dissociated pharmacologically based on their permanence or disappearance when muscarinic acetylcholine receptor antagonist atropine is administered to the animal.

Type 1 theta is associated with locomotion and REM sleep and is not found in anaesthetized animals, while type 2 is typical of urethane anaesthesia (Kramis, Vanderwolf, and Bland 1975). The medial septum sets the pace of Type 1 theta in the hippocampus (Fuhrmann et al. 2015; Hangya et al. 2009; Huh, Goutagny, and Williams 2010).

It has been shown that in freely moving rodents there is a relationship between type 1 theta power and animal speed (McFarland, Teitelbaum, and Hedges 1975). This is very relevant for us because we don't want potential behavioural differences in the speed of our two cohorts to be mistakenly read as a difference in the average power of theta. However, in head-fixed animals the picture is less clear (Supplementary materials in Ravassard et al. (2013); Haas et al. (2019); Chen et al. (2019)). We will need to take this into account.

---

#### 1.4.3 GAMMA OSCILLATIONS

---

High frequency oscillations have been observed and studied in a wide array of cortical regions (György Buzsáki and Wang 2012). While they are usually divided into slow and fast gamma, the exact boundaries of these two frequency bands are not consistent across studies. In our case, we will call slow gamma oscillations in the range of 30-80 Hz and fast gamma oscillations at higher frequencies. When occurring during periods of theta activity, gamma bursts are often modulated by theta, showing a preferred theta phase depending on their anatomical location and frequency. Contrary to theta, fast oscillatory activity is very transient in nature, limited to bursts of gamma activity.

Increases of gamma coherence across hippocampal structures have been linked to performance in specific tasks. In particular, it has been proposed that gamma oscillations may be a mechanism by which hippocampal activity is coordinated (Montgomery and Buzsáki 2007; Lasztóczy and Klausberger 2016). It has also been shown (Schomburg et al. 2014; Fernández-Ruiz et al. 2017) in the rat that the peak of cell firing and high-frequency (30-200 Hz) synchronization in upstream regions is reflected in the emergence of gamma oscillations in the LFP of the target dendritic layers and concomitant depolarization of the target dendritic compartments downstream.

Indeed, the pattern of principal cells preferences of theta phases described by Mizuseki et al., (2009) seems for the most part to be reflected in the modulation of gamma by theta phase within both the principal cell layer and the dendritic target laminae to which those cells population project, for example with gamma activity in CA1 stratum radiatum having the same preferred theta phase as the firing of principal cells and gamma in CA3 (Schomburg et al. 2014).

To isolate individual gamma burst, it is possible to use analytical techniques based on the detection of local maxima in the frequency, temporal and spatial domains and a further screening based on the separation between the selected burst, to avoid assigning the same burst to multiple adjacent layers (Sirota et al. 2008) [Fig. 5]. From existing work on high frequency synchronization in the entorhino-hippocampal circuit in Sirota lab as well as from recent publications (Schomburg et al. 2014; Lasztóczy and Klausberger 2014; 2016) emerges that gamma bursts detected in different dendritic laminas in hippocampus are related to gamma synchronization in the distinct afferent regions.

---

#### 1.4.4 RESPIRATION

---

While respiratory rhythm does not originate in the hippocampus, numerous studies have recently identified a correlation between respiratory oscillation and both cortical and hippocampal oscillatory activity in rodents, where this oscillation is abolished if respiration was diverted from the nose through a tracheotomy (Yanovsky et al. 2014; Lockmann et al. 2016), and humans, where the same happened if the respiratory flow was diverted from the nose to the mouth (Zelano et al. 2016). This signatures of respiration in the hippocampus have been attributed to re-afferent olfactory activity.

It has been shown that this respiratory oscillations provide temporal coordination of neuronal firing in cortical and limbic networks. During quiescence and non-REM sleep the limbic LFP activity is dominated by respiratory input, with the firing of single neurons being modulated by it (Karalis and Sirota 2018).

Given the important role of SWR in memory consolidation (Girardeau et al. 2009; Jadhav et al. 2012) and the difficulties in storing new memories that people affected by Alzheimer encounter, it is important to verify if between our two cohorts of mice there are significant differences in the modulation of hippocampal activity during quiescence by respiration.

---

### 1.5 ALZHEIMER'S DISEASE

---

First described in 1901 by German psychiatrist Alois Alzheimer, AD was originally only diagnosed in people aged between 45 and 65 years and considered a form of pre-senile dementia, until in 1977 it was recognized that symptoms between AD and senile dementia were identical and AD started to be diagnosed regardless of age (Boller and Forbes 1998; Berchtold and Cotman 1998).

AD is a degenerative disease, beginning with a subtle, but increasing, impairment in the ability to retain recent memories, while older memories are spared until later stages. With the progression of the disease other cognitive deficits arise, including visuo-spatial deficits, loss of orientation and behavioural changes (Bekris et al. 2010). The loss of orientation in particular has been proposed as a biomarker of AD, used to distinguish AD from other forms of neurodegenerative diseases (Lithfous, Dufour, and Després 2013).

Loss of olfaction is also an early marker of AD. For this reason, in the present study we also recorded from both olfactory bulbs and verified the role of respiration modulation of hippocampal activity.

From a pathophysiological perspective, AD is accompanied by the accumulation of amyloid- $\beta$  ( $A\beta$ ) plaques in the extracellular space and of neurofibrillary tangles (NFTs) of hyperphosphorylated microtubule-associated protein tau inside the neuron cell bodies.

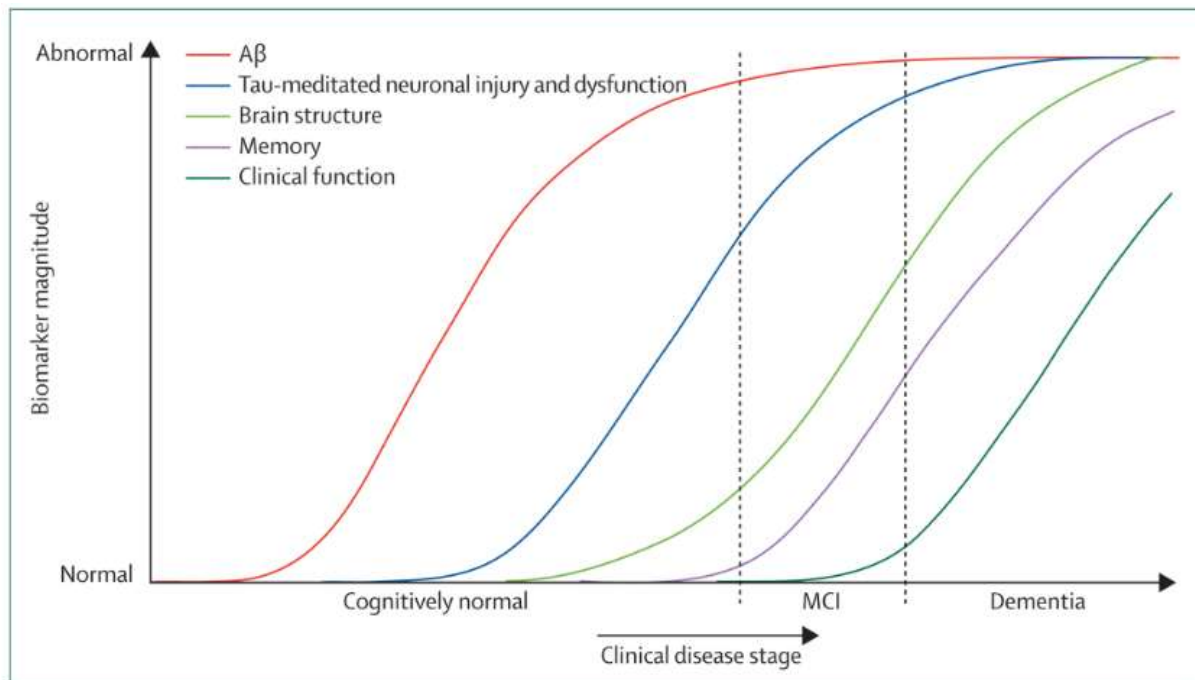


Figure 2: Progression of Alzheimer's Disease. Figure taken from Jack et al 2010. Reproduced with permission.

$A\beta$  plaques are composed of abnormally folded  $A\beta$  ( $A\beta_{40}$  and  $A\beta_{42}$ , depending on the number of amino acids) and they involve the entorhinal cortex and hippocampal formation to a lesser extent than NFTs, since it is Tau pathology that typically starts in these brain areas. AD patients present also widespread neuroinflammation and eventually brain atrophy, led by the loss of neurons and synapses (Lane, Hardy, and Schott 2018; Jack et al. 2010). Cholinergic cells in medial septum are particularly impacted by these changes. Given that  $A\beta$  plaques precede NFTs, and that amyloid pathology has been proposed to be the main mechanism of AD progression (Hardy and Allsop 1991; Selkoe 1991), in this study we will use an animal model of amyloid pathology.

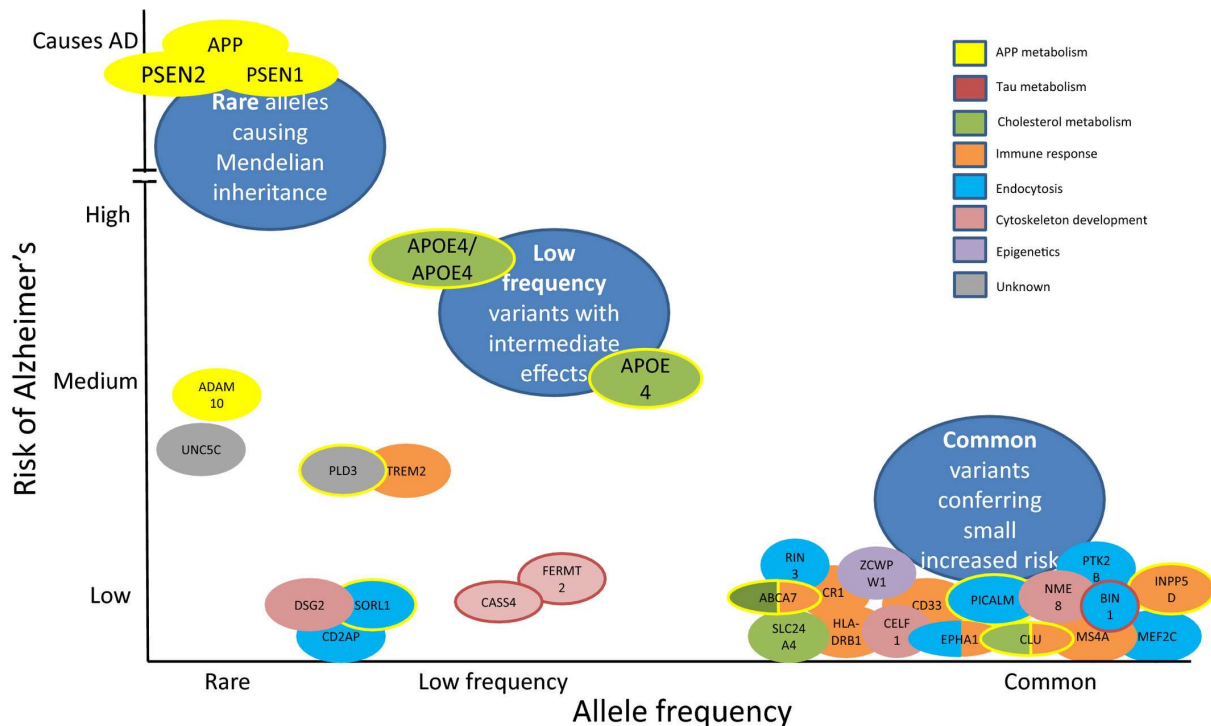


Figure 3: Alleles carrying increased AD risk. Figure taken from Lane, Hardy, and Schott 2018. Reproduced with permission.

The behavioural changes distinguishing AD must arise from changes in the underlying computation. Many studies indicate that in the hippocampus cross-frequency coupling between theta (4-10 Hz) and gamma (30-100 Hz) oscillations play a critical role in memory consolidation and retrieval (Buzsáki 2002; Hasselmo 2005; György Buzsáki and Moser 2013; Huxter et al. 2008; Mizuseki et al. 2009; Montgomery, Sirota, and Buzsáki 2008), and a correlation with working memory in the human brain has been reported (Chaieb et al. 2015; Rajji et al. 2017). Looking at early abnormalities in these oscillations might then shed new light on the mechanisms underlying AD and possibly indicating new markers disease's onset.

While the causes of AD are yet unknown, many genes have been linked to a higher risk of contracting the disease, with a few rare ones carrying a particularly elevated risk. Amongst these are mutations affecting amyloid precursor protein (APP) or presenilin 1 and 2 (PSEN1, PSEN2), which cause a rare familial form of AD, contributing to less than 0.5% of the cases (Lane, Hardy, and Schott 2018) (Figure 3). In this rare form of AD symptoms develop early, typically between 30 and 50 years of age. As we will see in the next section, these mutations have been used to create transgenic mouse models of AD.

---

### 1.5.1 ANIMAL MODELS OF AD

---

There are aspects of any disease that would be impossible to investigate in humans because of the invasiveness of the techniques needed to do so. For this reason, animal models are developed to mimic aspects of human diseases to be able to study them. Moreover, AD is a degenerative disease that in humans develops across the span of years, which prolongs the time of longitudinal human studies. In mice models of AD, the same progression can span months, making mouse models particularly convenient to study.

While the underlying causes of AD are unknown, and the overall progression of the disease seems to be driven by the deposition of amyloid- $\beta$  plaques (Murphy and Levine 2010). It is then reasonable to focus our study amyloid- $\beta$  pathology.

Many AD models exist, like APP23xPS45, used by Busche et al. (2008), which is a double transgenic line overexpressing both APP and mutant PSEN1; TgCRND8 mice overexpress mutant human APP at levels approximately 5-fold higher than wild type mice (Chishti et al. 2001); 5xFAD mice express human APP and PSEN1 having a five mutations linked to familial Alzheimer's disease (FAD), making them overproduce  $A\beta_{42}$  and show amyloid- $\beta$  plaques deposition starting from two months of age (Oakley et al. 2006).

As we see, amongst the multiple transgenic mice models created to study AD, many overexpress amyloid precursor protein (APP). This casts doubts on their validity, since that's not the case in AD patients and such overexpression has the potential to already alter brain dynamics. This is not the case of APP<sup>NL-G-F</sup> mice, where levels of  $A\beta$  protein are higher than in their wild type counterpart, without increasing overall APP (Saito et al. 2014). This model presents humanized APP gene with three mutations:

- NL ("Swedish"): responsible for the increase in  $A\beta$ , but not overall APP
- F ("Iberian"): responsible for an increase in the  $A\beta_{42}/A\beta_{40}$  ratio
- G ("Arctic"): responsible of promoting  $A\beta$  aggregation via reduced proteolytic degradation

In APP<sup>NL-G-F</sup> mice show cognitive deficits starting from the age of six months (Masuda et al. 2016).

This model is a model of Amyloid Pathology rather than the full AD, since it never presents tau neurofibrillary tangles.

---

#### 1.5.1.1 BEHAVIOUR

---

A common characteristic of rodent models of AD is presenting a memory impairment that becomes more severe with ageing. APP23 mice present memory deficit before  $A\beta$ -plaques deposition and that get more severe with age (Van Dam et al. 2003; Kelly et al. 2003). APP23xPS45 mice, obtained as a cross between APP23 mice and a mouse line overexpressing PSEN1, were reportedly tested in a discriminatory water maze task and in a Y maze, presenting no impairment at 2 months of age, but significantly reduced

performance in both tests at 6-8 months of age (Busche et al. 2008). Already at 3 months of age TgCRND8 mice show impairment in both acquisition and learning reversal as tested by the reference memory version of the Morris water maze (Chishti et al. 2001). This line is also more susceptible to seizures (Del Vecchio et al. 2004). As for 5xFAD mice, there are reports of impaired working memory (as tested with spontaneous alternation in the Y-maze) already at approximately 4 to 5 months of age (Oakley et al. 2006; Devi and Ohno 2010), while impaired spatial memory has been confirmed in 6 months old mice using the Morris Water Maze (Xiao et al. 2015). Female 5xFAD mice have also been reported to have changes in their social behaviour, specifically symptoms that point at an increased social anxiety (Kosel et al. 2019). This is particularly interesting because social withdrawal is also correlated with AD.

Related to our model in particular we can look at how having a different number of mutations impacts APP<sup>NL</sup>, APP<sup>NL-F</sup> and APP<sup>NL-G-F</sup> mice (Figure 4): while APP<sup>NL</sup> present almost no hallmark of AD, including very few biomarker (even at 18 months they don't exhibit sign of A $\beta$ -plaques), APP<sup>NL-F</sup> mice already show signs of memory loss in adult age (8+ months) and begin to exhibit compulsive behaviour. The model with the most deficits and higher presence of biomarkers remains however APP<sup>NL-G-F</sup>, the one used for the present study (Masuda et al. 2016).

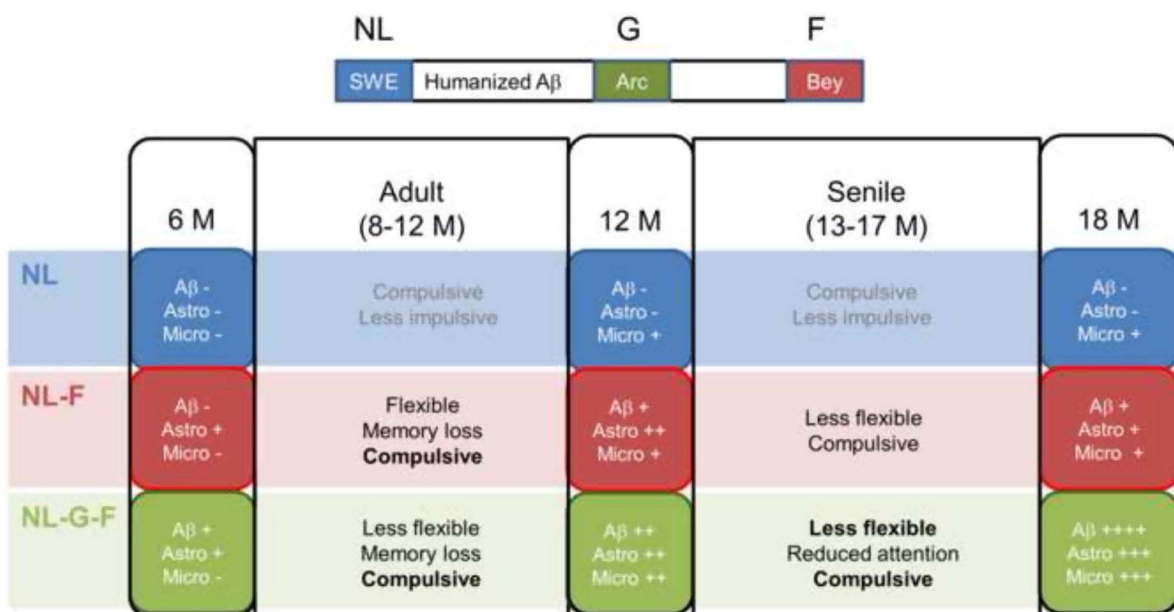


Figure 4: Deficit of APP Knock-In mice for different age groups (Masuda et al., 2016). Figure published with a [Creative Commons Attribution-NonCommercial-No Derivatives License](#), so present use is permitted

Dr. Kaichuan Zhu and Zagorka Bekjarova verified that the APP<sup>NL-G-F</sup> line used for the recordings analysed in this study presented the characteristic impairments in memory.

This was done in three experiments. The first was a test of spontaneous alternation in which the animals were given six minutes to freely explore a T-maze, documenting the

alternation between left and right turns at the decision point. Here, as expected, there are no significant differences between the two groups (Figure 5).

Then, the animals were subject to a Novel Object Recognition task where they were first familiarized with an object (old) and then presented with both the old object and a new one. WT mice spent significantly more time exploring the new object than they did with the old, while in  $APP^{NL-G-F}$  mice the difference in time spent exploring the two objects was not significantly different.

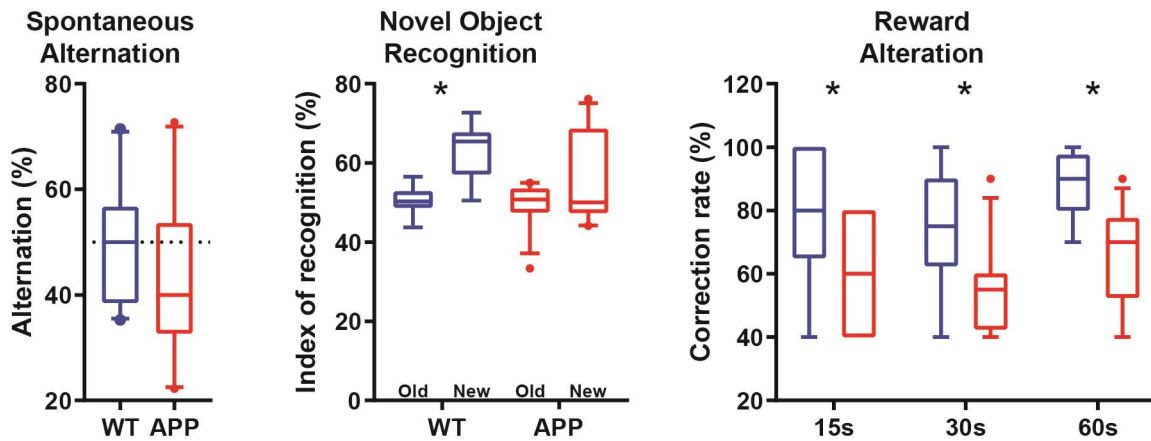


Figure 5: Behavioural effects on the  $APP^{NL-G-F}$  line. Spontaneous alternation: no significant differences. Novel Object recognition: WT, but not  $APP^{NL-G-F}$ , spend significantly more time in the proximity of the novel object. Reward alteration: for all tested delays  $APP^{NL-G-F}$  performance is significantly decreased. (Blue: WT, Red:  $APP^{NL-G-F}$ ).

Finally, the mice were presented with a new alternation task, this time rewarded. In the first half of the trial, the mouse was free to explore one of the two arms of the T-maze, at the end of which was the water reward. It was then held in a chamber at the beginning of the maze for an amount of time varying according to the trial (15 seconds, 30 seconds or 60 seconds) and was left with the choice of re-visiting the same arm or the unexplored one. The second part of the reward was at the end of the unexplored arm, thus incentivizing the mice to alternate between arms.  $APP^{NL-G-F}$  mice performed more poorly than WT mice for all time periods.

### 1.5.2 OSCILLATORY DYNAMICS IN AD

Oscillatory dynamics in AD patients and AD models has been discussed by many works, but very few utilize the same model, most recent,  $APP^{NL-G-F}$  model and older models of amyloid pathology over-express APP and thus lead to results that are more difficult to interpret. We are also amongst the first to use awake animals and, at the moment of this writing, the first to take advantage of the spatial resolution of silicon probes in this analysis.

### 1.5.2.1 OSCILLATORY DYNAMICS IN AD PATIENTS

Both quantitative and qualitative studies in humans have shown that alteration of normal EEG patterns are both an early stage predictor of (Helkala et al. 1991; Claus et al. 1998; Prichep et al. 2006), and correlated to (Brenner et al. 1986; Prichep et al. 1994; Jiang 2005; Onishi et al. 2005) the gravity of cognitive impairment shown by the patients. These abnormalities presented themselves in the form of a decrease in coherence and slowing of the EEG, with a relative increase in power of oscillations in the delta and theta band compared to faster oscillations (Adler, Brassens, and Jajcevic 2003).

### 1.5.2.2 OSCILLATORY DYNAMICS IN ANIMAL MODELS OF AD

*In vitro* studies have shown a decrease in theta-gamma cross-frequency coupling in a model of AD (TgCRND8 transgenic mice) (Goutagny et al. 2013), while in *in vivo* models reduced gamma oscillations were observed (Iaccarino et al. 2016). In both cases, this phenomena preceded the onset of plaque formations.

It was shown *in vivo* in anaesthetized 5 months old APP<sup>NL-G-F</sup> mice that gamma-theta cross-frequency coupling and phase locking of spiking activity were both reduced in the MEC, but the power and emergence of theta was not significantly affected (Nakazono et al. 2017).

A decrease in theta frequency, coupled with an increase in theta activity was found in a 5xFAD model (Siwek et al. 2015), with 5xFAD mice expressing humanized APP and PSEN1 transgenes with a total of five mutations linked to early onset familial AD (hence the name 5xFAD)

A decrease in SWR abundance has been described in multiple models of AD (apoE4-KI mice: (Gillespie et al. 2016) tau overexpression: (Ciupek et al. 2015) and amyloid  $\beta$  overexpression: (Nicole et al. 2016)). A decrease in SWR abundance is also an early predictor of learning and memory impairment in apoE4-KI mice (Jones et al. 2019).

While many of the early models of AD overexpress amyloid precursor protein (APP), making it unclear if the brain dynamics were suffering from this overexpression rather than the amyloid pathology, this is not the case of APP<sup>NL-G-F</sup> mice (Saito et al. 2014). This is not the case for 5xFAD models, but they present non-physiological combination of FAD mutations and marked intracellular A $\beta$  accumulation. For more in depth comparison between different mouse models of AD, see Jankowsky and Zheng (2017).

Moreover, these studies relied on tetrodes for data acquisition, thus not having the spatial resolution that silicon probes can provide. Most of the published analysis suffered from other methodological or conceptual shortcomings that make interpretation of the effects difficult.

---

### 1.5.3 UNIT ACTIVITY IN AD

---

It has been shown in the cortex of anaesthetized models of AD that, while many cells become silent, those close to amyloid plaques become hyperactive (Busche et al. 2008). However, the study of the MEC of behaving animals didn't show such hyperactive cells (Jun et al. 2020), but an impairment in place cell remapping was found, becoming increasingly more severe with the subject's age.

In APP<sup>NL-G-F</sup> mice it has been observed a disruption of grid cells in MEC that precedes disruption of place cells in the hippocampus, together with an impairment in remapping (Jun et al. 2020).

In the present study we will look at the activity pattern of hippocampal pyramidal cells, but not at their spatial modulation.

## 2. MATERIALS AND METHODS

---

### 2.1 BRAIN RECORDINGS AND ELECTROPHYSIOLOGY

---

Nowadays many techniques to obtain different metrics of brain activity are used in a clinical setting. Examples of these are MRI and EEG, providing in one case informations on the internal structure and status of the brain and in the other its activity as recorded on the scalp. Working with mice we can afford more invasive procedures, like those required for calcium imaging and deep electrophysiology.

Techniques like calcium imaging, a staple of AD research, allow the recording of high numbers of cells at the same time and their localization in respects to amyloid plaques. It comes however with two drawbacks: the difficulty imaging deeper structures without altering the brain excessively and the very low time resolution, in the time-scale of seconds. For this reason, in the present study we decided to use electrophysiological means of investigation, allowing us to record from the hippocampus and giving us a signal in the scale of milliseconds.

Indeed, while most communication between neurons – with the exception of gap-junctions – happens at the chemical level, signal transmission within a single neuron is associated with a distinct electrical current known as action potentials, caused by the ionic currents through the cellular membrane while the signal is travelling along the axon, away from the cell body (Hodgkin and Huxley 1952). These action potentials can be measured by electrodes sufficiently close to the neuron’s membrane, with much higher spatial and temporal precision than what is currently possible for their chemical counterpart.

Action potentials don’t just give us information about the time the neuron fires, their shape can also be used to infer neuronal types. Indeed, if we measure the time between the trough of the action potential to the rebound peak following it, we can use this information to infer the type of neuron we are recording from (Henze et al. 2000; Klausberger et al. 2003) (Figure 1).

The local field potential (LFP), is more difficult to interpret, being the result of multiple current generators and not the output of a single unit. While recorded unit activity is only local, LFP is an entanglement of close and distant activity, reflecting mainly synaptic currents (György Buzsáki, Anastassiou, and Koch 2012). However, this also brings the advantages of the study of LFP: LFP signals provide an averaged measurement of population activity while giving us a reading of the input reaching the local population.

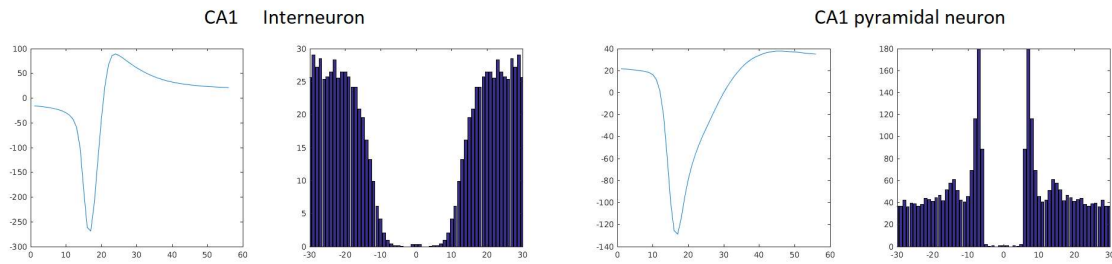


Figure 6: Average traces and auto-correlograms for a CA1 interneuron and a CA1 pyramidal neuron. Notice the different width of the action potentials.

The laminated structure of the hippocampus makes it the perfect region to study LFP signals, because the orderly arranged cell bodies and dendritic subregions makes it so that the contributions of individual cells gets summed constructively rather than cancel each other out. This means that we can measure very distinct signals in the extracellular space, and that these patterns of activity can be related to their anatomical position.

One of the advantages of using silicon probes is that they give us the ability to sample LFP with high spatial resolution and a defined distance between recording sites. This allows us to perform Current Source Density (CSD) analysis on the acquired data

The CSD is the Laplacian of the field potential and allows us to eliminate volume conductance from the signal and to individuate sources (a flow of positive ions exiting the neuron, or of negative ones entering into the neuron) and sinks (a flow of negative ions into the neurons or of positive ones exiting it) in the various layers as different phenomena occur in the brain (Einevoll et al. 2013).

In the present study we will use the CSD to assign anatomical layers to the channels of the probe and to estimate the strength of theta. We will also discuss observations made on both single unit activity and LFP.

## 2.2 SURGERIES AND DATA COLLECTION

The dataset analysed in this thesis was collected by Dr. Kaichuan Zhu with assistance from Monchen Cui and Zagorka Bekjarova.

### 2.2.1 SUBJECTS AND SURGERY

The subjects were 14 APP NL-G-F mice and 14 C57BL/6 mice (Wild Type – WT), of ages ranging from 6 to 12 months. All mice were male and were hosted in individual cages after surgery.

In a preparatory step for the experiment, mice were implanted with an headpost and a craniotomy above the hippocampal region was made. Subjects were anaesthetized with

three component anaesthesia agonist (Fentanyl, Midazolam, Medetomidin) and placed on a stereotaxic apparatus. To avoid hypothermia, the mice were placed on a heating pad. Vital parameters were monitored with a Kent Scientific MouseSTAT Pulse Oximeter and pain reflexes were regularly checked.

Six recording screws were implanted: 2 above the olfactory bulbs, 2 above prefrontal cortex, 1 above somatosensory cortex and 1 above visual cortex. On top of that, 2 grounding screws were implanted above cerebellum. This study makes use of the screws to track the respiration rhythm. Space was left for the craniotomy through which the recording probes would be inserted during head fixation.

All animal procedures were in accordance with the European Community Council Directive for the Care and Use of Laboratory Animals (86/609/ECC) and German Law for Protection of Animals and were approved by local authorities.

---

## 2.2.2 RECORDINGS

---

Recordings were made in head fixed animals on a circular treadmill. Above the treadmill there was a holder for the headpost and electrodes were inserted in the craniotomies using a micromanipulator. This setup was housed inside a Faraday cage to minimize external electromagnetic interference.

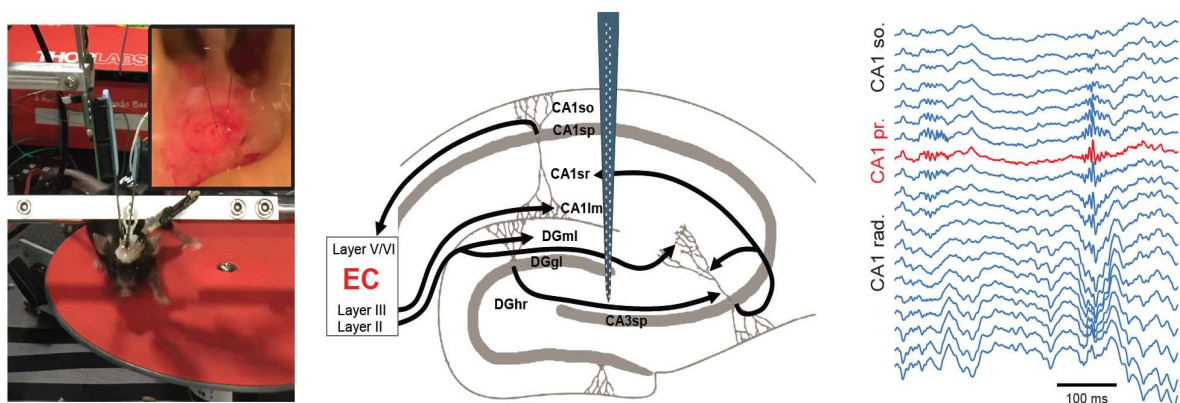


*Figure 7: Left: Experimental setup, with close-up to a craniotomy with two probes inserted. Middle: implantation schema, adapted from Petrantonakis and Poirazi (2014). Right: Example traces during a Sharp-wave ripple complex.*

The recordings were done through an Open Ephys acquisition board, which acquired both the LFP data coming from the silicon probe (sessions were recorded using either ASSY-77-M2 by Cambridge NeuroTech or A1x64-Poly2-6mm-23s-160 by NeuroNexus both having 64 channels and having active sites spanning approximately 1.9 mm) and the LFP data coming from the screws (2 over olfactory bulb, 2 over prefrontal cortex, 2 over parietal cortex). These were synchronized with video of the mouse face, separately recorded, the speed signal coming from the treadmill and the activity of a lick sensor.

The signal was recorded at a sampling rate of 30000 Hz and offline downsampled to 1250 Hz for the LFP analysis.

---

## 2.3 PREPROCESSING

---

All analysis was performed using MATLAB 2016b and 2019b. Spike sorting was performed using Kilosort 2 (Pachitariu, Steinmetz, Kadir, Carandini, and Harris 2016; Pachitariu, Steinmetz, Kadir, Carandini, and Harris 2016) and Phy (<https://github.com/cortex-lab/phy>).

The LFP signal was denoised using custom-developed EMG denoising algorithm. Briefly, an ICA model was fit in short data chunks and component that had most uniform loading across all channels and had large spectral content in the high frequency band was identified and removed from the signal. This procedure drastically reduced contamination of the LFP signal by EMG leading to false positive high frequency gamma and ripple detection, as well as distortion of the spectra.

Respiration is conventionally measured via a thermocouple in the nose, a pressure sensor, an electrode over olfactory epithelium or from olfactory bulb (OB) (Karalis and Sirota 2018). In preliminary analyses I found that the OB signal can be contaminated by the volume-conducted cortical slow wave signal. In order to extract reliable respiration signal, ICA decomposition was applied to all EEG signals. A reliable component with maximal loading on OB channels and stable respiration frequency between 2-4 Hz during immobility was found, consistent with published work (Karalis and Sirota 2018), and was used to extract phase and rate of respiration.

---

### 2.3.1 SPIKE SORTING AND CELL TYPE ATTRIBUTION

---

After manually separating clean units from clusters with multi-units activity (MUA), we computed in MATLAB various characteristics of the clusters, including spike waveshape width measured as time from trough to the rebounding peak in the action potential.

Hippocampal CA1 neurons were then divided between putative interneurons and putative pyramidal cells based on the width of the waveshape of their action potentials, with narrow action potentials (less than 0.55 msec) being assigned as putative inhibitory neurons (labelled interneurons) and wide as excitatory cells (labelled principal cells) (see Figure 6).

---

### 2.3.2 SPEED

---

Animals were free to run on a circular treadmill with a radius of 5 cm connected to a rotary encoder that samples at 600 pulses per rotation. The output of the rotary encoder

was recorded from the same Open Ephys acquisition board that recorded the electrophysiological signal, at the same 30000 Hz.

During the preprocessing phase, the number of pulses per 100ms was counted and was used to reconstruct the speed of the animal.

---

### 2.3.3 PUPIL SIZE

---

An infrared camera recorded the left side of the animals head, including the whiskers area and the eye. The size of the pupil was extracted using DeepLabCut (Mathis et al. 2018; Nath et al. 2019), tracking the top, bottom, left and right extreme of the pupil (see Figure 8) and then using those to calculate the average diameter in pixels. Since the camera was at slightly different distances for each animal, it is impossible to translate this pixel measure in millimetres.

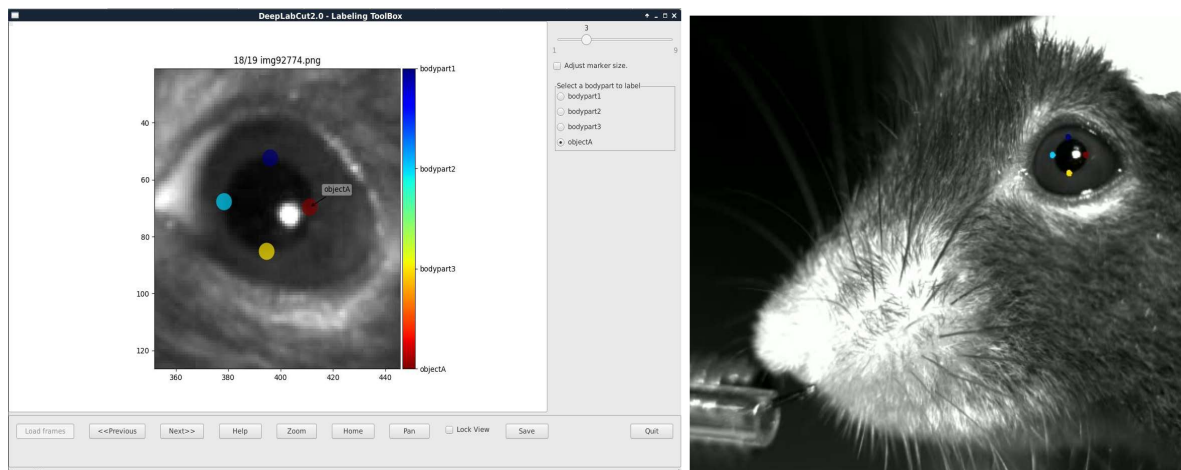


Figure 8: Left: Close-up of eye during marker positioning Right: Example frame with automatically detected markers delimiting the pupil.

To train DeepLabCut, 10 sessions with different light conditions and angle of recording were selected and relevant frames were manually scored.

---

## 2.4 ANALYTICAL METHODS

---

---

### 2.4.1 SPECTRAL ANALYSIS

---

The LFP power spectrum was calculated using multitaper estimates. The spectral window was 1-2 seconds for theta analysis and 100 ms for gamma analysis.

Theta periods were detected automatically using the ratio of the amplitude of the theta band (5-12 Hz) to the power of the delta band (1-4 Hz). Only theta periods taking place during locomotion were considered.

---

## 2.4.2 PHASE EXTRACTION

---

To extract the phase of theta, we first filter the signal with a Butterworth bandpass filter of order 4, with a pass band between 4 and 12 Hz. The Butterworth filter used is based on the standard Matlab implementation of it.

After filtering the signal, we use the Hilbert transform to obtain the instantaneous phase and amplitude of theta. The Hilbert transform is defined as:

$$H(u) = \frac{1}{\pi} p.v. \int_{-\infty}^{\infty} \frac{u(\tau)}{t-\tau} d\tau$$

where p.v. is the Cauchy principal value.

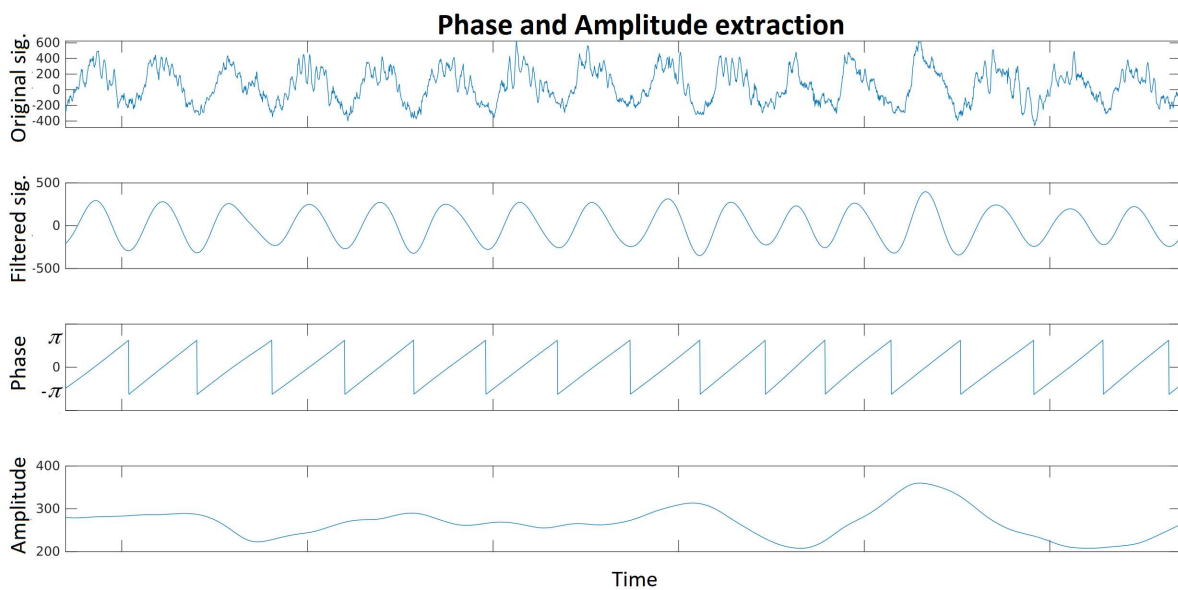


*Figure 9: Exemplification of the signal at various steps of our pipeline for phase and amplitude extraction. The original signal is filtered and then phase and amplitude are extracted through the Hilbert transform*

In practical terms, what this does is it rotates the negative and positive coefficients of the Fourier transform, giving us a complex signal when we started from a real one. Having a complex signal, we can easily obtain its phase and amplitude at any given moment in time.

As seen in Figure 9, peaks will have a phase of  $0^\circ$ , while troughs have a phase of  $180^\circ$ .

---

### 2.4.3 PAIRWISE PHASE CONSISTENCY (PPC)

---

In this study we will look at the theta and respiration modulation of spikes, times of gamma bursts and SWR, which requires us to have a measure of their angular preference.

There are various possible tests for angular preference, but many of these are biased by sample size. This is the case of phase-locking value, coherence measure and Rayleigh's resultant length. While the direction of the Rayleigh's resultant vector will be used to obtain the preferred phase (circular mean), an unbiased measure for the strength of modulation itself is required in case of a small sample size.

The Pairwise Phase Consistency is a measure of rhythmic synchronization that is not biased by sample size (Vinck et al. 2010). This is achieved by looking at pairs of observations rather than to all the observations together: if, for example, a neuron is consistently firing at a certain theta phase, pairs of spikes will on average present a small angular distance between each other.

---

### 2.4.4 GAMMA BURSTS DETECTION

---

While the analysis of the signal spectral content can give us a general idea of the strongest and most stationary components of oscillatory activity, gamma oscillations are better described as short lasting oscillatory events or gamma bursts. Conventionally, analysis of gamma oscillations assumes that their power and rate of occurrence is modulated by the phase of the slower oscillations, giving rise to a cross-frequency-coupling statistics. In the hippocampus, gamma oscillations during theta state are characterized by theta-gamma modulation index. However, this measure intrinsically emphasizes not the presence of the oscillation per se, but the strength of modulation by theta rhythm phase.

To provide more objective assessment of the gamma oscillations, our lab has developed analytical tools to isolate individual bursts of gamma activity. This is achieved by detecting local power maxima in the spatial, temporal and frequency domains. A subsequent screening is executed to avoid assigning the same burst to multiple adjacent layers (Sirota et al. 2008).

We can see a graphical example of this procedure in Figure 10.

On the left we have a slice of the frequency domain (for frequencies in the range 100-105 Hz), where each row corresponds to a channel of the silicon probe collecting the data. On the right we have the spectrogram for the channel in which the burst has been detected.

This method of description of gamma oscillations as discrete events allows to quantify separately the rate of their occurrence, modulation of their occurrence by theta phase and their power. Another conceptual advantage of such analysis of gamma oscillations is that it is agnostic to the ongoing brain state and does not rely on theta phase as a source

of non-stationarity. It becomes clear that ripple oscillations constitute a specific case of high frequency oscillations (120-200 Hz) that occur during quiescent state and are localized to CA1 pyramidale. In order to comply to a conventionally used detection of ripple oscillations they were further preselected to have power above 5 STD from the baseline distribution.

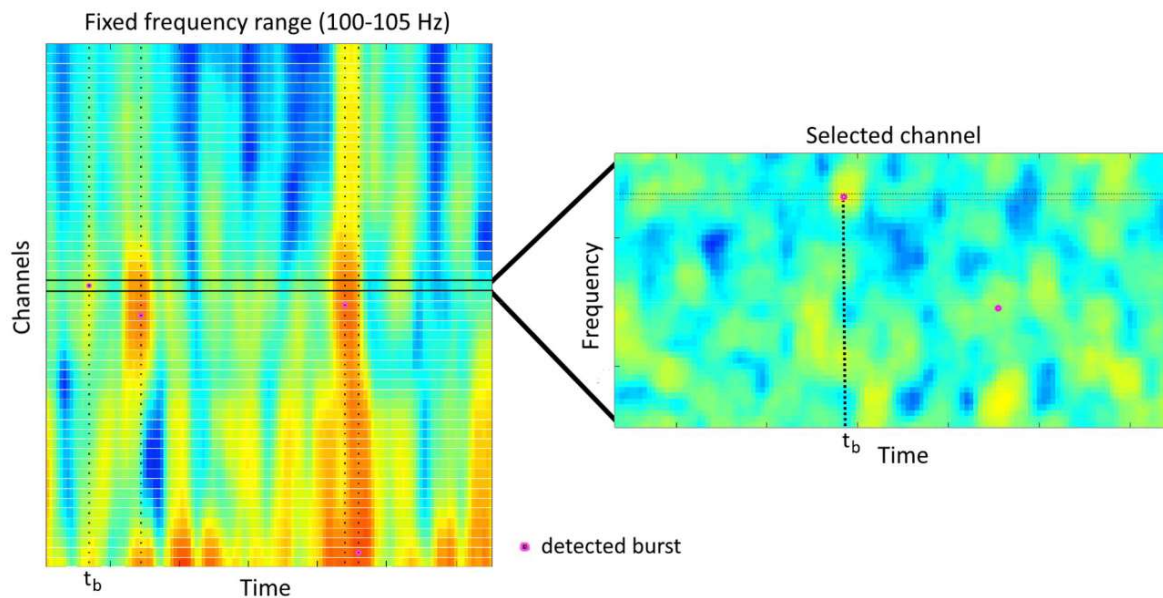


Figure 10: Right: spectral power in the range of 100-105Hz across channels in time. Left: Spectrogram of a single channel with detected burst.

## 2.5 STATISTICAL METHODS

To verify the presence of significant differences between WT and APP animals I used the Wilcoxon rank-sum test, a nonparametric alternative to the two-sample t-test.

Given that in most cases I am not only dividing the data between WT and APP animals, but also between young and old animals, I also used unequal two-way analysis of variance (ANOVA), since each value presented might be dependent both on our WT vs. APP comparison and from Young vs. Old.

Moreover, in multiple parts of the thesis I am testing multiple hypotheses (for example, that in any of six different layers gamma occurrences significantly change). When multiple hypotheses are tested, the chance of obtaining a false positive result increases. To compensate for that I used the Bonferroni correction.

As for the circular statistics used in determining the significance of theta/respiration modulation differences between WT and APP animals, I used the Kuiper test to verify the presence of shift in the preferred theta/respiration phase. The Kuiper test is a circular equivalent of the Kolmogorov–Smirnov test.

### 3. RESULTS

#### 3.1 BRAIN STATES

We first divided brain activity into its respective brain states and verified that the presence of periods of mobility (RUN, speed > 5 cm/s) and of quiescence (QUIET speed > 5 cm/s and no theta in pyramidal layer) was similarly distributed between the two groups (Figure 11).

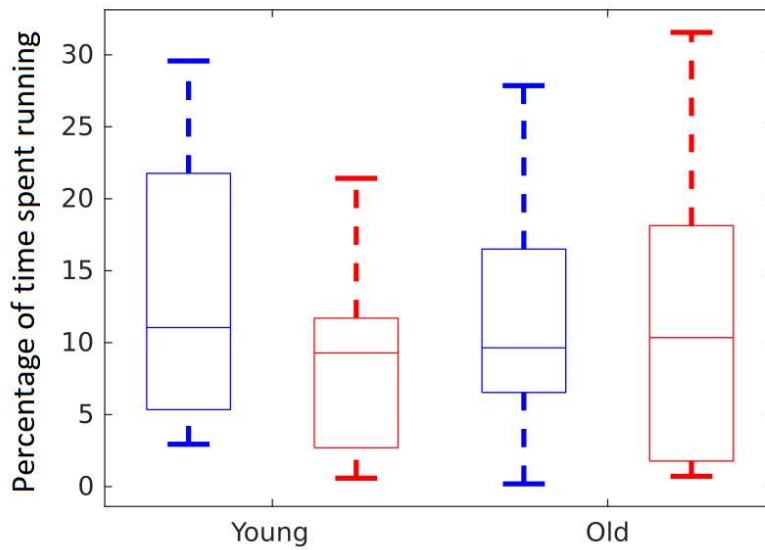


Figure 11: Percentage of time spent running for young (6-8 months old) and old (9+ months old) animals. (Blue: WT, Red: APP<sup>NL-G-F</sup>).

While our detection was based solely on the recorded speed of the animal and the theta/delta ratio present in the channel recording from CA1 pyramidal layer, pupil size and respiration observations were typically consistent with our state separation (Figure 12).

While theta power and activity are conventionally used for state detection in freely-moving animals, whether this definition of state is valid across all animals and genotypes in head-fixed condition is not known. To ascertain this, we used auxiliary variables indicating physiological state of arousal of the animal: the size of the pupil and respiration signal. In order to confirm that state segmentation based on theta power and locomotion is consistent with these variables we computed joint probability density between all variables: speed, pupil diameter, theta frequency, theta power, respiration frequency, respiration power. Typical example of such analysis (Figure 13, lower triangle) shows that during running (around the same speed level  $\sim 0.3$  cm/s) pupil diameter increases, theta amplitude increases, theta frequency stabilizes at  $\sim 7$  Hz, respiration frequency increases above 5 Hz and respiration amplitude increases. All

these state-related changes in the different state-related variables are therefore correlating, to a variable extent between each other, as seen in pairwise joint probability density plots. To quantify these relationships across sessions and group by genotype, we computed rank correlation (Spearman correlation coefficient) between all pairs of variables, which to some extent captures the degree and direction of relationship (Figure 13, upper triangle). Due to large number of sources of variability in the correlation coefficient values across sessions, the two groups do not show any statistical differences to each other.

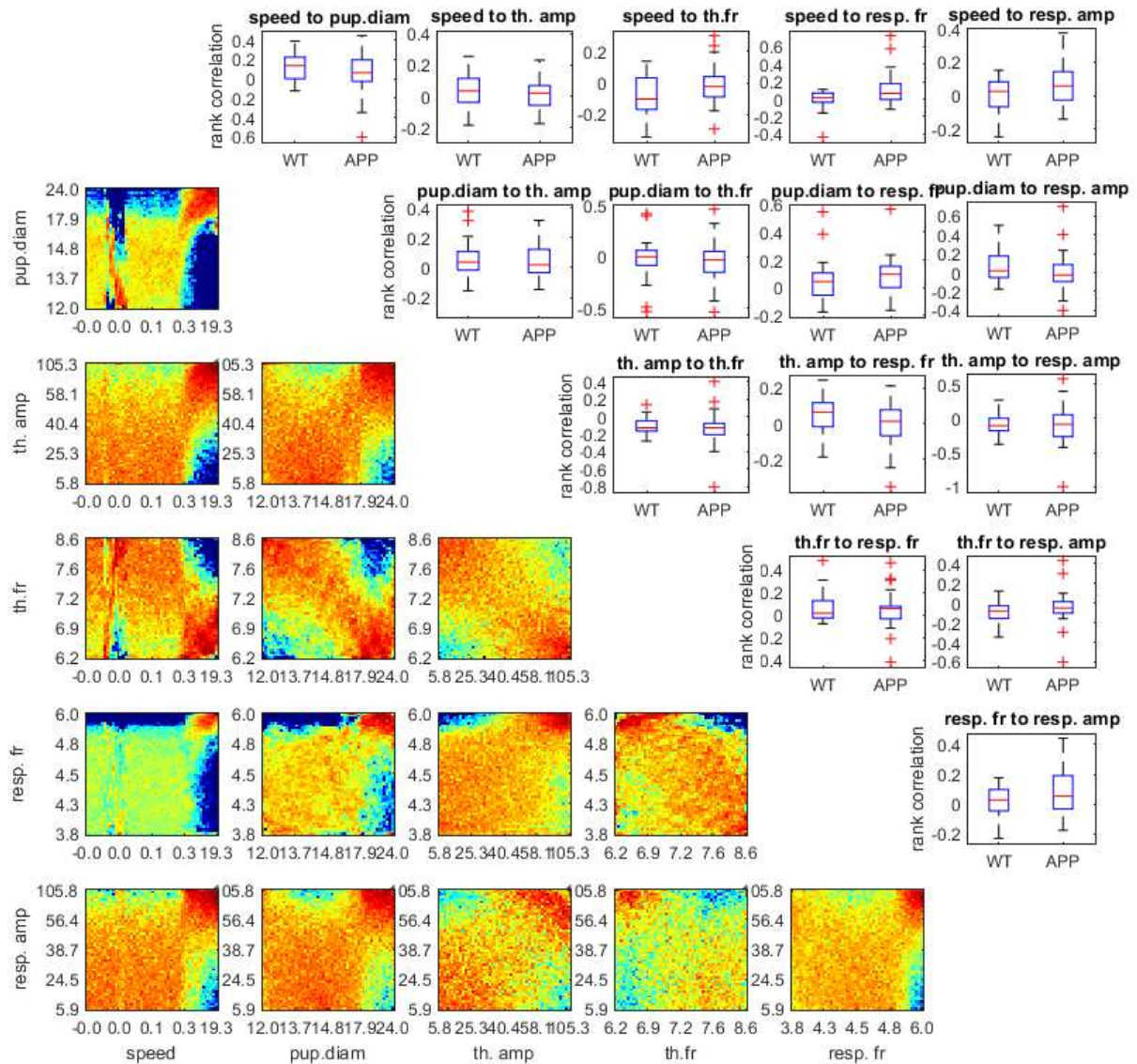


Figure 12: Brain state change is associated with correlated change in multiple physiological variables. Bottom-left triangle, pairwise joint probability density plots between speed, pupil diameter, theta frequency, theta power, respiration frequency, respiration power for an example session. Top-right triangle, matching arrangement plots summarizing group statistics of spearman correlation coefficient for WT(n=30)/APP<sup>NL-G-F</sup>(n=26) sessions.

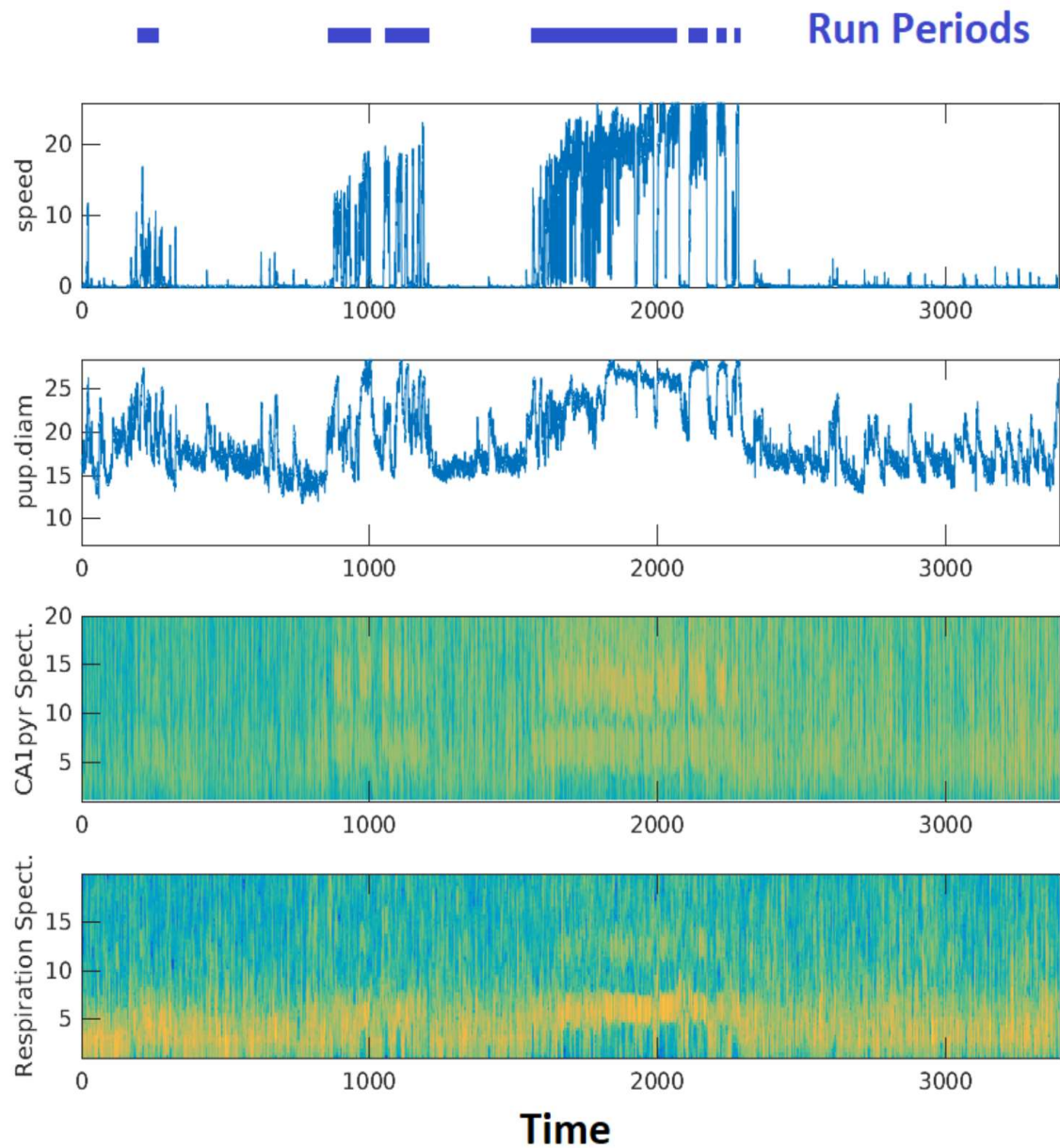


Figure 13: Blue bars on top: detected locomotion periods. From top to bottom: Speed, pupil dilation, CA1 pyramidal layer spectrogram, respiration spectrogram.

### 3.2 ANATOMICAL LOCALIZATION

As the next step, pyramidal layer of CA1 was identified by looking at the frequency content of the channels and identifying the one that has a peak for high (120-130 Hz) frequencies. Once we have identified CA1 pyramidal layer we can use it to detect ripples in quiescent periods. We also take the channel positioned three channels above CA1 pyramidal layer as the channel we use to detect theta.

The correct localization of CA1 and its layers is important for multiple reasons. First of all, the LFP reflects synaptic input and as such gives us an information about the activity of upstream brain regions. To know which brain regions we are talking about, we need to know the anatomical location we are recording from. Moreover, we want to be able to attribute types to the units we record, and we know that pyramidal cells will be located in CA1 pyramidal layer.

In the SWR-triggered CSD we can see the strong sink in radiatum (the “sharp wave”) due to CA3 input to CA1, corresponding to channels 34-38 in Figure 10. Here the current splits, generating a source in pyramidal layer (channels 29-33, as determined already with the PSD) and another in stratum lacunosum-moleculare Channels (channels 41-47).

In the theta-triggered CSD we can see the two theta dipoles: the first, having theta CA1 lacunosum-moleculare reflecting the input from layer 3 of the MEC and originating a passive return current in CA1 radiatum; the second, formed by a sink in DG molecular layer caused by the activity of layer 2 of the MEC and a passive return current in the

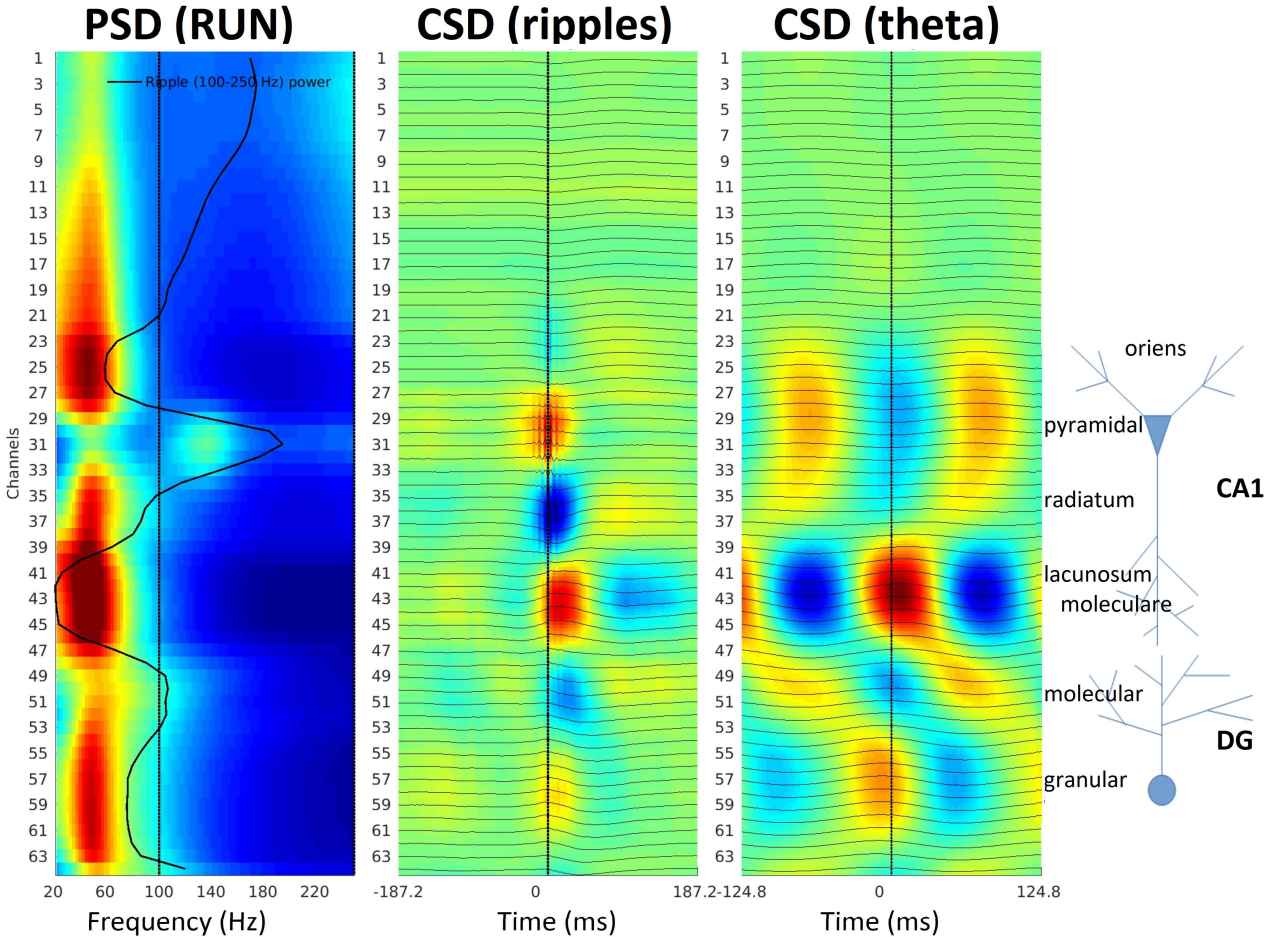


Figure 14: Left: PSD across channels (colour: power) Centre: averaged CSD triggered on ripple occurrences (t=0: ripple peak power) Right: averaged CSD triggered on the trough of theta in orians (t=0: through of theta). Blue: sinks; Red: sources

granule cell layer. We can see how the same channels as before are identified as part of CA1 lacunosum-moleculare and CA1 radiatum (Figure 14).

While anatomical localization would benefit from histology, the nature of the experiment (with repeated insertions in head-fixed mice) makes it impossible to use histological means to unequivocally attribute the channels. However, thanks to the analysis of CSD we are able to identify CA1, DG and their layers accurately. At this level of investigation, we don't see differences between WT and APP<sup>NL-G-F</sup> mice.

---

### 3.3 LFP ANALYSIS

---

As discussed in section 1.4.3, various oscillatory patterns in the hippocampus have been related to cognition and performance in multiple tasks. Given the impairment shown by APP<sup>NL-G-F</sup> mice, it is important to verify if there are differences in the hippocampal rhythms.

---

#### 3.3.1 THETA

---

The most prominent oscillation in the hippocampal circuit is theta (4-10 Hz). As already discussed, theta oscillations appear altered in both human patients with AD and in various animal models of the disease. However, there are still no studies investigating them in APP<sup>NL-G-F</sup>, a better model of AD than those that preceded it.

There are multiple aspects of theta that we want to investigate:

- Its relationship to speed, to avoid confounding factors in our subsequent analysis.
- Its power and average frequency
- Its modulation of gamma bursts

---

##### 3.3.1.1 THETA IN DIFFERENT LAYERS

---

Since theta originates as a dipole with contributions from multiple upstream regions, we want first to verify that the ratio between the strength of theta in the different hippocampal layers isn't varying between APP<sup>NL-G-F</sup> and WT animals (Fig 15).

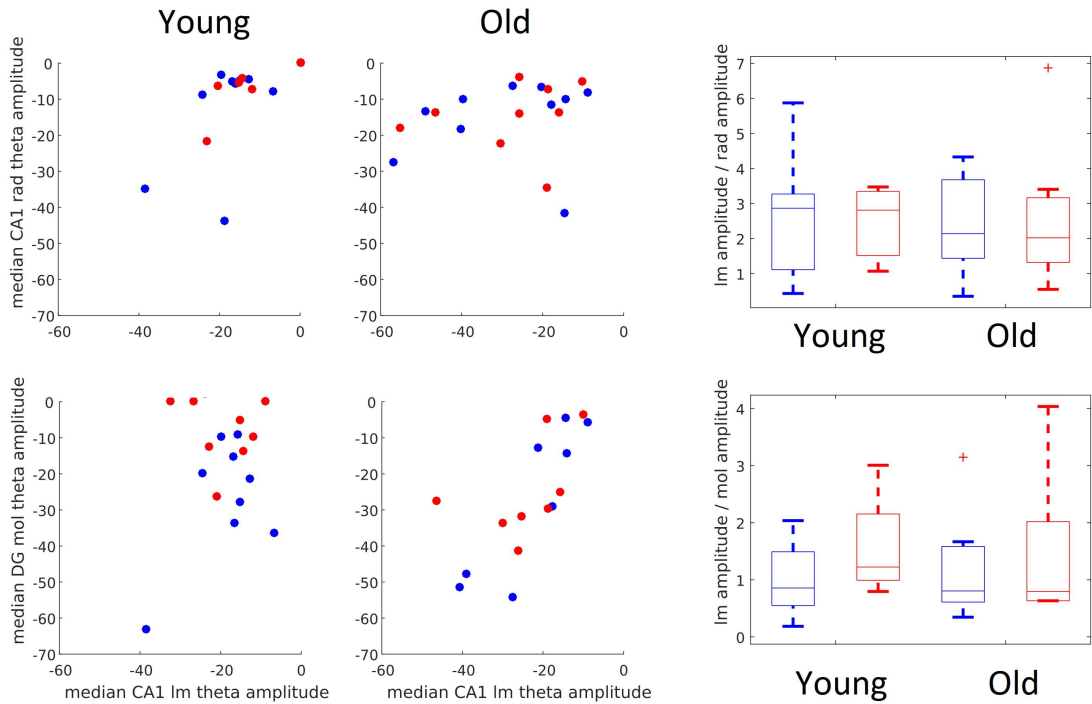


Figure 15: Left: scatter plots of median CA1 radiatum and DG molecular amplitude vs. median CA1 lacunosum moleculare amplitude. Right: ratio of CA1 lacunosum moleculare amplitude on CA1 radiatum (Top) and on DG mol (Bottom). (Blue: WT, Red:  $APP^{NL-G-F}$ ).

### 3.3.1.2 THETA AND SPEED

While in freely moving rodents there is ample literature describing a relationship between theta and speed (McFarland, Teitelbaum, and Hedges 1975), the results in head-fixed animals are not yet clear (Supplementary materials in Haas et al. (2019; Ravassard et al. (2013; Chen et al. (2019)). It is thus necessary to ascertain if and how speed modulates theta in our setup.

Our results were contradictory, with some animals presenting no speed modulation of theta (Figure 16, Top-Left) and others presenting it (Figure 16, Bottom-Left). Looking at the histogram of the rank correlation values we see that modulation of theta frequency (here we show its inverse, the cycle period) and of theta amplitude varies between a slightly negative and a slightly positive association, almost centred at zero (Figure 17).

Finally, we need to verify if this lack of correlation was due to a lag between the speed peak and the increase in theta power (Figure 18).

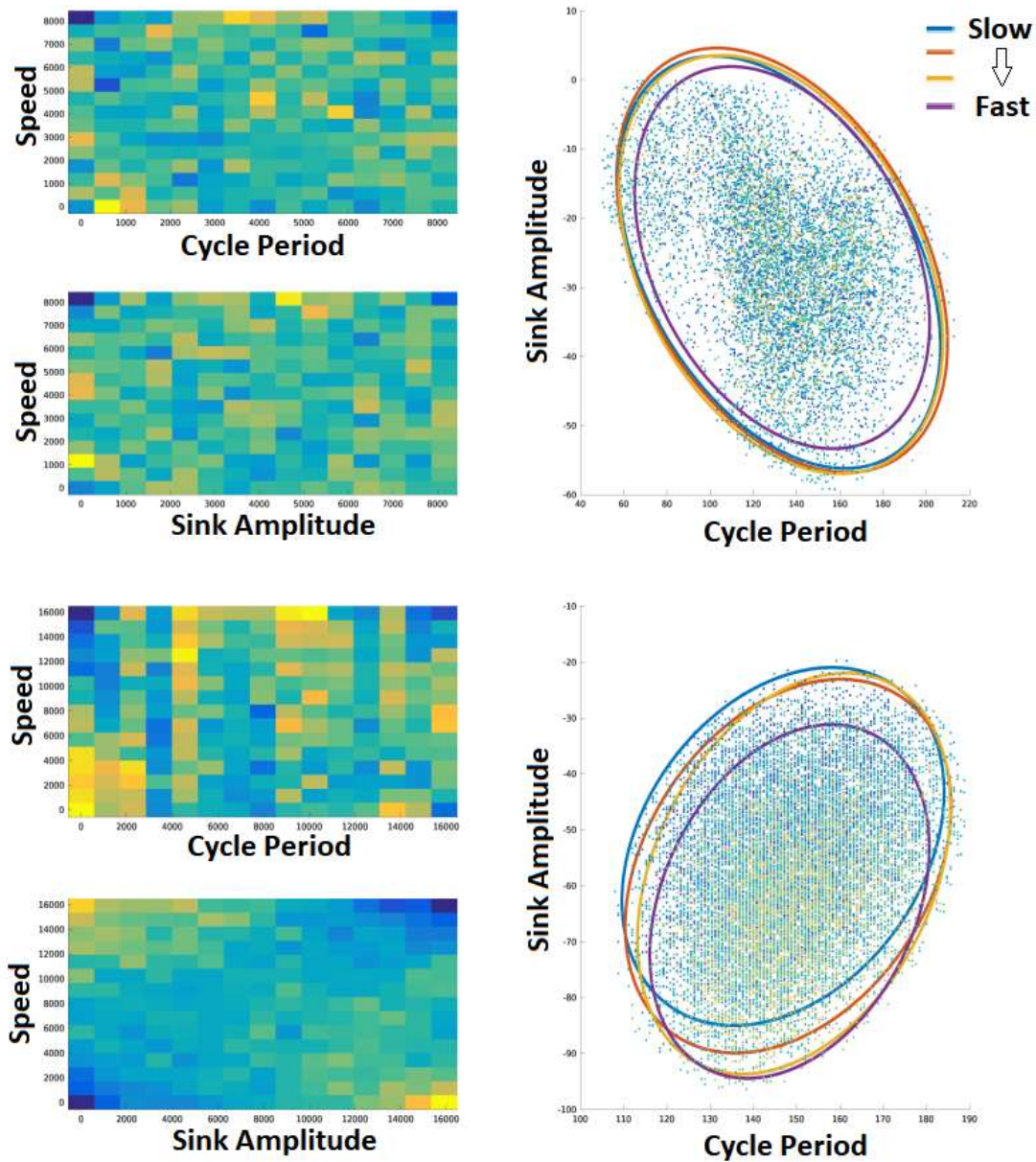


Figure 16: Left: joint probability density for two different animals for speed vs. cycle period (Top) and speed vs. sink amplitude (Bottom). Right: sink amplitude on cycle period, Colour: speed (colour scale from blue (slow) to yellow (fast)). The ellipses represent the confidence area per different speed percentiles for the same animal as Left.

## Rank Correlation

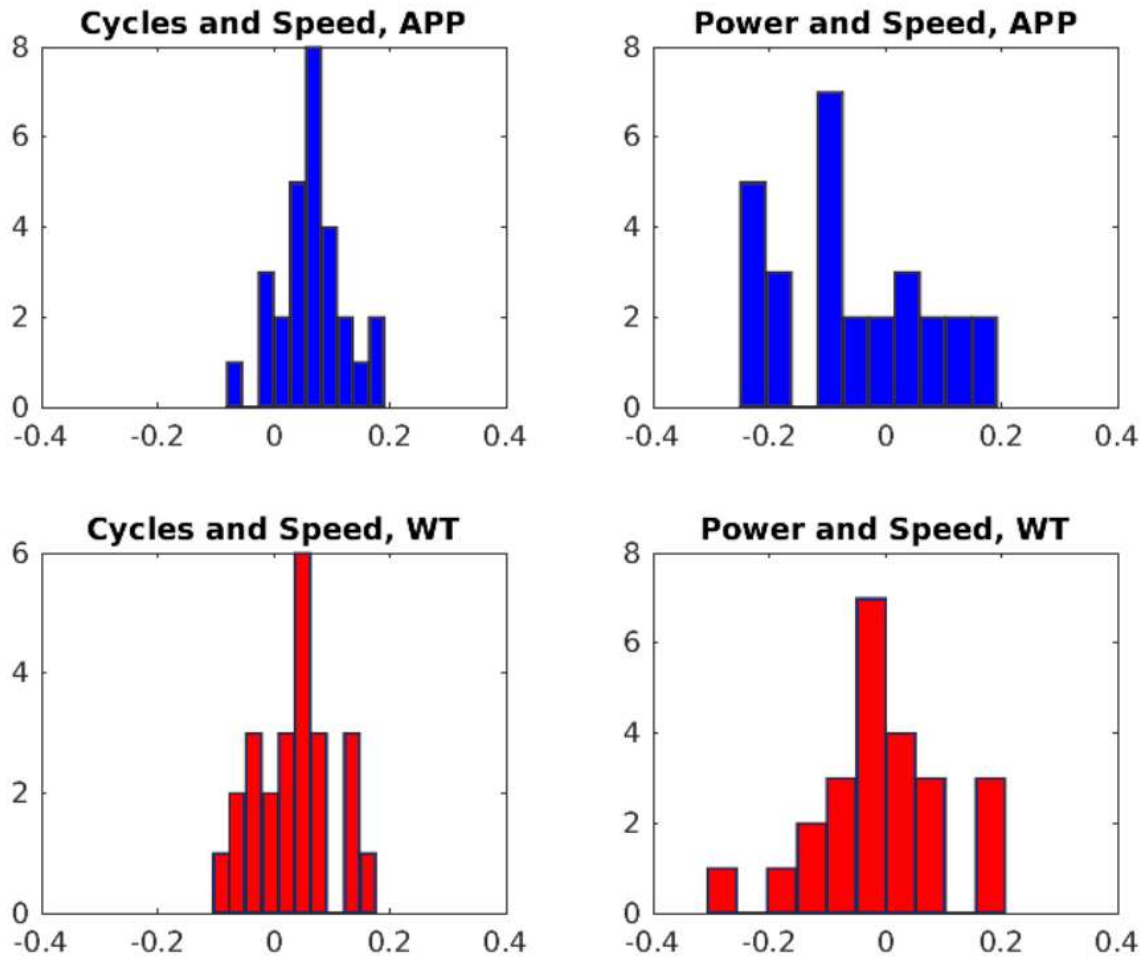


Figure 17: Rank correlation between cycle length and speed (Left) and power and speed (Right) for WT (Top) and APP<sup>NL-G-F</sup> (Bottom) mice.

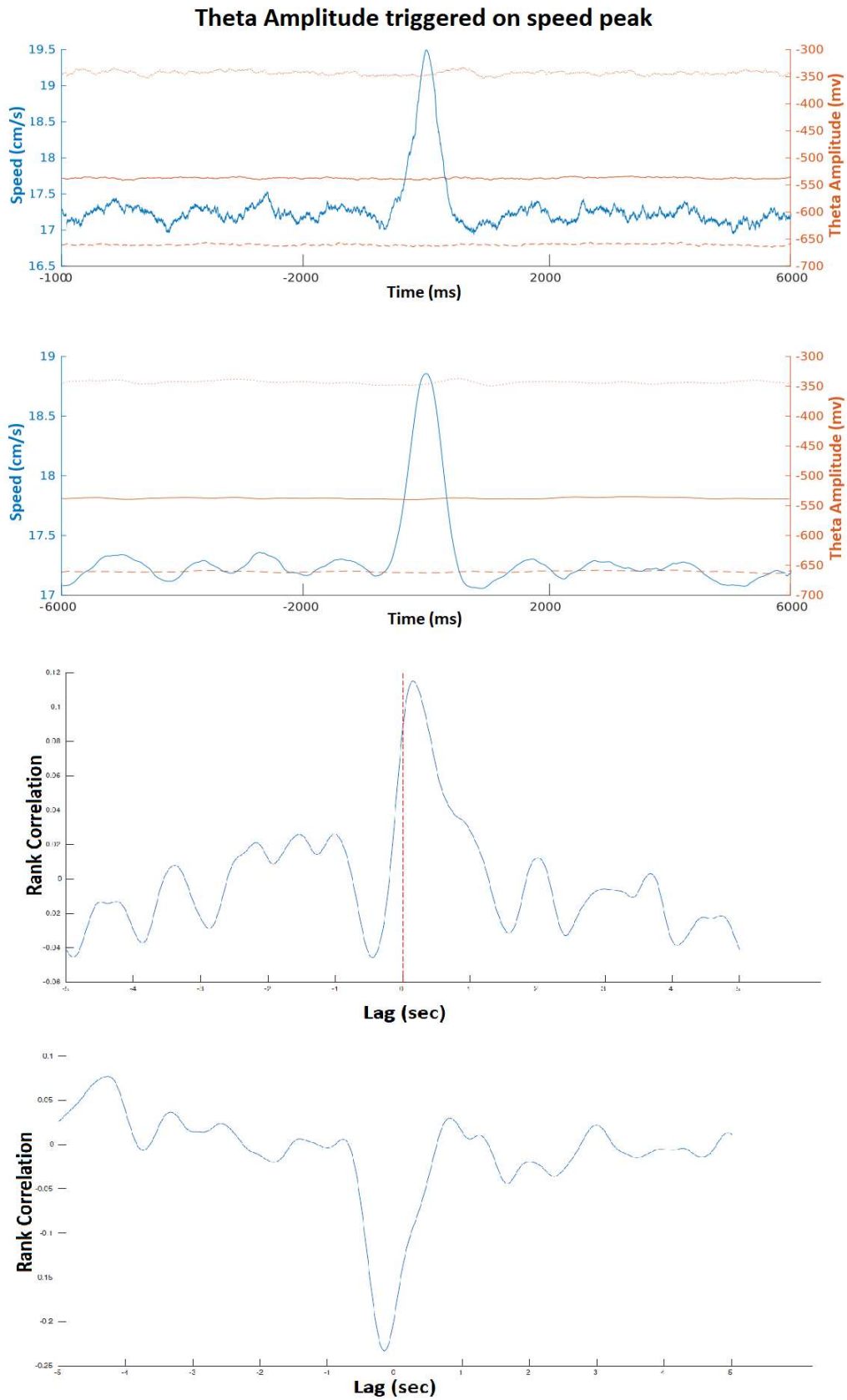
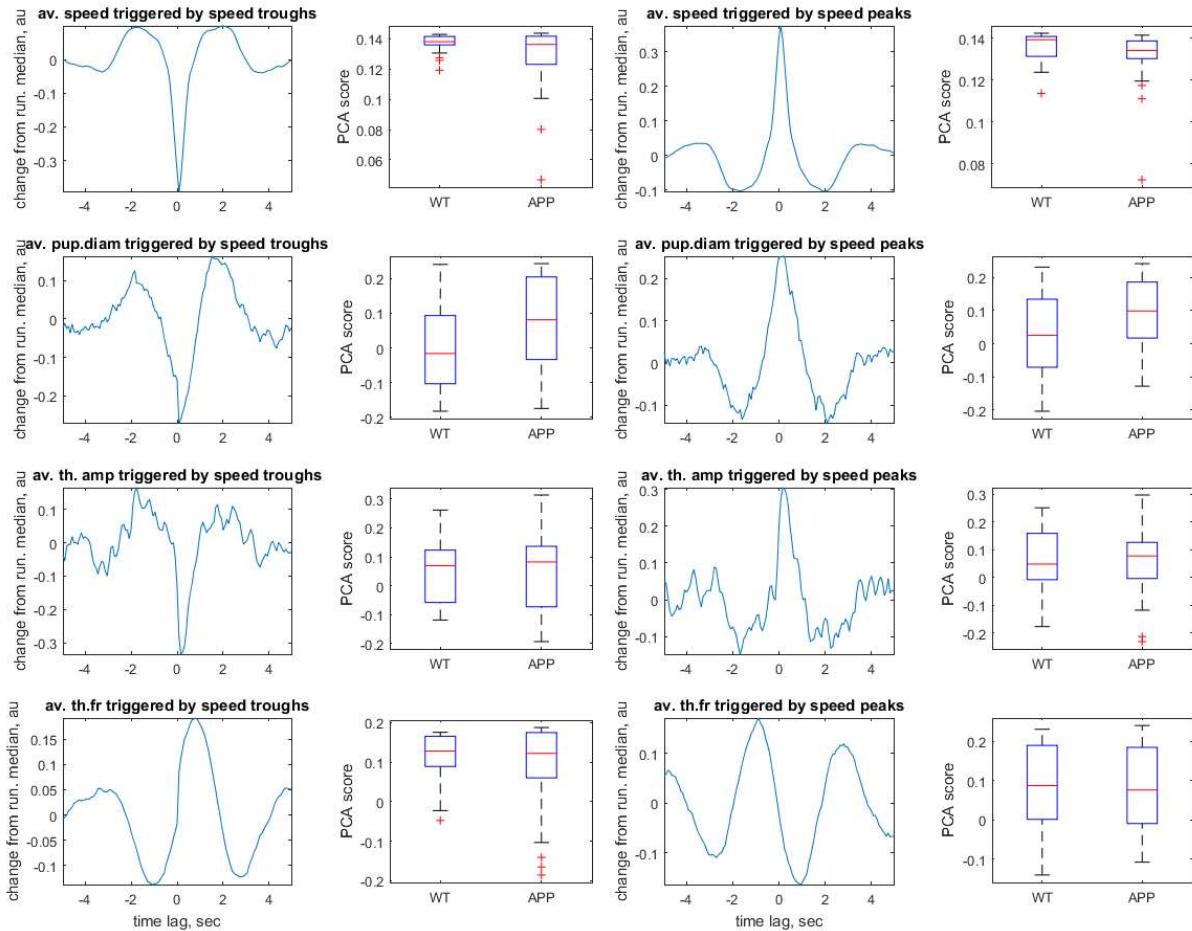


Figure 18: Top: speed peak triggered average of Theta Amplitude in CA1 Im. The thick, orange line represent theta amplitude, while the thin lines are its 25% and 75% percentile. Bottom: rank correlation for multiple lag values for two different animals

As we can see in the example sessions shown in Figure 18, results can dramatically vary between sessions, with some showing an increase of theta amplitude that has its maximum a few milliseconds after the peak in speed (second to last plot) and others in which not only this peak is not present, but we even find a negative correlation between speed peak and theta amplitude (last plot).



*Figure 19: Fine time scale relationship between speed transients and pupil and theta dynamics. Top to bottom, triggered average speed, pupil diameter, theta amplitude and theta frequency (median filtered prior to averaging). Left two columns, first PCA eigenvector for averages triggered by troughs in speed and box-plot group statistics of the corresponding scores across all sessions ( $n=30/26$ ). Right two columns, triggered by peak in speed.*

It is possible, that other sources of animal arousal state contribute to the changes of theta power and frequency. As shown earlier, on a coarse time scale fluctuations in speed, theta power and pupils size are correlated. We investigated whether fast changes of the speed, associated with stops or accelerations, are also temporally correlated in a consistent manner with theta frequency and power changes, as well as pupil size. To this end we detected troughs or peaks of speed and computed average fluctuations in all high-pass-filtered time series of all the variables. To assess how variable the resultant speed trough/peak centred time-courses are, we performed PCA analysis across all

sessions and represented typical response of each variable with the first eigenvector, and group data variability with the scores of the first principal component (Figure 19).

Typical dynamics in most data was that of decrease in pupil size during speed troughs and increase during peaks, but in both WT and APP groups some animals showed opposite dynamics as evidenced by the negative PC score. Interestingly, troughs/peaks of speed were associated with delayed and moderate, on average, increase/decrease in theta frequency, comparable between groups. This analysis suggests that detail study of theta parameters might require revisiting our characterization of locomotion on the treadmill as non-stationary behaviour and depart from simplistic zero or fixed-lag correlations to speed.

### 3.3.1.3 THETA POWER AND AVERAGE FREQUENCY

We now move to examine the theta oscillations themselves, looking at their power and average frequency during periods of locomotion (minimum speed: 2 cm/s). Since the

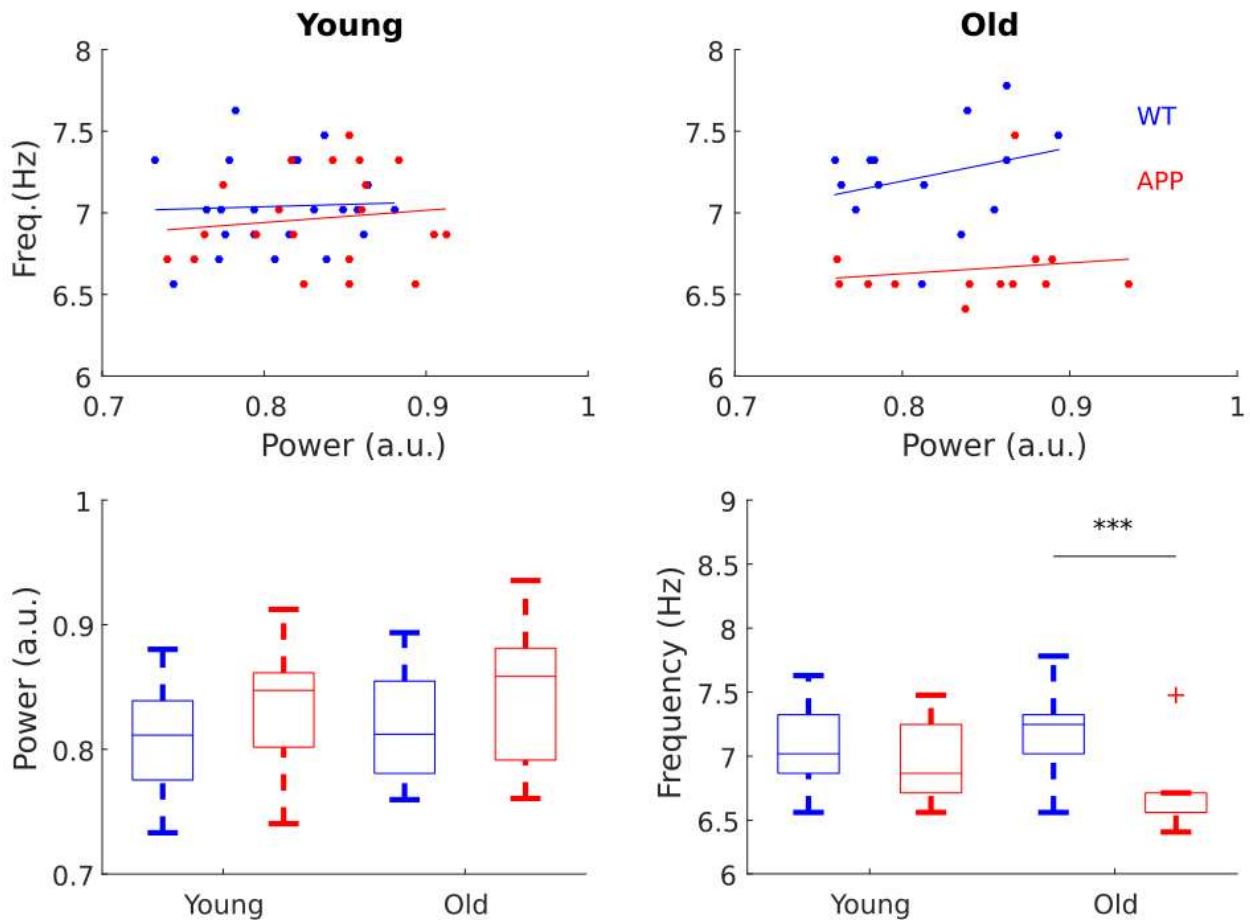


Figure 20: Theta frequency, but not its power, in the old  $APP^{NL-G-F}$  cohort is lower than in WT animals ( $p < 0.00001$ ). This is not true for the younger cohorts.

Top: frequency vs. power for young (Left) and old (Animals). Lines are linear fit. Bottom Left: power for young and old animals. Bottom Right: frequency for young and old animals (Blue: WT, Red:  $APP^{NL-G-F}$ ).

results were equivalent at all speed ranges, Figure 20 is computed for the whole active state regardless of speed.

For this analysis (and some subsequent ones) the animals were divided into two groups: young (6-8 months old) and old (9-12 months old). We find a significant decrease in theta frequency in the old  $APP^{NL-G-F}$  mice compared to the WT cohort. This effect is present only for the older cohort and not in the younger one, suggesting it as an effect of continuous neurodegeneration.

To better visualize the difference, we plot the distribution of frequency and power for the four cohorts (Figure 21).

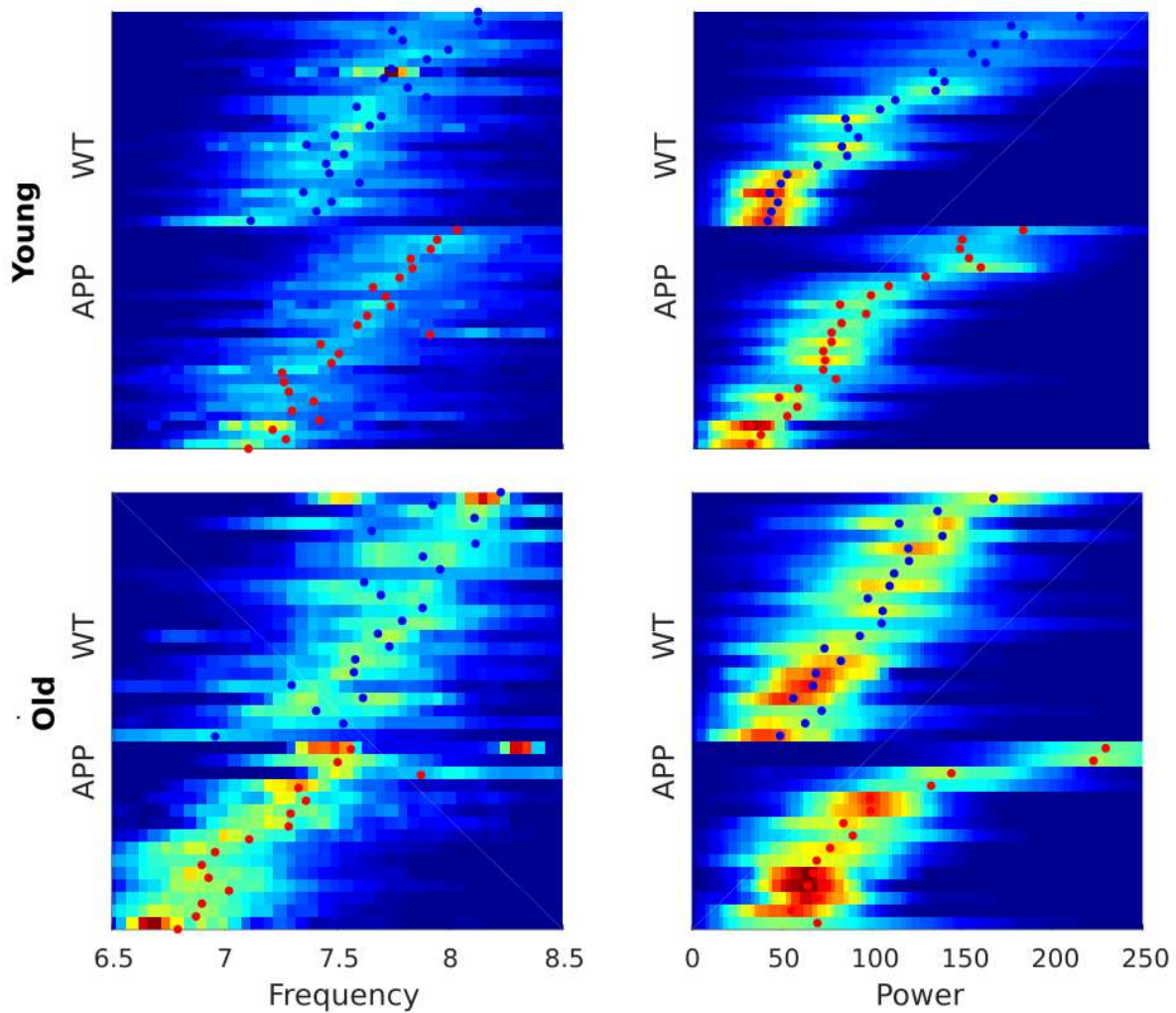


Figure 21: Distribution of frequency (Left) and power (Right) of the theta spectrum ordered by mean value for young (Top) and old (Bottom) animals. Dots indicate the median value. (for the dots: Blue: WT, Red:  $APP^{NL-G-F}$ ).

### 3.3.1.4 FIRST THETA HARMONIC AND ASYMMETRY

Since theta oscillations aren't perfectly sinusoidal, they produce harmonics. This can be useful to quantify their distance from a sinusoidal oscillation. Comparing the theta/1<sup>st</sup> harmonic ratio between APP<sup>NL-G-F</sup> mice and WT mice could thus show us if the shape of theta is changing between the two cohorts.

There is no significant difference in the harmonic/theta rate between the two cohorts (Figure 22).

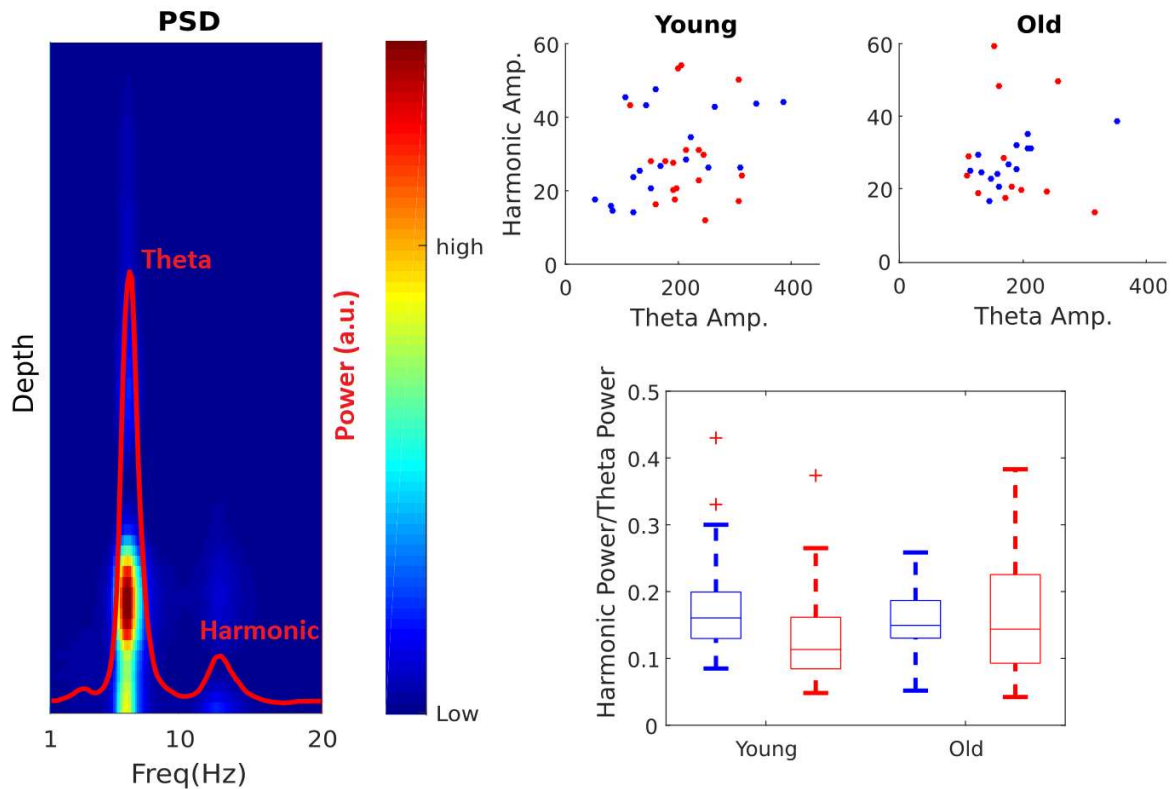


Figure 22: Left: PSD showing theta and its first harmonic across depth. Red overlay: spectral power in CA1Im (Single session example). Top-Right: Scatter plot showing the power of the harmonic and the power of theta for the two groups. Each dot represents a session. Bottom-Right: Harmonic power/Theta power ratio across sessions. (Blue: WT, Red: APP<sup>NL-G-F</sup>).

Another useful measure to capture the shape of theta waves is that of asymmetry, which we used as defined by Belluscio et al. (2012):

$$\log\left(\frac{\text{ascending phase}}{\text{descending phase}}\right)$$

so that a value of zero equals to a symmetric wave-shape.

As seen in Figure 23, we can conclude that there are no significant differences in the shape of theta between APP<sup>NL-G-F</sup> mice and WT mice.

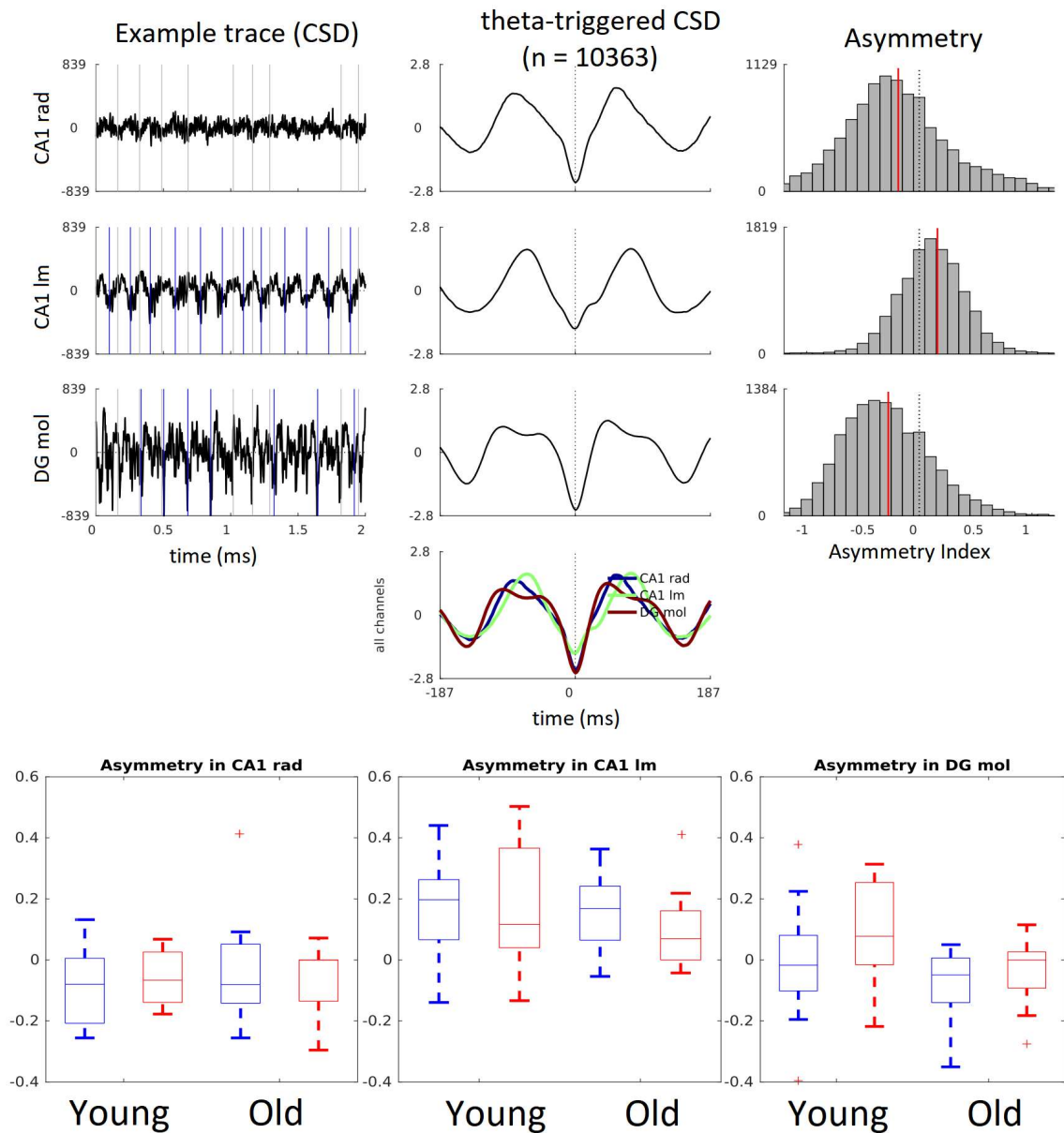


Figure 23: Top-Left: example CSD traces of multiple theta cycles for CA1 rad, CA1 lm and DG mol. Top-Centre: theta triggered CSD for CA1 rad, CA1 lm and DG mol, Top-Right: asymmetry distribution for the same session in CA1 rad, CA1 lm and DG mol. Bottom: asymmetry across all sessions, divided between young and old animals. (Blue: WT, Red:  $APP^{NL-G-F}$ ).

While the results regarding the relationship between theta and the animal's speed remain inconclusive, we can see a significant decrease in the average frequency of theta and no significant changes in its power, shape and relative strength across layers. We want now to look at events in the gamma range, which can reflect input from the upstream regions (EC in the case of gamma in CA1lm and DGmol) and local output (in CA1pyr).

### 3.3.2 GAMMA

We then performed cross-frequency coupling analysis, as conventionally used in the field to characterize diverse gamma oscillations. To this end we computed the strength of theta phase modulation of gamma power using power-weighted resultant vector, yielding strength and associated preferred theta phase for each LFP channel.

A first look at the theta-gamma modulation of the LFP doesn't show a qualitative difference between the two cohorts (Figure 24). At this level of description we can already identify various gamma modes, clusters of gamma activity with similar frequency and theta phase preference.

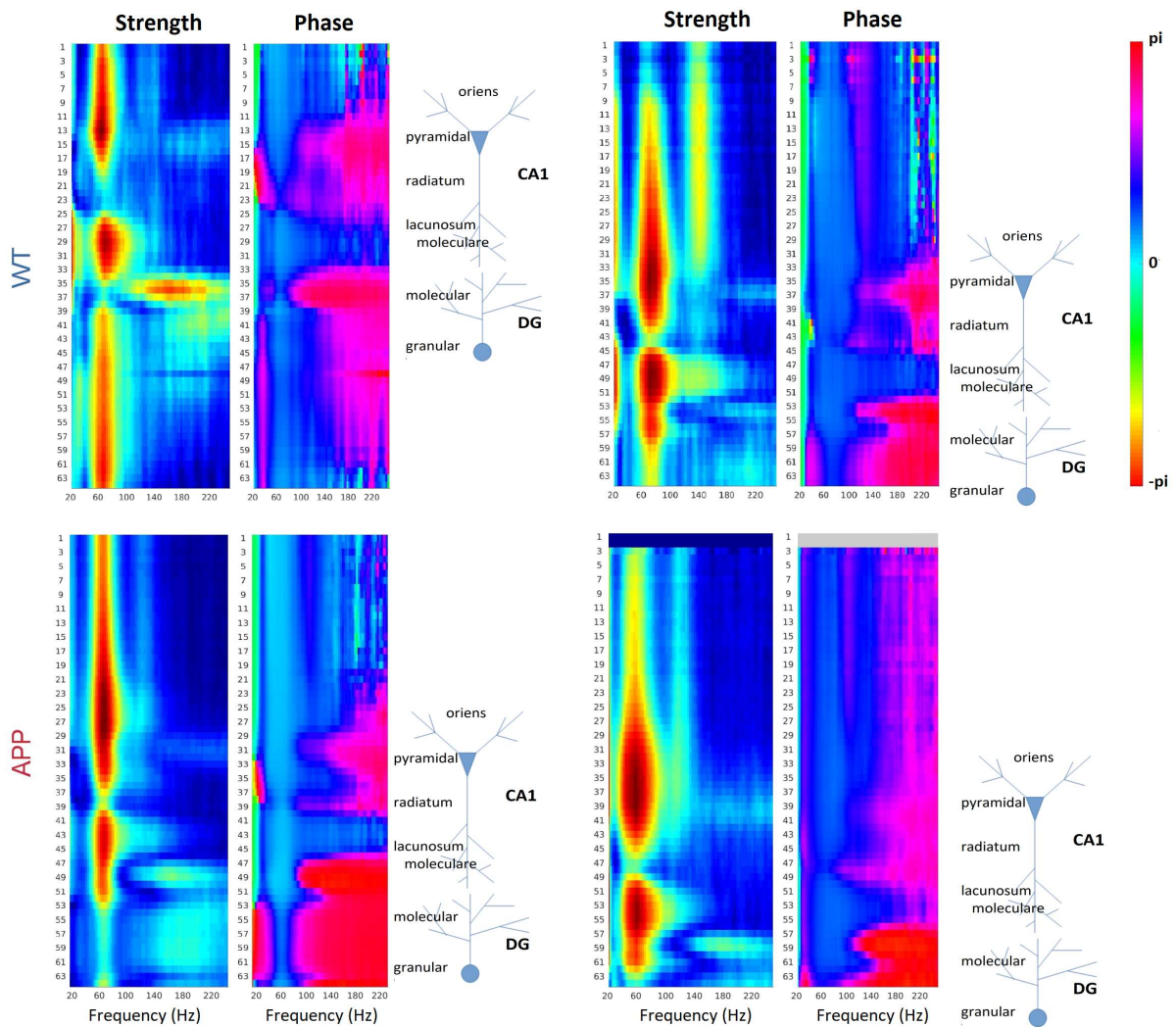


Figure 24: Theta Gamma modulation (strength and phase) for four different animals  
Phase =  $\pi$ : peak of theta as measured in oriens. (Top: two WT mice, Bottom: two  $APP^{NL-G-F}$  mice).

Looking at Figure 24 we can see that the frequency that is more strongly modulated across the hippocampus is centred around 60 Hz and happens in the descending phase of theta (blue colour in the phase plot). The fact that this modulation extends to the

cortex is due to volume conductance. In radiatum we can see a less strongly modulated, but consistently present, gamma mode at around 30-40 Hz riding the peak of theta (purple-red colour in the phase plot). We can also see strong modulation of fast gamma (140-220 Hz) in CA1 lm and DG mol, again at the peak of theta (red colour in the phase plot).

While this analysis could give qualitative assessment of the different gamma oscillations, there are number of shortcomings associated with volume conduction, mixing between gamma power and theta modulation of gamma occurrence. Hence we resorted to a more accurate method for assessing gamma dynamics, treating gamma oscillations as anatomically and frequency localized transient bursts.

### 3.3.2.1 GAMMA AS GAMMA BURSTS

---

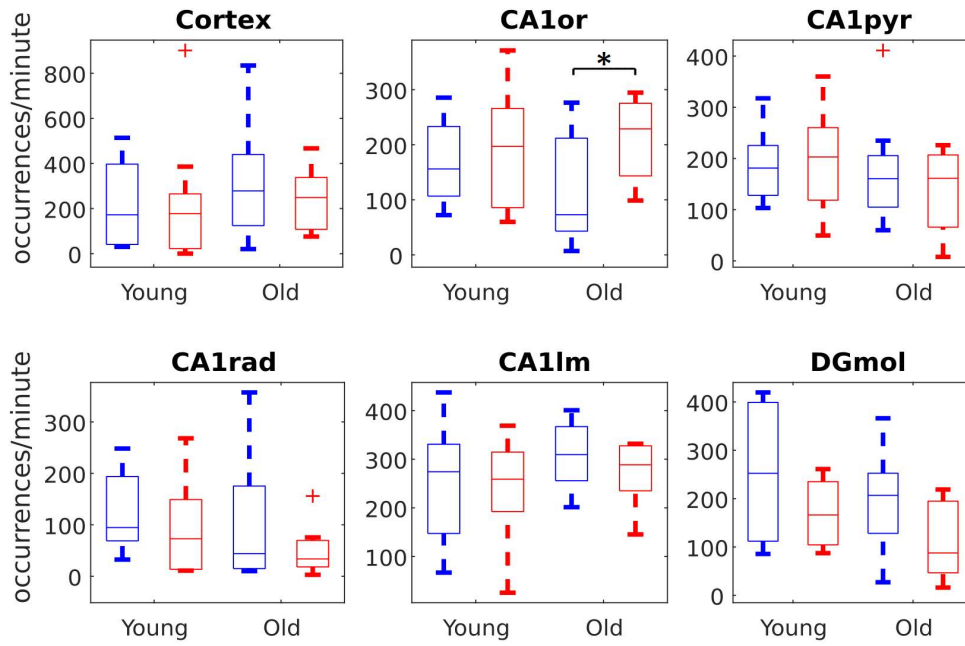
As described in the method section, we identified the individual gamma bursts and then treated them similarly to units: clustering them on the basis of their anatomical location, preferred theta phase and frequency.

By doing so, we can count the single occurrences and verify whether their rate is changed, finding an increase in the occurrence of slow gamma bursts in CA1 oriens for old APP<sup>NL-G-F</sup> mice for both RUN periods (Figure 25) and periods of immobility (Figure 26). During the RUN periods we can see an increase in the gamma occurrences for slow gamma in oriens, while for immobility periods we see more changes: not only a reduced occurrence of slow gamma in CA1 lacunosum moleculare and DG molecular, but also of fast gamma in CA1 pyramidalia (which is not caused by a reduction in SWR, as we will see in Figure 33) and in CA1 lacunosum moleculare. All these changes seem to appear only in older animals. We do this by dividing gamma into slow (40-100 Hz) and fast (100-200 Hz) gamma.

We find different gamma modes, all occurring for both wild type and APP animals. In Figure 27 we see an example from one of the APP animals, the same represented in the bottom left of Figure 24.

From Figure 27 we can see that in most layers of the hippocampus we can identify two gamma modes: one at high frequency and one for slow gamma, with different preferred theta phase. Exceptions to this are found in CA1 radiatum, where a third, slower, mode can be seen (frequencies 30-40 Hz) and CA1 lacunosum moleculare and DG granular layer where both high and low frequency gamma have the same preferred theta phase.

## Slow Gamma



## Fast Gamma

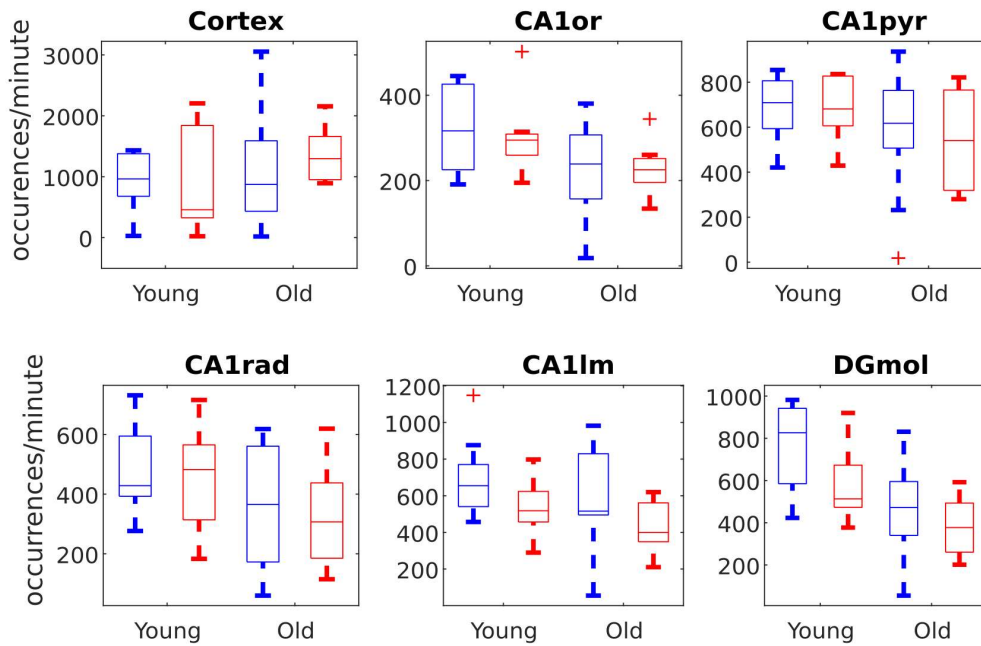
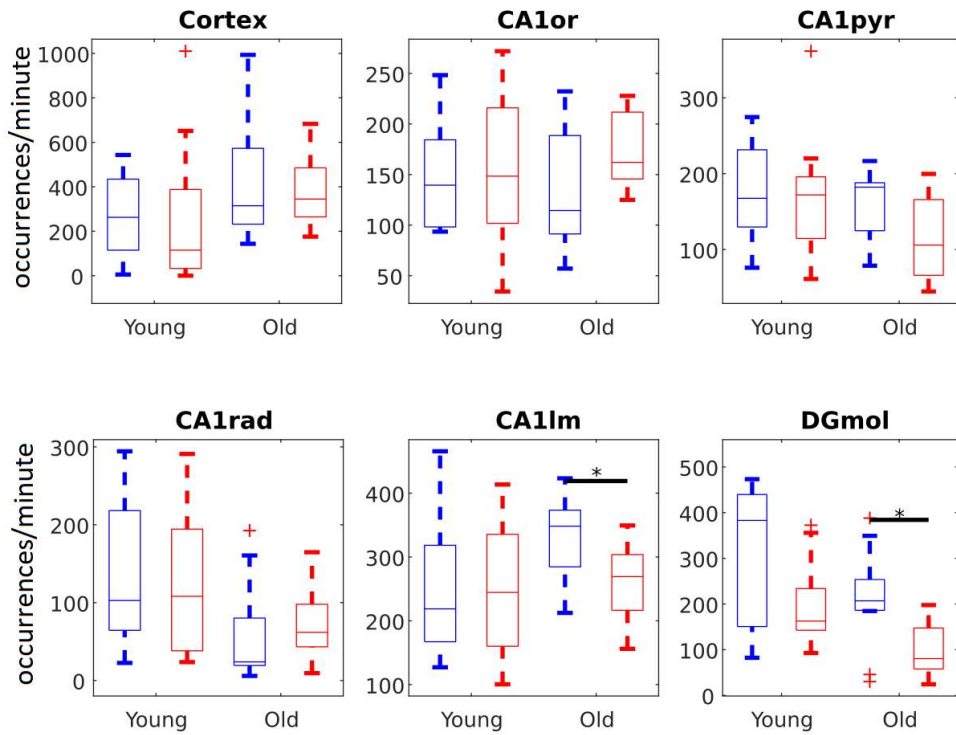


Figure 25: Rate of occurrence of gamma bursts divided by anatomical layer for RUN periods (Blue: WT, Red:  $APP^{NL-G-F}$ ).

# Slow Gamma



# Fast Gamma

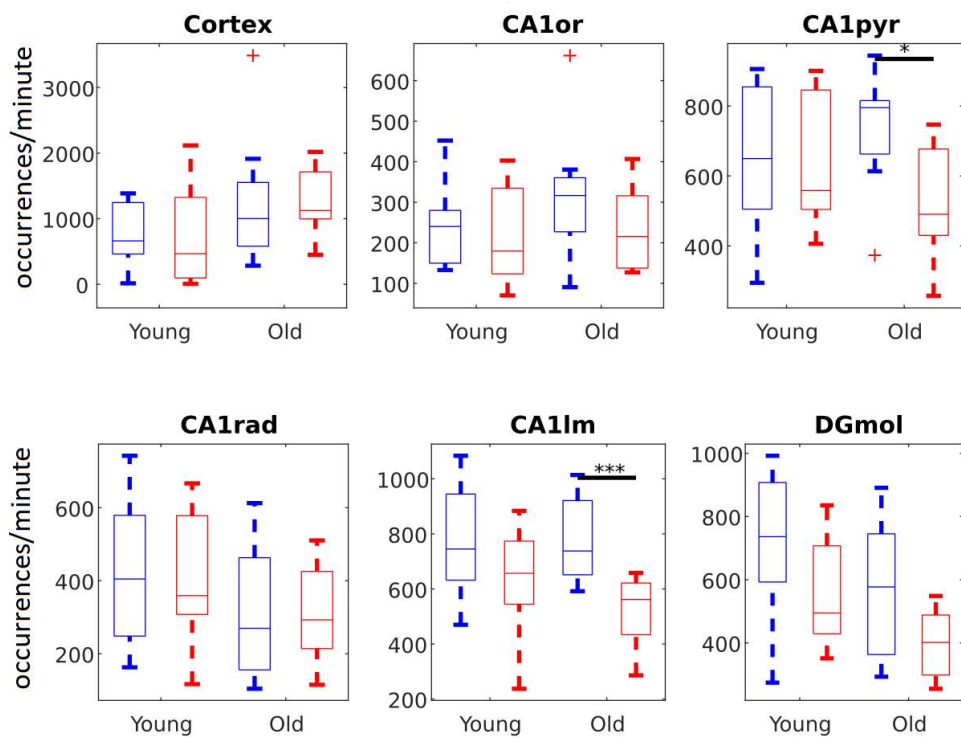


Figure 26: Rate of occurrence of gamma bursts divided by anatomical layer for quiescent periods (Blue: WT, Red:  $APP^{NL-G-F}$ ).

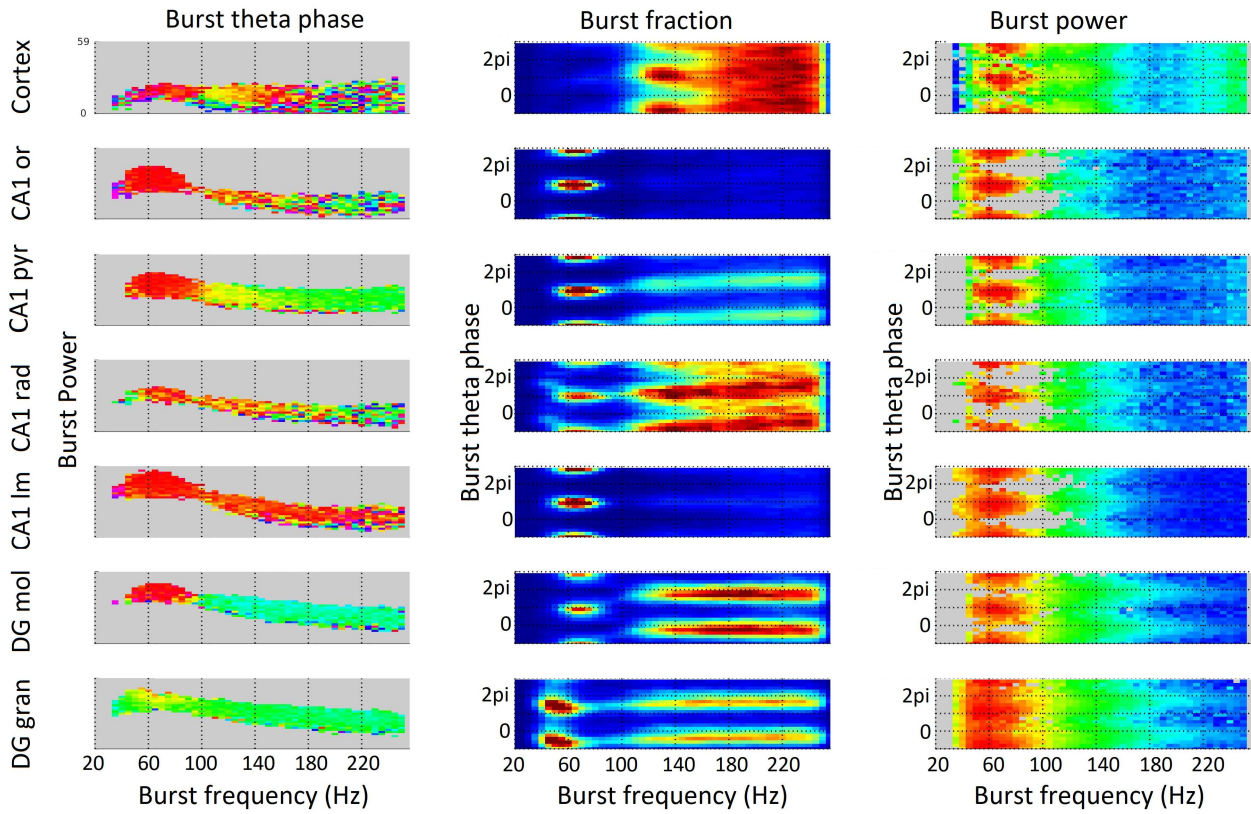


Figure 27: Left: burst power on burst frequency, colour: burst theta phase Center: fraction of bursts on burst frequency, colour: fraction of bursts. Right: burst theta phase on burst frequency, colour: burst power. Top to Bottom: Layers from Cortex to DG mol.

# Slow Gamma

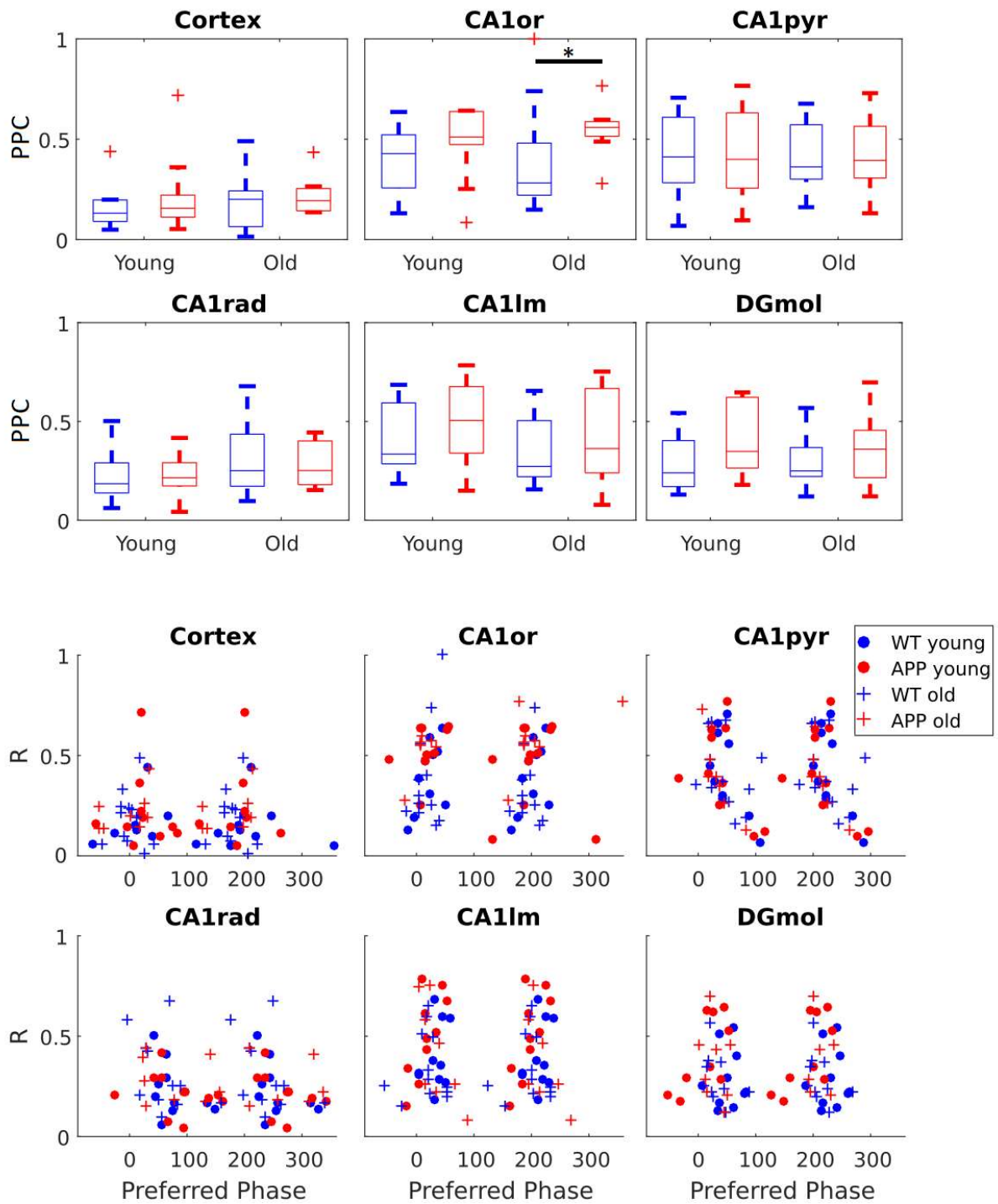


Figure 28: Theta Gamma Modulation for slow gamma (40-100 Hz). Top: PPC across sessions for young and old animals, per layer (Blue: WT, Red: APP<sup>NL-G-F</sup>). Bottom: resultant length R vs. preferred phase across sessions per layer (Blue: WT, Red: APP<sup>NL-G-F</sup>; Circles: Young, Crosses: Old).

# Fast Gamma

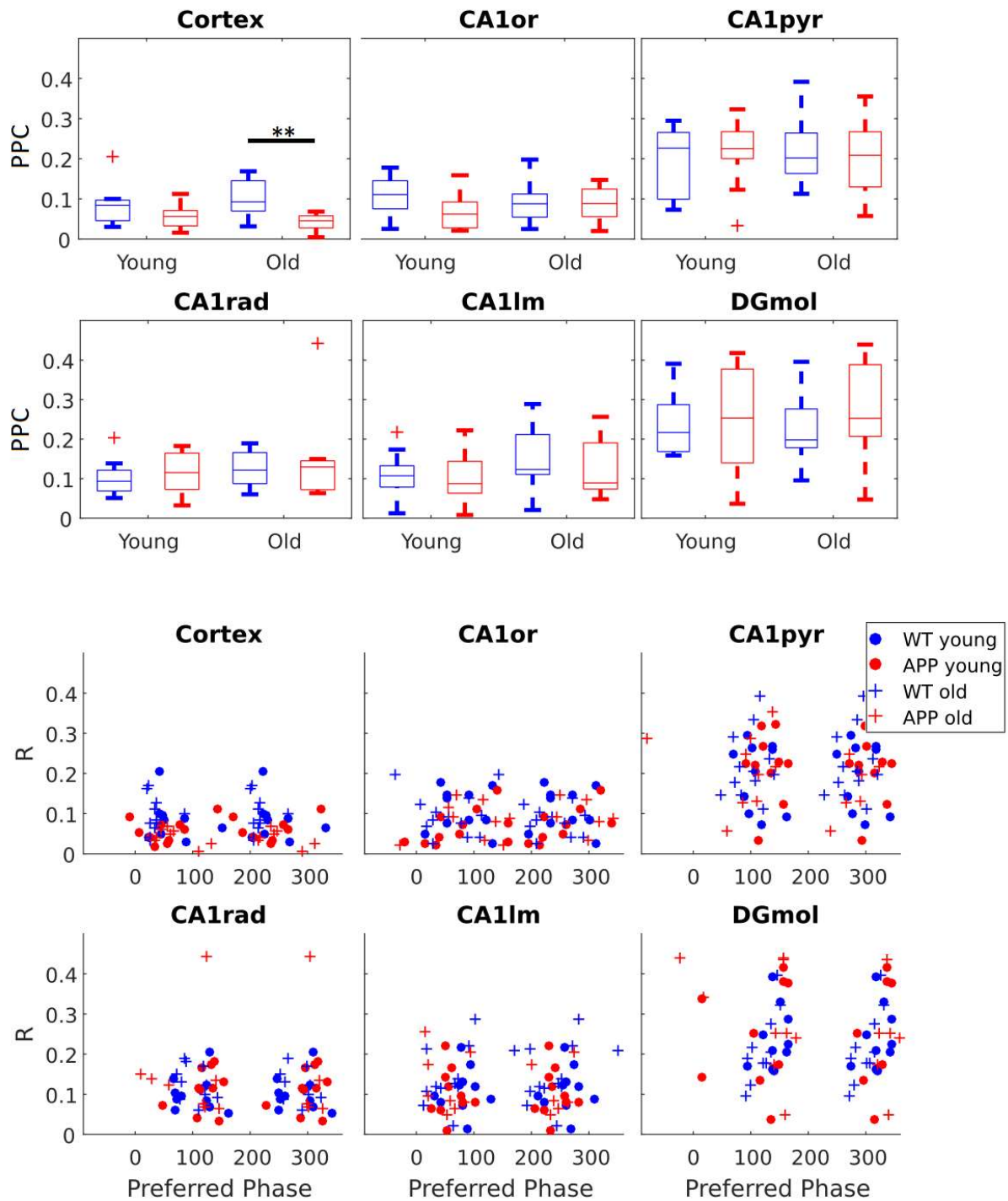
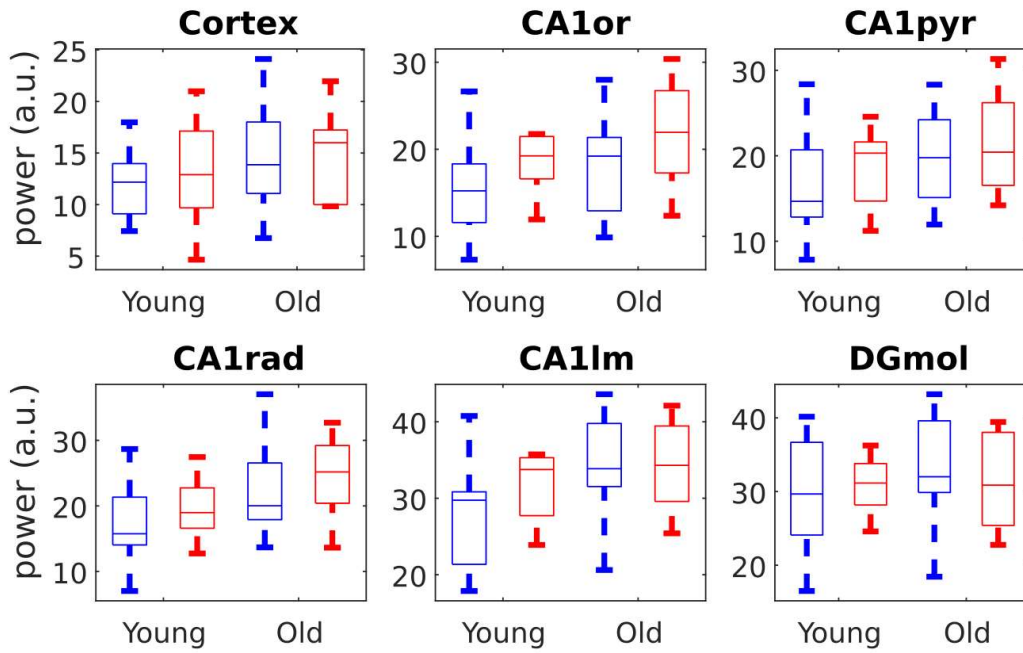


Figure 29: Theta-gamma modulation for Fast Gamma (100-200 Hz). Top: PPC across sessions for young and old animals, per layer (Blue: WT, Red:  $APP^{NL-G-F}$ ). Bottom: resultant length R vs. preferred phase across sessions per layer (Blue: WT, Red:  $APP^{NL-G-F}$ ; Circles: Young, Crosses: Old).

# Slow Gamma



# Fast Gamma

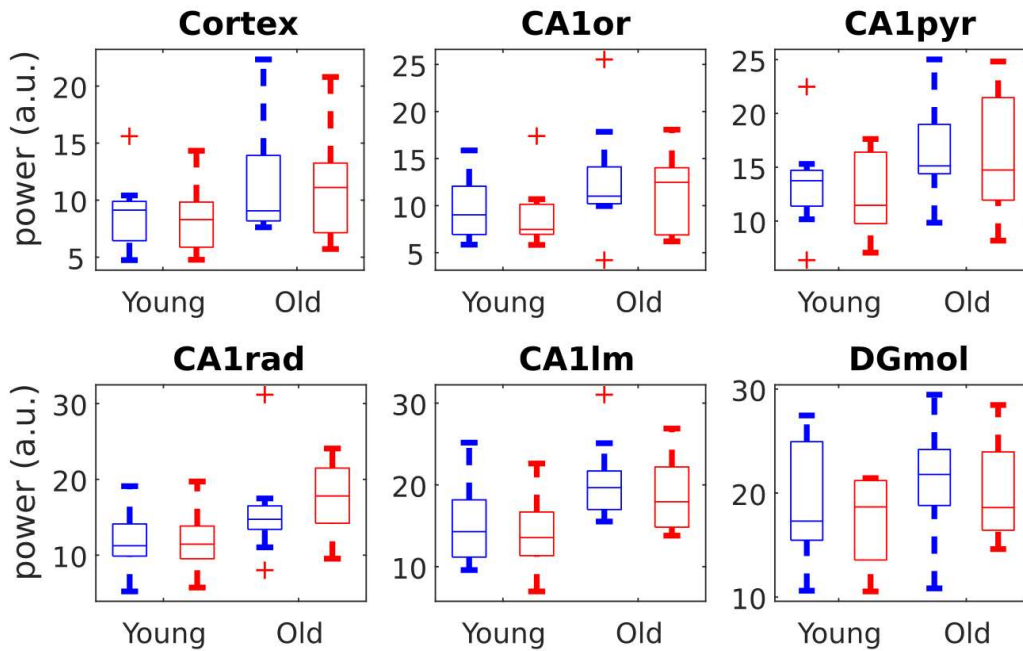
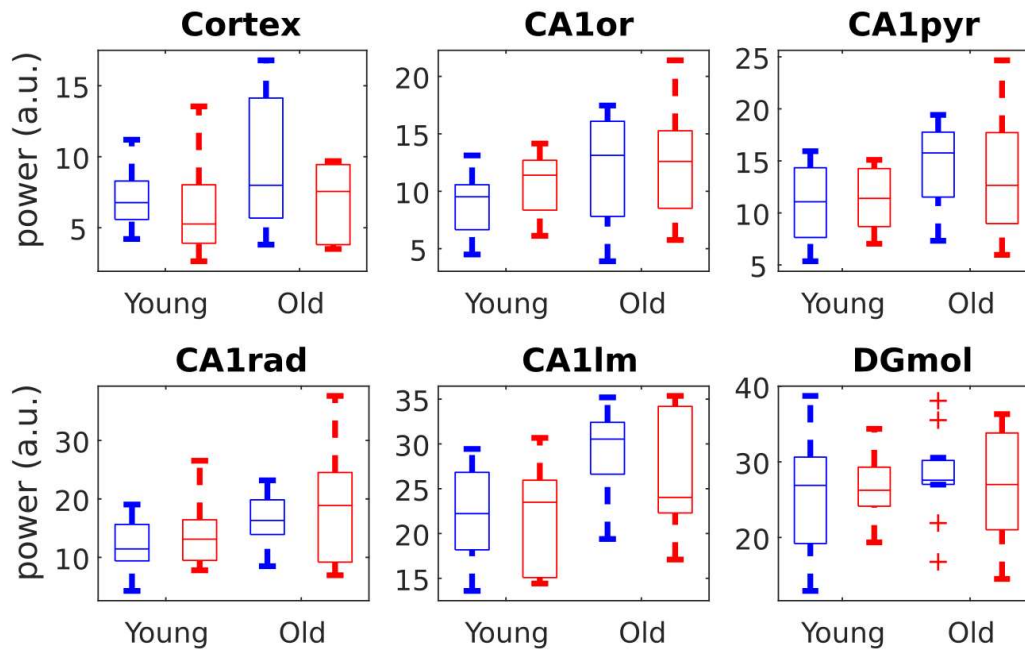


Figure 30: Gamma power for RUN periods divided by anatomical layer (Blue: WT, Red:  $APP^{NL-G-F}$ ).

# Slow Gamma



# Fast Gamma

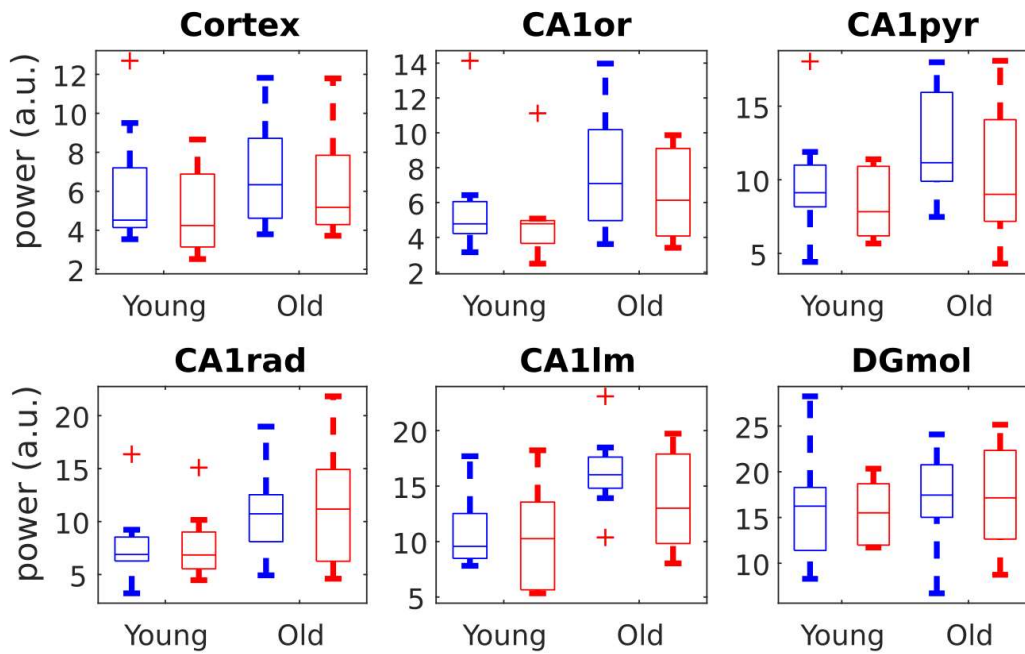


Figure 31: Gamma power for quiescent periods divided by anatomical layer. (Blue: WT, Red:  $APP^{NL-G-F}$ ).

This schema seems common to both APP<sup>NL-G-F</sup> and WT mice.

We can now look at the Pairwise Phase Consistency (PPC) as a metric of modulation strength. To better visualize the modulation we also perform a Rayleigh test and take resultant length and preferred phase for each session (Figures 28 and 29).

While the difference in preferred phase are not significant, we can see a distinct increase in theta modulation of slow gamma oscillations in CA1 oriens in the case of older animals.

In the case of fast gamma there is no significant difference neither in modulation strength nor in phase preference for any hippocampal layer, but there is a decreased modulation of gamma bursts in cortex.

Overall, regardless of age and genotype, we see that fast gamma bursts are significantly less modulated by theta than slow gamma bursts.

We conclude analysing the power of gamma bursts (Figures 30 and 31), not finding any significant difference between the two cohorts.

While there were little changes during the active state, we found a very interesting decrease of gamma occurrences in CA1lm and DGmol during the resting state: gamma in these areas is a proxy of EC activity, the first area affected by AD. This reduction in occurrences could thus be due to reduced activity in layer 2 and 3 of EC during the resting state. Armed with this knowledge, let's now look at what other changes occur during the resting state

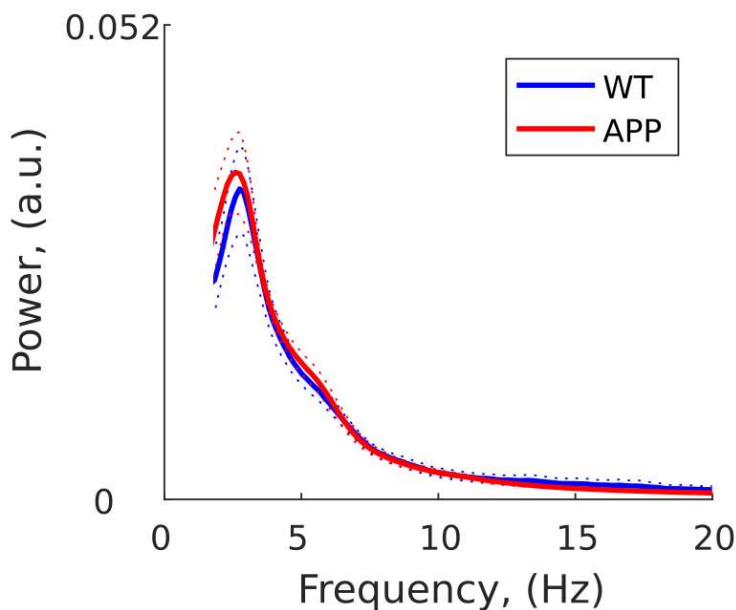


Figure 32: Mean respiration power and frequency for WT and APP animals. Dotted lines are SEM. No significant difference. (Blue: WT, Red: APP<sup>NL-G-F</sup>).

---

### 3.3.3 RESTING STATE

---

Theta oscillations are not the only rhythm organizing activity in hippocampus. During resting states, when theta oscillations are not present (we are thus excluding bouts of sniffing), many neurons across the limbic system are modulated by the respiratory rhythm (Karalis and Sirota 2018). In this brain state, in the hippocampus, we can also observe the sharpwave ripples, a well studied signature signal of this brain region. Below I describe the results of analysis of these two main dynamics with respect to hippocampal activity.

Before that, we verify that the slow oscillation due to respiration in hippocampus is the same between APP<sup>NL-G-F</sup> and WT animals (Figure 32).

---

#### 3.3.3.1 SHARPWAVE RIPPLES

---

During resting states we also have the occurrence of SWR. As a first step, we verify if their occurrence rate changes in APP<sup>NL-G-F</sup> animals compared to WT (Figure 33). We don't find any significant change, an interesting result given how in Figure 26 we had seen a decrease in occurrence rate of fast gamma activity (which includes the frequency range to which SWR belong).

Next, we look at the distribution of SWR frequency, power and duration (Figure 34)

Here we find that the frequency of ripples is significantly, though moderately, decreased in APP<sup>NL-G-F</sup> of all ages, while power and duration of the ripples increase in the older cohorts only. Since the frequency of a ripple, the amplitude of its sharp-wave and its power are related (Stark et al. 2014), we need to verify that the change in frequency is not explained away by a change in one of the other two metrics. For this reason we plot the ripple frequency at its peak versus the normalized amplitude of the sink in CA1

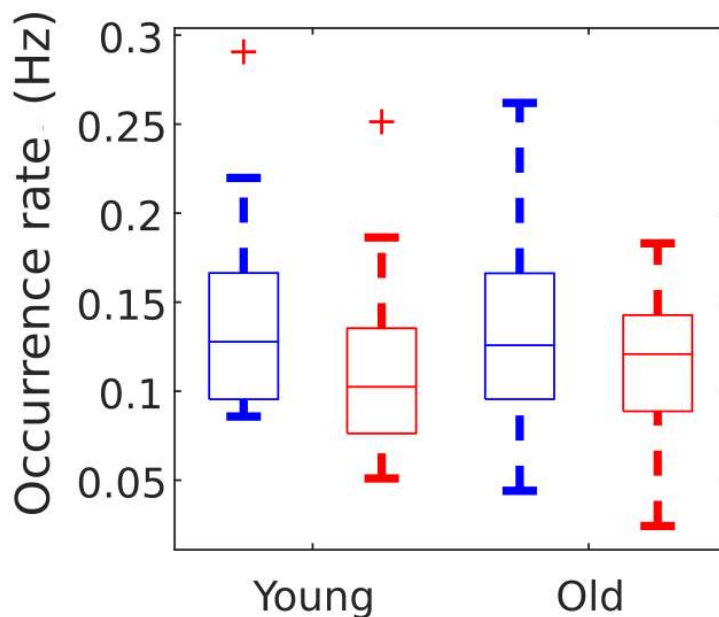


Figure 33: Ripple occurrence rate for quiescent periods.  
(Blue: WT, Red: APP<sup>NL-G-F</sup>).

radiatum (Figure 26) and do a linear fit of the results, showing clearly how the reduction in frequency remains once the power reduction is accounted for.

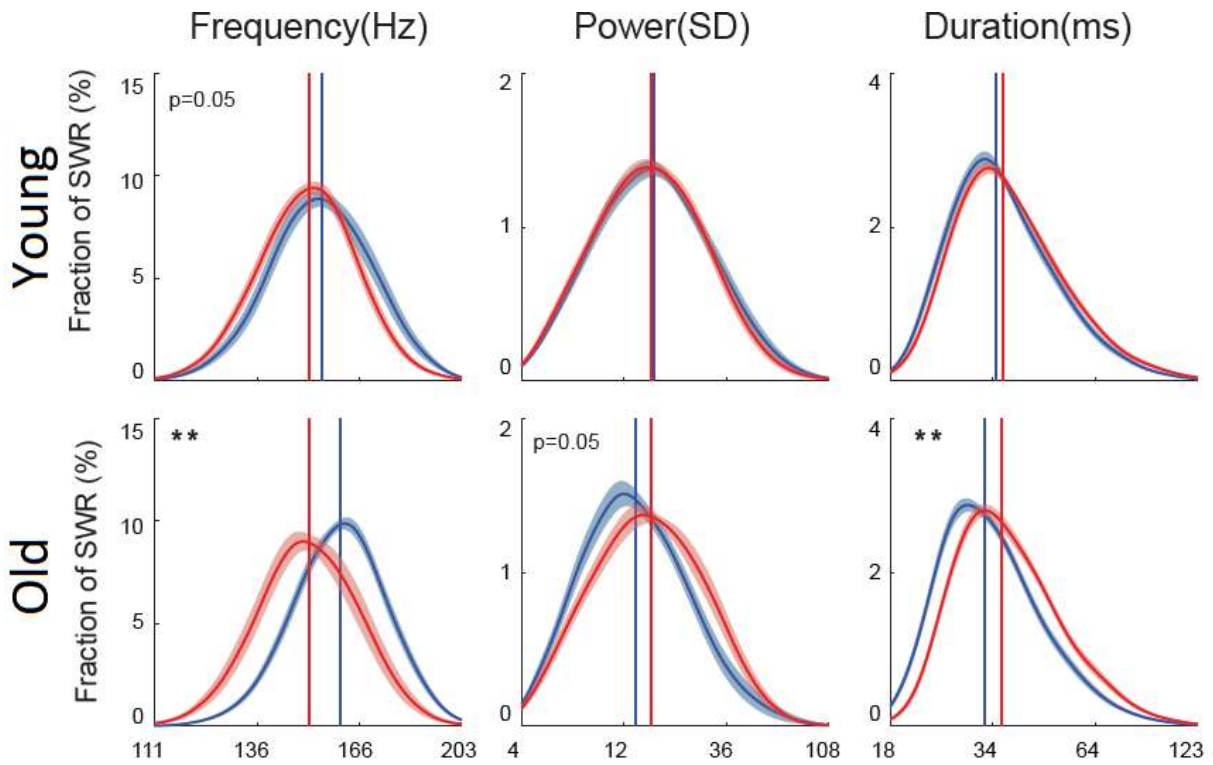


Figure 34: Distribution of the mean of SWR frequency, power and duration. The shadow is the standard error of the mean (SEM) (Blue: WT, Red:  $APP^{NL-G-F}$ ).

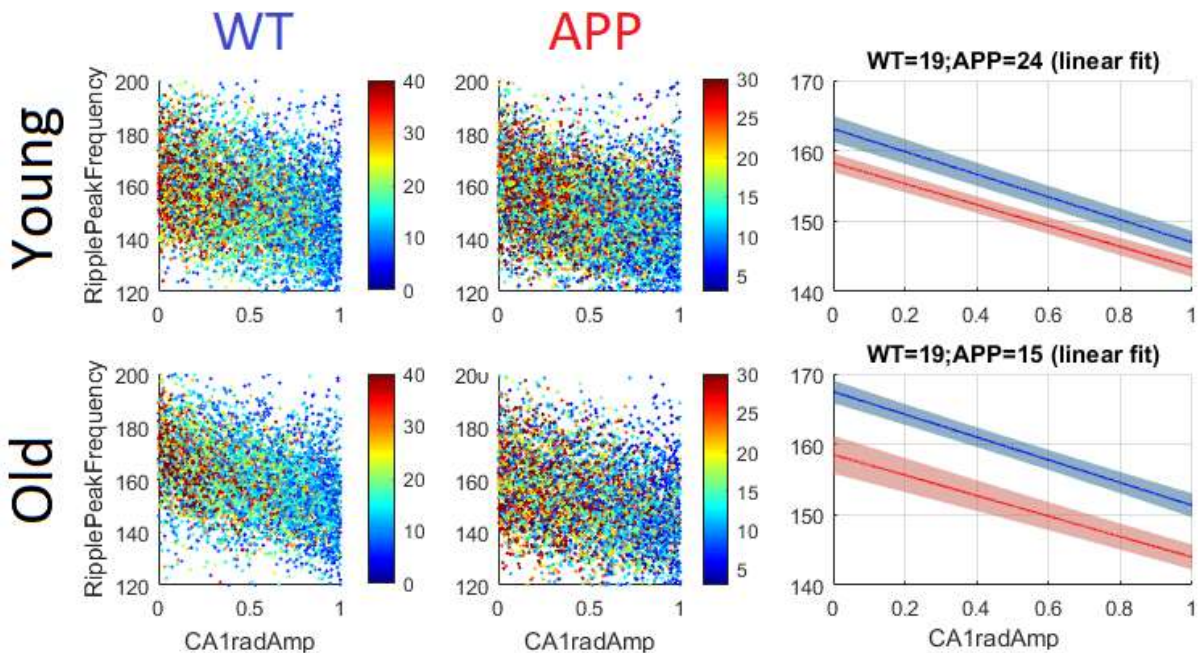


Figure 35: Left: frequency of the ripple at its peak versus normalized amplitude of the sink in CA1 radiatum, where 0 represents deepest sink of the session and 1 the shallowest. Right: linear fit.(Blue: WT, Red:  $APP^{NL-G-F}$ ).

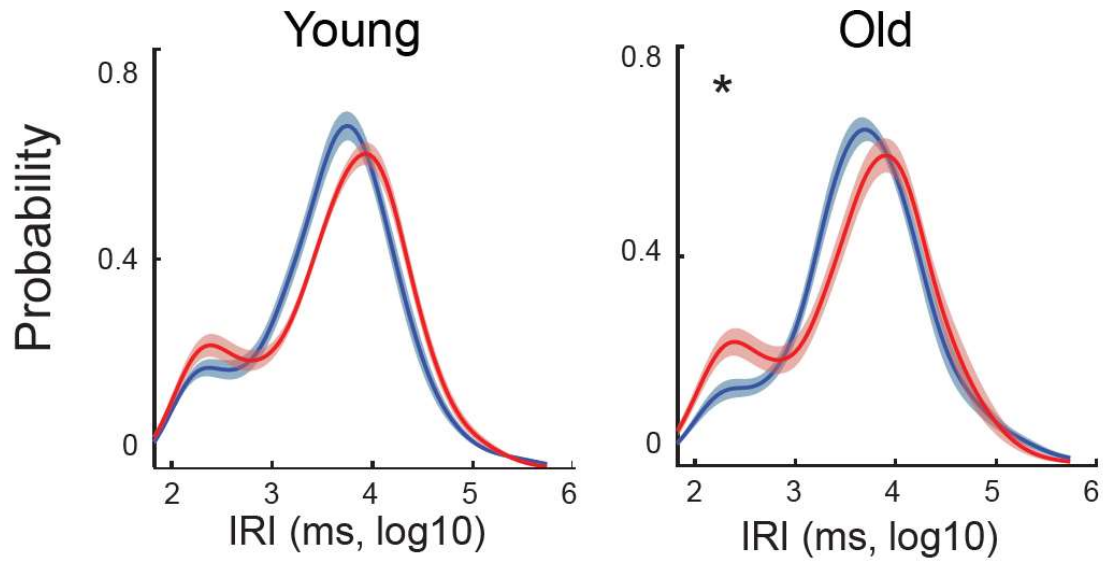


Figure 36: Probability the duration of Inter-Ripple Interval (IRI) will be of a specific length. (Blue: WT, Red:  $APP^{NL-G-F}$ )

After a SWR, the next SWR can follow after either a brief (<1000 ms) or a long period of time. We want to see if the structure of this inter-ripple interval (IRI) is altered in  $APP^{NL-G-F}$  mice. To do so we first look at the IRI distribution (Figure 36), then we look at both the length of the IRI for short-interval and long-interval ripples (Figure 37, Top) and at the probability that the next interval will be short or long (Figure 37, Bottom).

What we find is that in old  $APP^{NL-G-F}$  mice the length of short IRI is reduced and their probability is increased, while for young  $APP^{NL-G-F}$  mice it is the probability of long IRI that is significantly increased compared to WT animals (Figure 37).

Finally, we're interested in seeing how strongly modulated by respiration SWRs are, and if this changes in  $APP^{NL-G-F}$  mice. To do so we compute the PPC for young (6-9 months) and old (10+ months) animals. We find that in older animals ripple modulation decreases (Figure 38).

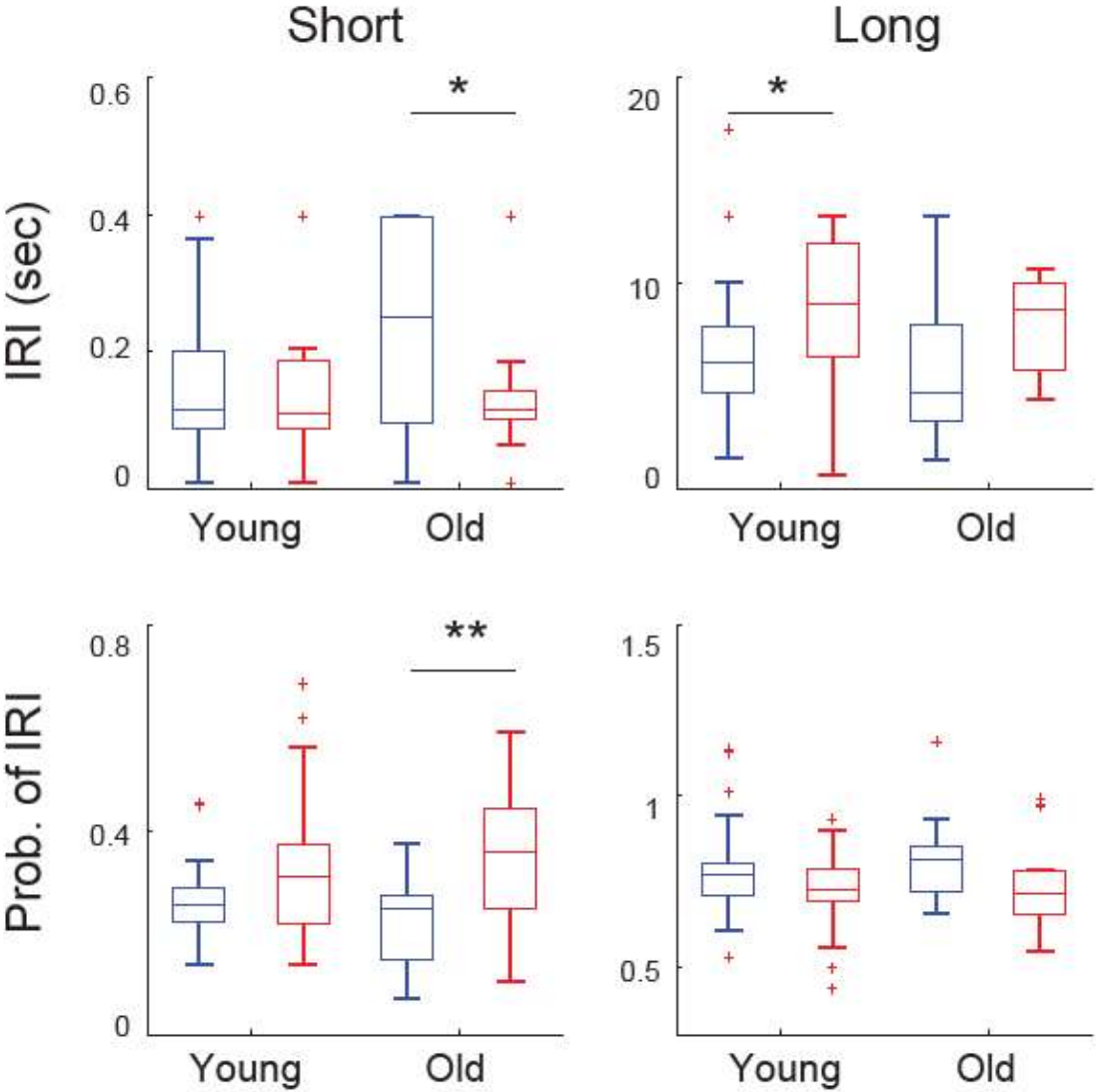


Figure 37: Duration of Inter-Ripple Interval (IRI) for ripples directly following a ripple (Left) or arriving after a long pause (Right). Bottom: Probability of the next interval being short (Left) or long (Right) (Blue: WT, Red:  $APP^{NL-G-F}$ ).

We have seen that ripples, while still present, have a reduced frequency and increased duration, while their rate of occurrences doesn't change.

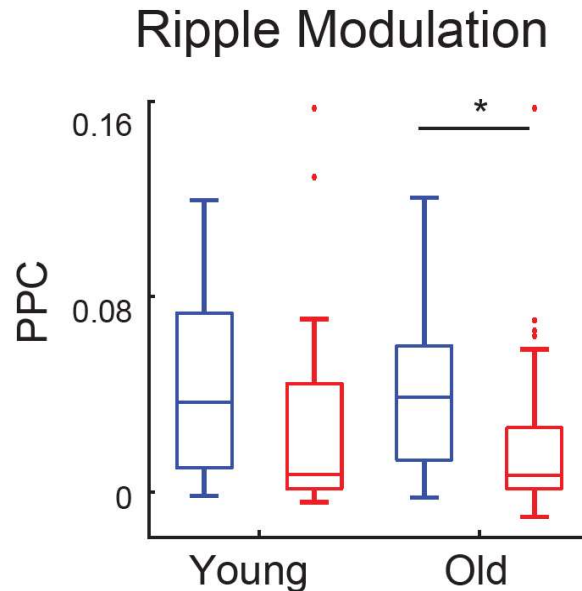


Figure 38: Changes in how SWRs are modulated by respiration (Blue: WT, Red:  $APP^{NL-G-F}$ ).

### 3.4 UNIT ACTIVITY

As previously discussed (1.5.3 Unit activity in AD), we expect to see alteration in neuronal activity in the hippocampus proper and, potentially, in the cortex above. These alterations can be different in nature, starting from differences in the average firing rate of the neurons up to more subtle differences in their modulation by theta oscillations.

#### 3.4.1 FIRING RATE AND BURSTINESS

Given that brain activity is correlated to the behavioural state of the animal, we cannot simply compute the average firing rate across the whole session, but we instead need to compute it separately for running periods and quiescent ones. In the left panels of Figure 39 we can see the value of the firing rate for these two states in the two different conditions. No significant difference was found between the two groups.

In the right panel of Figure 39 we can see the percentage of inactive cells (firing rate < 0.2 Hz), normally active (firing rate between 0.2-20 Hz) and hyperactive (firing rate > 20 Hz) cells. Contrary with what previously reported by Busche et al. (2008) in cortical neurons, but in line with what found by Jun et al. (2020) in MEC, we didn't find an increase of hyperactive cells in the hippocampus of APP<sup>NL-G-F</sup> mice compared to WT.

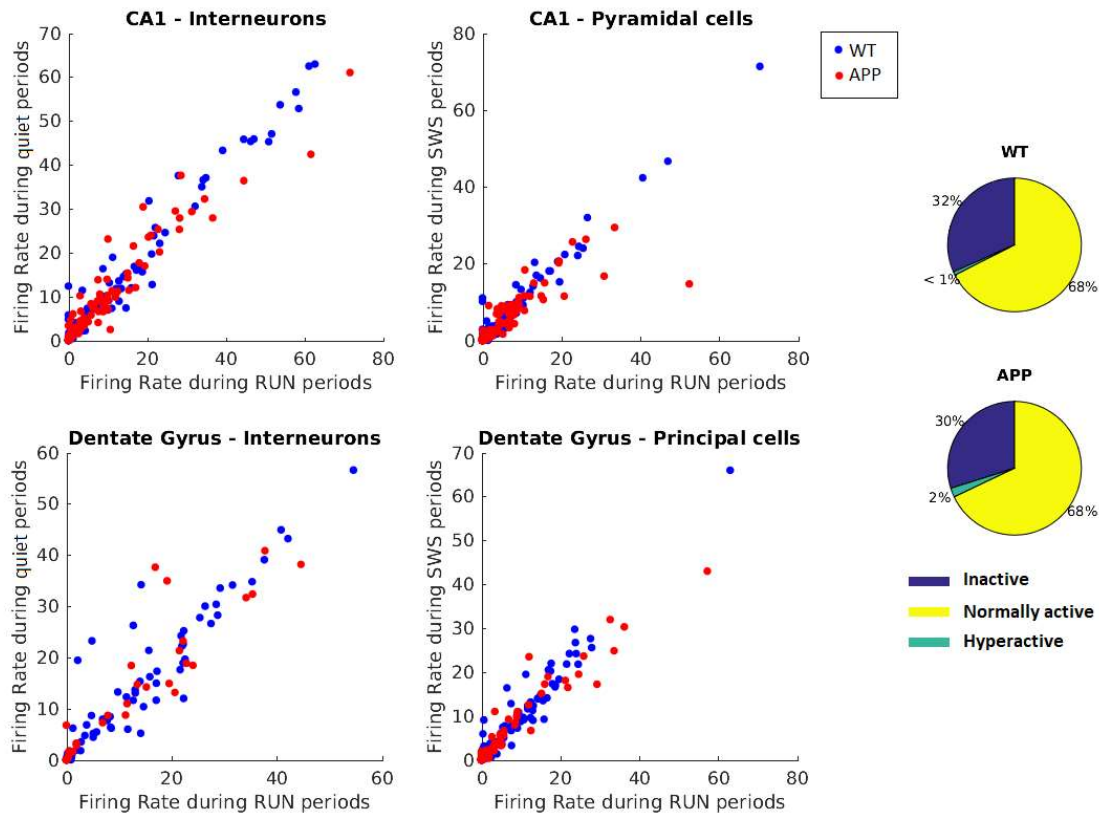


Figure 39: Right: Firing rate during RUN periods vs. firing rate during quiescent periods for cells of CA1 and DG. (Blue: WT, Red: APP<sup>NL-G-F</sup>). Left: Proportion of inactive, normally active and hyperactive cells in WT and APP animals. The difference between the group is not significant.

Another measures of cell activity can be given by the “burstiness” of a cell, here defined as the number of bursts divided by the number of action potentials, where “bursts” are defined as being events in which the cell emits a train of three or more action potentials with an inter-spike interval of less than 6 ms (Figure 40).

Looking at this metric, what we see is a significant decrease in burstiness of principal cells located in the cortex above hippocampus ( $p < 0.0001$ ), and in interneurons located in CA1 ( $p = 0.006$ ) and DG ( $p = 0.0003$ ) with the ranksum test.

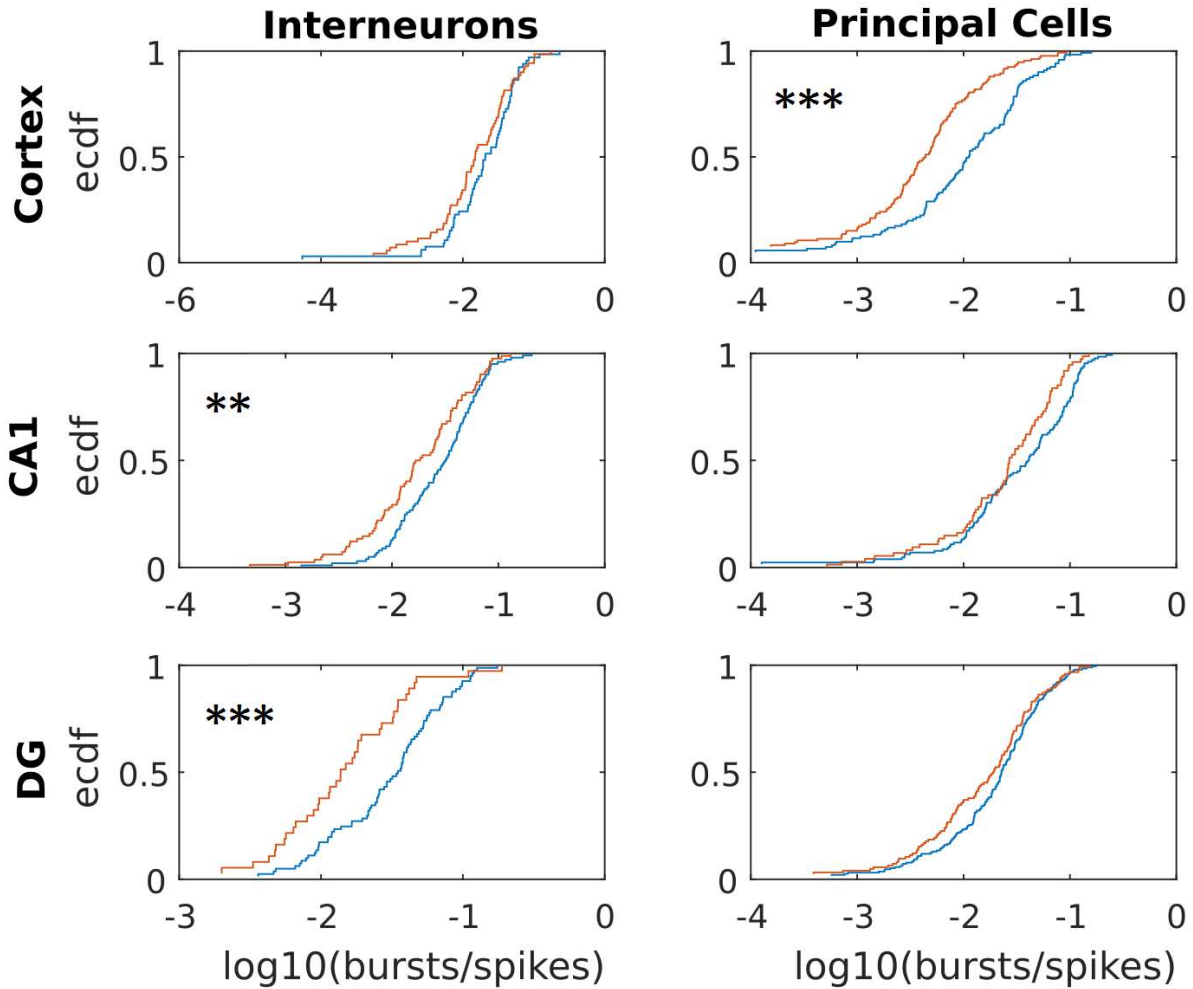


Figure 40: Empirical CDF of bursts/action potentials for interneurons and principal cells in Cortex, CA1 and in DG (Blue: WT, Red: APP<sup>NL-G-F</sup>).

We have seen that there are no significant differences in the firing rate of hippocampal and cortical neurons. However, the average firing rate of neurons (even comparing different states) is a very rough measurement of unit activity. Knowing that theta modulates the activity of units, it is sensible to now look at potential changes in the strength and preferred phase of this modulation.

---

### 3.4.2 THETA MODULATION OF NEURONS

---

Another important measure is theta modulation of neuronal activity, since, as discussed, it has been shown how theta has an important role in modulating hippocampal activity (Section 1.4.2). Indeed, we found theta-modulated cells in all areas we recorded from, although this modulation was less consistent in the cortex. The theta modulation for some example cells can be found in Figure 41.

The strength of modulation didn't vary in CA1 (pyramidal cells:  $p = 0.85$ , interneurons:  $p=0.51$ ), nor in DG (principal cells:  $p= 0.67$ , interneurons:  $p=0.06$ ) between APP<sup>NL-G-F</sup> and WT mice, but in both CA1 and Dentate Gyrus we can see a shift in the preferred theta phase of units, whose significance is here calculated using the Kuiper test (Figure 42).

In conclusion, the overall firing rate did not differ between APP<sup>NL-G-F</sup> and WT mice, while burstiness did. The theta modulation of pyramidal cells in CA1 and principal cells in DG was altered, with cells preferring on average a different phase of theta.

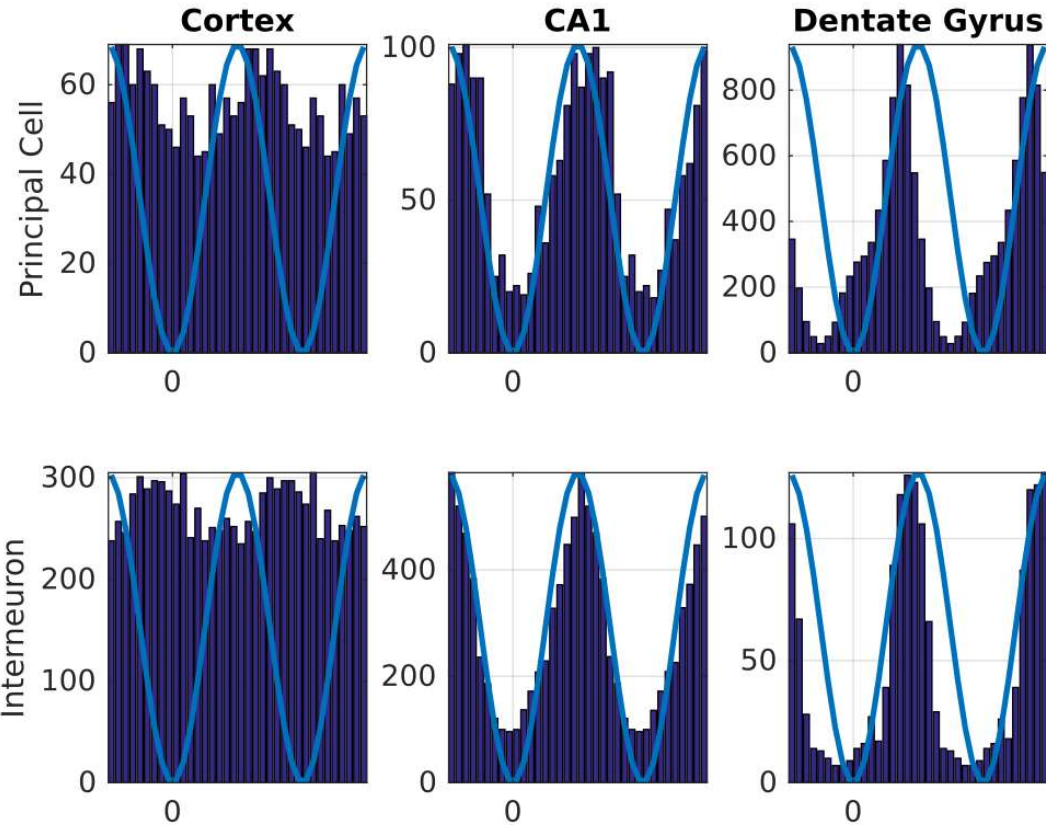


Figure 41: Theta modulation of example cells from different brain regions: count of spikes in one session per theta phase.

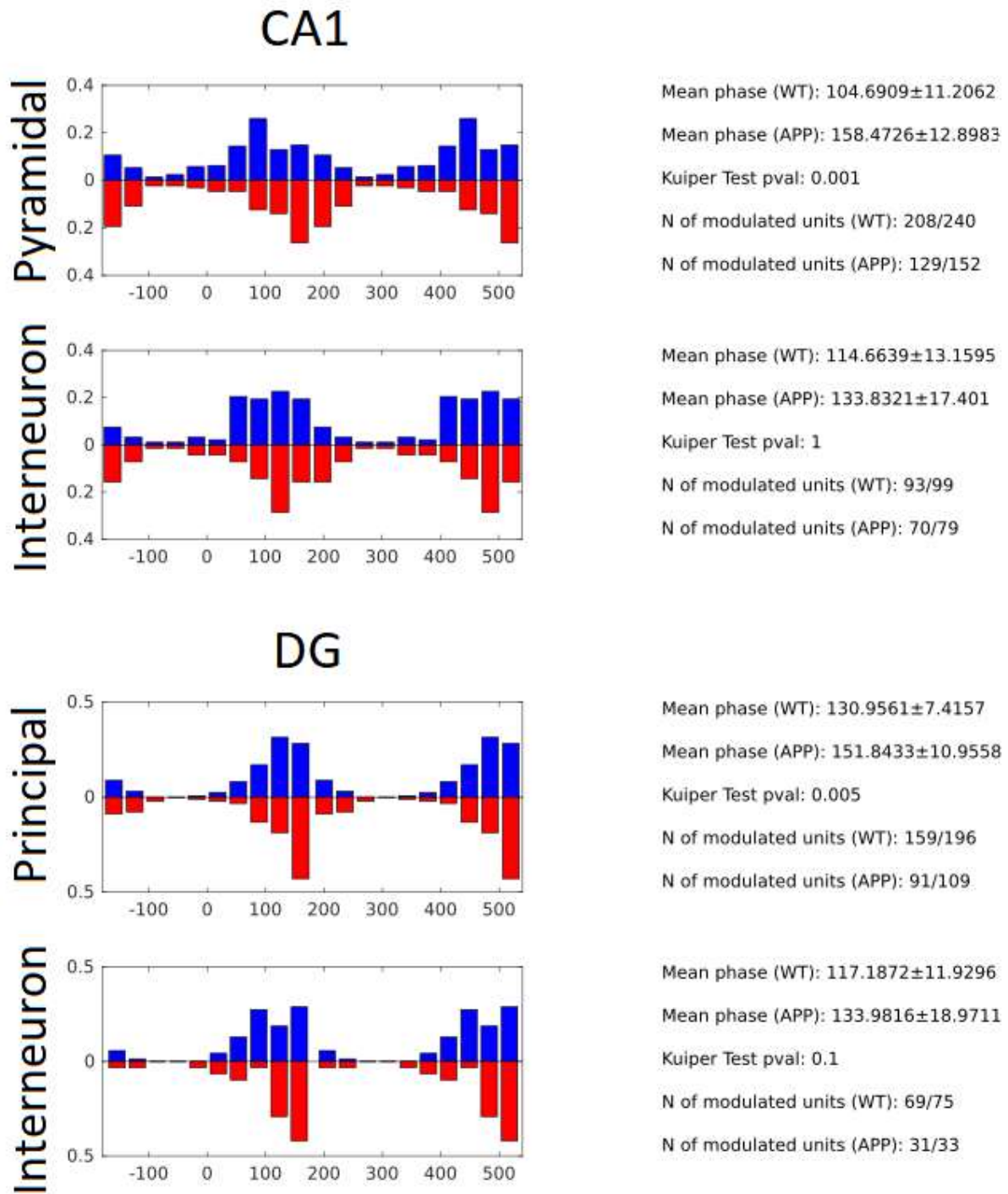


Figure 42: Histogram of preferred theta phases (Blue: WT, Red:  $APP^{NL-G-F}$ ).

### 3.4.3 RESPIRATION MODULATION OF NEURONS

Having access to respiration data via the oscillatory activity of the two Olfactory Bulbs, we can investigate if and how respiration entrainment of units differs between APP<sup>NL-G-F</sup> and WT mice.

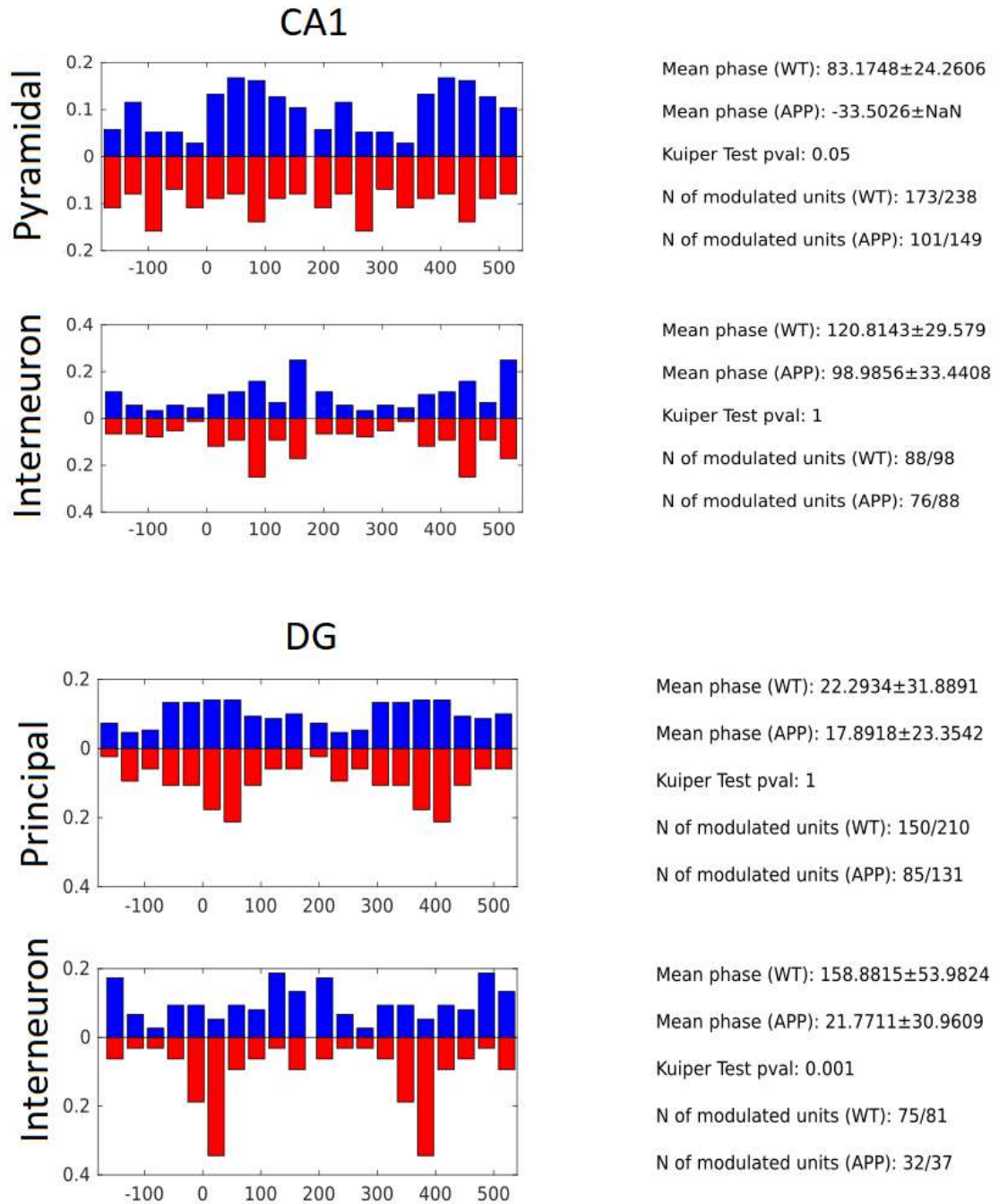


Figure 43: Histogram of preferred respiration phases (Blue: WT, Red: APP<sup>NL-G-F</sup>).

We see that in CA1 pyramidal neurons are less modulated (pyramidal neurons:  $p= 0.0002$ , interneurons:  $p= 0.76$ ), that in DG the modulation doesn't vary (principal cells:  $p=0.72$ , interneurons:  $p=0.76$ ), and that in DG interneurons fire at a different phase of theta altogether.

We also see a phase shift in pyramidal neurons in CA1 and in interneurons in DG (Figure 43).

We have seen an interesting shift in preferred phase of theta in principal cells, and of preferred phase of respiration in CA1 pyramidal cells. Interneurons in DGmol also had a shift in preferred phase of respiration. It's important to remember that this doesn't necessarily mean that the same cells fire later than it normally would, but it could instead mean that the balance between the amount of early-firing and late-firing neurons is different.

To summarize, we have seen minimal changes at the system level during the active state, the most prominent of which is a significant decrease in the average frequency of theta. For this reason, if brain activity in the active state contributes to the deficit, the changes can only be at the cellular level. I looked then at the theta modulation of Units and saw that there is a shift in preferred phase. The resting state has presented more significant changes: gamma occurrences in CA1lm and in Dgmol have diminished, which points at a diminished engagement of EC. Moreover, respiratory modulation of sharp wave-ripples is diminished.

## 4. DISCUSSION

---

Our results have shown multiple subtle differences between APP<sup>NL-G-F</sup> and WT mice.

One of our original questions was related to the differences in oscillatory patterns between APP<sup>NL-G-F</sup> and WT mice, which we need to discuss separating the effects on theta, those on gamma, and those on sharp-wave ripples.

### 4.1 THETA

---

For most of our analysis we have used the CSD rather than the LFP of our signal, since it gives us more insight into the different pathways by allowing us to see the problem in terms of sinks and sources of current and to ignore volume conduction.

The results regarding speed modulation of theta remain inconclusive, given the huge inter-group variety of responses, with some animals having theta being modulated by speed and others not. This is in itself interesting if we consider how theta power reflects synchrony of upstream regions, synaptic connectivity strength, density of local neuronal populations and placement of the electrode. While the last two cannot be modulated by behaviour in the observed timescale, synchrony of upstream regions and synaptic connectivity strength can be modulated by various factors, including neuromodulatory state, strength of various external (for example, the optic flow) and internal (vestibular) inputs that are modulated by linear and angular speed and acceleration. While locomotion in head-fixed mice is more controlled than in freely-moving ones, it seems that there are differences in the behavioural and brain-state dynamics across animals that simple control of speed does not provide. Preliminary analysis of the speed transients showed that the pupil dynamics are not consistently fluctuating with speed, suggesting that the dynamics of neuromodulatory inputs, most likely norepinephrine, are not consistently correlated with locomotion bouts. In contrast, speed frequency but not power changes did follow speed transients. Further complex analysis of these joint sources of variability would be required to assess changes of theta power across groups.

The multiple sources of variability of theta power give rise to complex power distribution with broader variance than difference between animals and groups. For this reason, there is no way to conclude if theta power changes in APP<sup>NL-G-F</sup> mice compared to WT controls. This is in line with Nakazono et al. (2017), which showed how power and emergence of theta did not change in APP<sup>NL-G-F</sup> mice.

Looking at the decrease in theta frequency (reported also by Siwek et al. (2015) in 5xFAD mice), since it remains in the physiological range it is unlikely that this decrease is part of the cause of impairment. It could however be an important early marker of changes occurring at the level of medial septum, where theta rhythm is generated.

There are multiple possible causes: given that the theta rhythm is generated in the medial septum, there could be changes in the GABA-ergic pacemaker mechanism there, or changes in the hippocampal feedback to medial septum. It is also known that cholinergic cells in medial septum are affected early by AD (Francis 2005; H. Ferreira-Vieira et al. 2016), which leads to the reduction of cholinergic tone and thus a reduction in excitation. Finally, amyloid pathology might give raise to unreported changes hyperpolarization-activated cyclic nucleotide-gated (HCN) receptors expressing GABAergic cells in the medial septum, which are amongst those responsible for the pacing of theta rhythm (Hangya et al. 2009; Varga et al. 2008).

This frequency change might have a functional role in the decreased performance of APP animals, given how it has been shown that reducing hippocampal theta frequency by cooling the medial septum leads to an increase of errors in spatial tasks (Petersen and Buzsáki 2020). This is in line with the reduction of theta frequency in a 5xFAD model of AD (Siwek et al. 2015).

The waveshape of theta reflects nonlinear theta cycle dynamics in the upstream pathways. For this reason, we have investigated it in two ways: first looking at the ratio between theta and its first harmonic, and later looking at its asymmetry coefficient. In both cases, we have not found significant differences between APP<sup>NL-G-F</sup> and WT mice.

---

## 4.2 GAMMA

---

We have identified multiple gamma modes in both APP<sup>NL-G-F</sup> and WT mice. There were significant differences between the two cohorts in two areas (slow gamma in CA1 oriens and fast gamma in the cortex).

The technique that we used, consisted in detecting gamma bursts as localized activity in the anatomical, frequency and spatial domains. This gives us a less biased approach to decompose gamma frequency activity in its components. In recent years multiple publications have suggested that gamma bursts detected in dendritic laminae might be related to afferent activity (Schomburg et al. 2014; Lasztóczy and Klausberger 2014; 2016).

In light of these, the modes that we identify (both for APP<sup>NL-G-F</sup> and WT mice) in CA1 radiatum will reflect activity in CA3, while the ones identified in CA1 lacunosum moleculare and DG molecular layer would respectively reflect activity in layer III and II of the MEC.

While previous studies had already shown reduced gamma oscillations (Iaccarino et al. 2016), thanks to our use of silicon probes we were able to pinpoint the anatomical layers in which there was a decreased rate of gamma occurrences. Indeed, we have shown a decrease in gamma occurrences during quiescent states in CA1 lm (both slow and fast gamma) and in DG mol (slow gamma). Given that these layers are receiving projections from MEC our observations are consistent with a degeneration of this area, which is

known to be the first affected by AD. It is also worth noting that, contrary to Iaccarino et al. 2016, we are using multiple animals for our statistical results and not only one per group, as in their study.

However, we didn't see this decrease during RUN states, which are dominated by theta. It is known that slow oscillations modulate gamma in CA1 lacunosum moleculare and DG molecular layer (Isomura et al. 2006). The reason we don't see the decrease during theta states might be that septal dynamics are sufficient to entrain EC circuits and drive gamma occurrence, while during sleep slow oscillations (UP states) and gamma generation are more likely internally generated in EC and thus more affected by its degeneration.

Interestingly, we also observed an increased theta modulation in APP<sup>NL-G-F</sup> mice compared to WT is the slow gamma mode in CA1 oriens. Likely candidates for the origin of gamma in this layer are inputs from CA2 or CA3.

---

#### 4.3 SHARP-WAVE RIPPLES

---

We have also seen a decrease of the ripple frequency. Similarly to what happens to theta, the slowing down of ripples does not exceed physiological value and thus does not seem to justify memory loss by itself, but it could be a marker for synaptic alterations in the hippocampus. However, it indicates a change in the amount of excitation to pyramidal cells and interneurons in the hippocampus, as indicated by the model in (Geisler, Brunel, and Wang 2005).

Contrary to what previously reported by Gillespie et al. (2016), Ciupek et al. (2015) and Nicole et al. (2016), we didn't observe any reduction in identified SWR. However, we saw a decrease in gamma in the ripple frequency when this was not accompanied by sharp-waves. Studies relying on tetrodes and single electrodes and thus lacking the description in the space domain might have erroneously attributed this reduction of non-SWR gamma events to SWR.

It has been shown that there is a relationship between ripple frequency, its power and the amplitude of its sharp-wave (Stark et al. 2014). In our case, even accounting for sink amplitude we can see that the ripple frequency is reduced in APP<sup>NL-G-F</sup> mice compared to WT controls. This is a compelling argument for changes in the input-output conversion in CA1 cells and, potentially, a rewiring of the circuit such as to cause a shift in the excitation/inhibition balance, which in turn would bring a reduction of the frequency. A similar reduction in SWR frequency has been previously reported in ageing rats (Wiegand et al. 2016).

We also observed a decrease of the inter-ripple interval, together with an increase in probability of a ripple shortly following another. Recurrence of ripples at 100 ms comes either from re-entrance loop (Kloosterman et al. 2003) or sleep spindles (Sirota et al. 2003), while infraslow (5-10 sec) periodicity of ripples likely comes from system-wide

Mayer rhythm connected to blood pressure fluctuations (Sirota et al 2003). Changes in the Inter-ripple-interval from slower to faster might reflect increased excitability of sharp-wave generating CA3 circuit or stronger re-entrance loop.

---

#### 4.4 RESPIRATION

---

Respiration has been connected to slow oscillatory activity in the limbic system, providing a scaffolding for the underlying computation and able to modulate SWRs and UP and DOWN states, with consequent effects on memory consolidation (Karalis and Sirota 2018). In our APP<sup>NL-G-F</sup> mice we find a decreased modulation of sharpwave ripples by respiration. This would lead to a reduced coupling between UP states and SWRs, since this is provided by respiration. Since this entrainment is lively mediated by an unknown corollary discharge mechanism with long-projecting neurons (Karalis and Sirota 2018) it is possible that such long-projecting neurons degenerate in AD, similarly to long-projecting neuromodulatory cells.

---

#### 4.5 SINGLE UNITS

---

One of the original questions of this study is if and what changes happen in the firing of single neurons in the hippocampus and the above cortical area. An important difference between our finding and current literature is that we didn't find hyperactive cells as Busche et al. (2008) did. However, the study of the MEC of behaving animals also didn't show such hyperactive cells (Jun et al. 2020). This could be due to the brain area we decided to study (Busche et al. imaged from the cortex), the animal model used (which was the same as in Jun et al., while Busche et al. Used double-transgenic APP23xPS45 mice, overexpressing both APP and mutant PSEN1) or the fact that in Busche et al. the animals were anaesthetized.

We have also observed changes in the preferred theta phase of pyramidal neurons in CA1 and of principal cells in DG, without a significant change in the intensity of modulation. This might affect the way in which neurons engage in theta sequences organization, since integration of inputs from different upstream networks will be shifted. It is important to notice that this change in the average preferred theta phase doesn't necessarily reflect cells firing at a different phase compared to what they normally would do, but could also be explained by cells firing in certain preferred theta phases being more or less active, shifting the balance to a different average preferred theta phase.

This change in preferred phase reflects a change in the balance between theta-coupled excitatory or inhibitory inputs. Since we have shown that the theta amplitude in CA1 lacunosum moleculare, CA1 radiatum and DG moleculare did not significantly change between cohorts, what is likely to have changed is local inhibition, mostly linked to feed-

forward disinhibition (arising from the septal drive of local interneurons) and feed-back inhibition (through, for example, basket cells).

This differs with the results found for respiration, where pyramidal cells in CA1 showed a clear decrease in modulation, but only DG interneurons showed a change in preferred phase.

---

## 4.6 CONCLUSIONS

---

The present study found only very subtle changes in the electrophysiological activity of the hippocampus during the active state, but stronger changes during the resting one. What can this mean, given the obvious cognitive deficits shown by the animals?

First, we need to remember that also the changes registered during the active state might be relevant: the accumulation of these subtle changes could bring them to be functionally relevant. However, given the high variability of metrics such as theta or SWR frequency within an animal, this seems unlikely.

For this reason, studies concentrating on the active state should look at the connection of functional deficits to microscopic changes (for example in synaptic plasticity, neuromodulation, cell assembly formation, etc.) which did not directly translate into macroscopic changes in the network dynamics. It is also important to remember that while studying brain rhythms in connection to memory is useful to understand network mechanisms, the parameters of these rhythms (power, frequency, occurrence rate) are affected by so many variables that they themselves cannot be reliable metrics of cognitive abilities.

Moreover, while many people report correlation between various oscillatory parameters and cognitive function, the reported correlation might be caused by a common factor affecting both function and oscillations. A causal link between oscillation parameters and cognitive function is not actually demonstrated. This applies to theta, gamma and SWRs. Indeed, even studies suppressing hippocampal activity during SWR cannot prove a causal link between SWR and memory formation, since they might be disrupting something else.

The last question we asked at the beginning of this study is if there a distinguishable progression of electrophysiological changes for mice of different ages. Our study has shown electrophysiological differences between APP<sup>NL-G-F</sup> mice of different age groups. Age is an important factor in the build-up of amyloid plaques and correlates with the severity of the impairment, as expected for a degenerative pathology. In our case, we can say that the first behavioural impairments precede the electrophysiological effects we are measuring, meaning that our findings might not be useful biomarkers for early detection of the pathology.

Given our results, the most promising direction of investigation is looking at resting states, possibly in a set-up that allows for sleep recordings. The difference in results among different brain states also casts doubts on the interpretation of *in vitro* studies and of recordings obtained for anaesthetized animals.

## BIBLIOGRAPHY

---

- Adler, G., S. Brassens, and A. Jajcevic. 2003. "EEG Coherence in Alzheimer's Dementia." *Journal of Neural Transmission* 110 (9): 1051–58. <https://doi.org/10.1007/s00702-003-0024-8>.
- Amaral, David G., Helen E. Scharfman, and Pierre Lavenex. 2007. "The Dentate Gyrus: Fundamental Neuroanatomical Organization (Dentate Gyrus for Dummies)." *Progress in Brain Research*. Elsevier. [https://doi.org/10.1016/S0079-6123\(07\)63001-5](https://doi.org/10.1016/S0079-6123(07)63001-5).
- Andersen, Per, Richard Morris, David Amaral, Tim Bliss, and John O' Keefe. 2009. *The Hippocampus Book*. Oxford University Press. <https://doi.org/10.1093/acprof:oso/9780195100273.001.0001>.
- Başar, Erol, Canan Başar-Eroğlu, Bahar Güntekin, and Görsev Gülmen Yener. 2013. "Brain's Alpha, Beta, Gamma, Delta, and Theta Oscillations in Neuropsychiatric Diseases: Proposal for Biomarker Strategies." *Supplements to Clinical Neurophysiology*, 62:19–54. Elsevier B.V. <https://doi.org/10.1016/B978-0-7020-5307-8.00002-8>.
- Bekris, Lynn M., Chang En Yu, Thomas D. Bird, and Debby W. Tsuang. 2010. "Review Article: Genetics of Alzheimer Disease." *Journal of Geriatric Psychiatry and Neurology*. NIH Public Access. <https://doi.org/10.1177/0891988710383571>.
- Belluscio, Mariano A., Kenji Mizuseki, Robert Schmidt, Richard Kempter, and György Buzsáki. 2012. "Cross-Frequency Phase-Phase Coupling between Theta and Gamma Oscillations in the Hippocampus." *Journal of Neuroscience* 32 (2): 423–35. <https://doi.org/10.1523/JNEUROSCI.4122-11.2012>.
- Berchtold, N. C., and C. W. Cotman. 1998. "Evolution in the Conceptualization of Dementia and Alzheimer's Disease: Greco-Roman Period to the 1960s." *Neurobiology of Aging* 19 (3): 173–89. [https://doi.org/10.1016/S0197-4580\(98\)00052-9](https://doi.org/10.1016/S0197-4580(98)00052-9).
- Berger, Hans. 1929. "Über Das Elektrenkephalogramm Des Menschen." *Archiv Für Psychiatrie Und Nervenkrankheiten* 87 (1): 527–70. <https://doi.org/10.1007/BF01797193>.
- Boller, François, and Margaret M. Forbes. 1998. "History of Dementia and Dementia in History: An Overview." *Journal of the Neurological Sciences*. Elsevier. [https://doi.org/10.1016/S0022-510X\(98\)00128-2](https://doi.org/10.1016/S0022-510X(98)00128-2).
- Bragin, Anatol, Jerome Engel, Charles L. Wilson, Itzhak Fried, and Gyorgy Buzsáki. 1999. "High-Frequency Oscillations in Human Brain." *Hippocampus* 9 (2): 137–42. [https://doi.org/10.1002/\(SICI\)1098-1063\(1999\)9:2<137::AID-HIPO5>3.0.CO;2-0](https://doi.org/10.1002/(SICI)1098-1063(1999)9:2<137::AID-HIPO5>3.0.CO;2-0).

- Brenner, R P, R F Ulrich, D G Spiker, R J Scwabassi, C F Reynolds, R S Marin, and F Boller. 1986. "Computerized EEG Spectral Analysis in Elderly Normal, Demented and Depressed Subjects." *Electroencephalography and Clinical Neurophysiology* 64 (6): 483–92. [https://doi.org/10.1016/0013-4694\(86\)90184-7](https://doi.org/10.1016/0013-4694(86)90184-7).
- Busche, Marc Aurel, Gerhard Eichhoff, Helmuth Adelsberger, Dorothee Abramowski, Karl Heinz Wiederhold, Christian Haass, Matthias Staufenbiel, Arthur Konnerth, and Olga Garaschuk. 2008. "Clusters of Hyperactive Neurons near Amyloid Plaques in a Mouse Model of Alzheimer's Disease." *Science* 321 (5896): 1686–89. <https://doi.org/10.1126/science.1162844>.
- Buzsáki, György. 1989. "Two-Stage Model of Memory Trace Formation: A Role for 'Noisy' Brain States." *Neuroscience* 31 (3): 551–70. [https://doi.org/10.1016/0306-4522\(89\)90423-5](https://doi.org/10.1016/0306-4522(89)90423-5).
- Buzsáki, György. 2002. "Theta Oscillations in the Hippocampus." *Neuron*. Cell Press. [https://doi.org/10.1016/S0896-6273\(02\)00586-X](https://doi.org/10.1016/S0896-6273(02)00586-X).
- Buzsáki, György. 2009. *Rhythms of the Brain*. Oxford University Press. <https://doi.org/10.1093/acprof:oso/9780195301069.001.0001>.
- Buzsáki, György. 2015. "Hippocampal Sharp Wave-Ripple: A Cognitive Biomarker for Episodic Memory and Planning." *Hippocampus* 25 (10): 1073–1188. <https://doi.org/10.1002/hipo.22488>.
- Buzsáki, György, Costas A. Anastassiou, and Christof Koch. 2012. "The Origin of Extracellular Fields and Currents-EEG, ECoG, LFP and Spikes." *Nature Reviews Neuroscience*. <https://doi.org/10.1038/nrn3241>.
- Buzsáki, György, Zsolt Horváth, Ronald Urioste, Jamille Hetke, and Kensall Wise. 1992. "High-Frequency Network Oscillation in the Hippocampus." *Science* 256 (5059): 1025–27. <https://doi.org/10.1126/science.1589772>.
- Buzsáki, György, and Edvard I. Moser. 2013. "Memory, Navigation and Theta Rhythm in the Hippocampal-Entorhinal System." *Nature Neuroscience*. <https://doi.org/10.1038/nn.3304>.
- Buzsáki, György, and Xiao-Jing Wang. 2012. "Mechanisms of Gamma Oscillations." *Annual Review of Neuroscience* 35: 203. <https://doi.org/10.1146/ANNUREV-NEURO-062111-150444>.
- Ramon y Cajal. 1901. "Sobre Un Ganglio Especial de La Corteza Esfeno Occipital."
- Ramon y Cajal. 1904. "Textura Del Sistema Nervioso Del Hombre y de Los Vertebrados, Tomo II, Primera Parte." *Imprenta y Libreria de Nicolas Moya, Madrid, Reprinted by Graficas Vidal Leuka, Alicante 1992, 399–402*.

- Canto, Cathrin B., Floris G. Wouterlood, and Menno P. Witter. 2008. "What Does the Anatomical Organization of the Entorhinal Cortex Tell Us?" *Neural Plasticity*. Hindawi Publishing Corporation. <https://doi.org/10.1155/2008/381243>.
- Chaieb, Leila, Marcin Leszczynski, Nikolai Axmacher, Marlene Höhne, Christian E. Elger, and Juergen Fell. 2015. "Theta-Gamma Phase-Phase Coupling during Working Memory Maintenance in the Human Hippocampus." *Cognitive Neuroscience* 6 (4): 149–57. <https://doi.org/10.1080/17588928.2015.1058254>.
- Chen, Guifen, Yi Lu, John A. King, Francesca Cacucci, and Neil Burgess. 2019. "Differential Influences of Environment and Self-Motion on Place and Grid Cell Firing." *Nature Communications* 10 (1): 1–11. <https://doi.org/10.1038/s41467-019-08550-1>.
- Chishti, M. Azhar, Dun Shen Yang, Christopher Janus, Amie L. Phinney, Patrick Horne, Jacqueline Pearson, Robert Strome, et al. 2001. "Early-Onset Amyloid Deposition and Cognitive Deficits in Transgenic Mice Expressing a Double Mutant Form of Amyloid Precursor Protein 695." *Journal of Biological Chemistry* 276 (24): 21562–70. <https://doi.org/10.1074/jbc.M100710200>.
- Ciuppek, Sarah M., Jingheng Cheng, Yousuf O. Ali, Hui Chen Lu, and Daoyun Ji. 2015. "Progressive Functional Impairments of Hippocampal Neurons in a Tauopathy Mouse Model." *Journal of Neuroscience* 35 (21): 8118–31. <https://doi.org/10.1523/JNEUROSCI.3130-14.2015>.
- Claus, Jules J., Vincent I. H. Kwa, Saskia Teunisse, Gerard J. M. Walstra, Willem A. van Gool, J. Hans T. M. Koelman, Lo J. Bour, and Bram W. Ongerboer de Visser. 1998. "Slowing on Quantitative Spectral EEG Is a Marker for Rate of Subsequent Cognitive and Functional Decline in Early Alzheimer Disease." *Alzheimer Disease & Associated Disorders* 12 (3): 167–74. <https://doi.org/10.1097/00002093-199809000-00008>.
- Dam, Debby Van, Rudi D'Hooge, Matthias Staufenbiel, Chris Van Ginneken, Frans Van Meir, and Peter P. De Deyn. 2003. "Age-Dependent Cognitive Decline in the APP23 Model Precedes Amyloid Deposition." *European Journal of Neuroscience* 17 (2): 388–96. <https://doi.org/10.1046/j.1460-9568.2003.02444.x>.
- Devi, Latha, and Masuo Ohno. 2010. "Phospho-EIF2 $\alpha$  Level Is Important for Determining Abilities of BACE1 Reduction to Rescue Cholinergic Neurodegeneration and Memory Defects in 5XFAD Mice." *PLoS ONE* 5 (9). <https://doi.org/10.1371/journal.pone.0012974>.
- Ego-Stengel, Valérie, and Matthew A. Wilson. 2010. "Disruption of Ripple-Associated Hippocampal Activity during Rest Impairs Spatial Learning in the Rat." *Hippocampus* 20 (1): 1–10. <https://doi.org/10.1002/hipo.20707>.
- Einevoll, Gaute T., Christoph Kayser, Nikos K. Logothetis, and Stefano Panzeri. 2013. "Modelling and Analysis of Local Field Potentials for Studying the Function of Cortical

- Circuits.” *Nature Reviews Neuroscience*. Nat Rev Neurosci. <https://doi.org/10.1038/nrn3599>.
- Fernández-Ruiz, Antonio, Azahara Oliva, Gergő A. Nagy, Andrew P. Maurer, Antal Berényi, and György Buzsáki. 2017. “Entorhinal-CA3 Dual-Input Control of Spike Timing in the Hippocampus by Theta-Gamma Coupling.” *Neuron* 93 (5): 1213-1226.e5. <https://doi.org/10.1016/j.neuron.2017.02.017>.
- Francis, Paul T. 2005. “The Interplay of Neurotransmitters in Alzheimer’s Disease.” *CNS Spectrums*. MBL Communications. <https://doi.org/10.1017/s1092852900014164>.
- Fuhrmann, Falko, Daniel Justus, Liudmila Sosulina, Hiroshi Kaneko, Tatjana Beutel, Detlef Friedrichs, Susanne Schoch, Martin Karl Schwarz, Martin Fuhrmann, and Stefan Remy. 2015. “Locomotion, Theta Oscillations, and the Speed-Related Firing of Hippocampal Neurons Are Controlled by a Medial Septal Glutamatergic Circuit.” *Neuron* 86 (5): 1253–64. <https://doi.org/10.1016/j.neuron.2015.05.001>.
- Fyhn, Marianne, Sturla Molden, Menno P. Witter, Edvard I. Moser, and May Britt Moser. 2004. “Spatial Representation in the Entorhinal Cortex.” *Science* 305 (5688): 1258–64. <https://doi.org/10.1126/science.1099901>.
- Geisler, Caroline, Nicolas Brunel, and Xiao Jing Wang. 2005. “Contributions of Intrinsic Membrane Dynamics to Fast Network Oscillations with Irregular Neuronal Discharges.” *Journal of Neurophysiology* 94 (6): 4344–61. <https://doi.org/10.1152/jn.00510.2004>.
- Gillespie, Anna K., Emily A. Jones, Yuan Hung Lin, Mattias P. Karlsson, Kenneth Kay, Seo Yeon Yoon, Leslie M. Tong, et al. 2016. “Apolipoprotein E4 Causes Age-Dependent Disruption of Slow Gamma Oscillations during Hippocampal Sharp-Wave Ripples.” *Neuron* 90 (4): 740–51. <https://doi.org/10.1016/j.neuron.2016.04.009>.
- Girardeau, Gabrielle, Karim Benchenane, Sidney I. Wiener, György Buzsáki, and Michaël B. Zugaro. 2009. “Selective Suppression of Hippocampal Ripples Impairs Spatial Memory.” *Nature Neuroscience* 12 (10): 1222–23. <https://doi.org/10.1038/nn.2384>.
- Goutagny, Romain, Ning Gu, Chelsea Cavanagh, Jesse Jackson, Jean-Guy Chabot, Rémi Quirion, Slavica Krantic, and Sylvain Williams. 2013. “Alterations in Hippocampal Network Oscillations and Theta-Gamma Coupling Arise before A $\beta$  Overproduction in a Mouse Model of Alzheimer’s Disease.” *European Journal of Neuroscience* 37 (12): 1896–1902. <https://doi.org/10.1111/ejn.12233>.
- H. Ferreira-Vieira, Talita, Isabella M. Guimaraes, Flavia R. Silva, and Fabiola M. Ribeiro. 2016. “Alzheimer’s Disease: Targeting the Cholinergic System.” *Current Neuropharmacology* 14 (1): 101–15. <https://doi.org/10.2174/1570159x13666150716165726>.

- Haas, Olivia V., Josephine Henke, Christian Leibold, and Kay Thurley. 2019. "Modality-Specific Subpopulations of Place Fields Coexist in the Hippocampus." *Cerebral Cortex* 29 (3): 1109–20. <https://doi.org/10.1093/cercor/bhy017>.
- Hafting, Torkel, Marianne Fyhn, Sturla Molden, May-Britt Moser, and Edvard I. Moser. 2005. "Microstructure of a Spatial Map in the Entorhinal Cortex." *Nature* 436 (7052): 801–6. <https://doi.org/10.1038/nature03721>.
- Hangya, Balázs, Zsolt Borhegyi, Nóra Szilágyi, Tamás F. Freund, and Viktor Varga. 2009. "GABAergic Neurons of the Medial Septum Lead the Hippocampal Network during Theta Activity." *Journal of Neuroscience* 29 (25): 8094–8102. <https://doi.org/10.1523/JNEUROSCI.5665-08.2009>.
- Hardy, John, and David Allsop. 1991. "Amyloid Deposition as the Central Event in the Aetiology of Alzheimer's Disease." *Trends in Pharmacological Sciences*. Trends Pharmacol Sci. [https://doi.org/10.1016/0165-6147\(91\)90609-V](https://doi.org/10.1016/0165-6147(91)90609-V).
- Hasselmo, Michael E. 2005. "What Is the Function of Hippocampal Theta Rhythm? - Linking Behavioral Data to Phasic Properties of Field Potential and Unit Recording Data." *Hippocampus*. John Wiley & Sons, Ltd. <https://doi.org/10.1002/hipo.20116>.
- Helkala, E L, V Laulumaa, R Soikkeli, J Partanen, H Soininen, and P J Riekkinen. 1991. "Slow-Wave Activity in the Spectral Analysis of the Electroencephalogram Is Associated with Cortical Dysfunctions in Patients with Alzheimer's Disease." *Behavioral Neuroscience* 105 (3): 409–15. <https://doi.org/10.1037//0735-7044.105.3.409>.
- Henze, Darrell A., Zsolt Borhegyi, Jozsef Csicsvari, Akira Mamiya, Kenneth D. Harris, and György Buzsáki. 2000. "Intracellular Features Predicted by Extracellular Recordings in the Hippocampus in Vivo." *Journal of Neurophysiology* 84 (1): 390–400. <https://doi.org/10.1152/jn.2000.84.1.390>.
- Hodgkin, A. L., and A. F. Huxley. 1952. "A Quantitative Description of Membrane Current and Its Application to Conduction and Excitation in Nerve." *The Journal of Physiology* 117 (4): 500–544. <https://doi.org/10.1113/jphysiol.1952.sp004764>.
- Huh, Carey Y.L., Romain Goutagny, and Sylvain Williams. 2010. "Glutamatergic Neurons of the Mouse Medial Septum and Diagonal Band of Broca Synaptically Drive Hippocampal Pyramidal Cells: Relevance for Hippocampal Theta Rhythm." *Journal of Neuroscience* 30 (47): 15951–61. <https://doi.org/10.1523/JNEUROSCI.3663-10.2010>.
- Huxter, John R., Timothy J. Senior, Kevin Allen, and Jozsef Csicsvari. 2008. "Theta Phase-Specific Codes for Two-Dimensional Position, Trajectory and Heading in the Hippocampus." *Nature Neuroscience* 11 (5): 587–94. <https://doi.org/10.1038/nn.2106>.
- Iaccarino, Hannah F., Annabelle C. Singer, Anthony J. Martorell, Andrii Rudenko, Fan Gao, Tyler Z. Gillingham, Hansruedi Mathys, et al. 2016. "Gamma Frequency Entrainment

- Attenuates Amyloid Load and Modifies Microglia.” *Nature* 540 (7632): 230–35.  
<https://doi.org/10.1038/nature20587>.
- Isomura, Yoshikazu, Anton Sirota, Simal Özen, Sean Montgomery, Kenji Mizuseki, Darrell A. Henze, and György Buzsáki. 2006. “Integration and Segregation of Activity in Entorhinal-Hippocampal Subregions by Neocortical Slow Oscillations.” *Neuron* 52 (5): 871–82. <https://doi.org/10.1016/j.neuron.2006.10.023>.
- Jack, Clifford R., David S. Knopman, William J. Jagust, Leslie M. Shaw, Paul S. Aisen, Michael W. Weiner, Ronald C. Petersen, and John Q. Trojanowski. 2010. “Hypothetical Model of Dynamic Biomarkers of the Alzheimer’s Pathological Cascade.” *The Lancet Neurology*. Lancet Publishing Group. [https://doi.org/10.1016/S1474-4422\(09\)70299-6](https://doi.org/10.1016/S1474-4422(09)70299-6).
- Jadhav, Shantanu P., Caleb Kemere, P. Walter German, and Loren M. Frank. 2012. “Awake Hippocampal Sharp-Wave Ripples Support Spatial Memory.” *Science* 336 (6087): 1454–58. <https://doi.org/10.1126/science.1217230>.
- Jankowsky, Joanna L. and Zheng, Hui. "Practical considerations for choosing a mouse model of Alzheimer’s disease" *Mol Neurodegener.* 2017; 12: 89. doi: 10.1186/s13024-017-0231-7
- Jiang, Zheng-yan. 2005. “Study on EEG Power and Coherence in Patients with Mild Cognitive Impairment during Working Memory Task.” *Journal of Zhejiang University SCIENCE B* 6 (12): 1213–19. <https://doi.org/10.1631/jzus.2005.B1213>.
- Jones, Emily A., Anna K. Gillespie, Seo Yeon Yoon, Loren M. Frank, and Yadong Huang. 2019. “Early Hippocampal Sharp-Wave Ripple Deficits Predict Later Learning and Memory Impairments in an Alzheimer’s Disease Mouse Model.” *Cell Reports* 29 (8): 2123–2133.e4. <https://doi.org/10.1016/j.celrep.2019.10.056>.
- Jun, Heechul, Allen Bramian, Shogo Soma, Takashi Saito, Takaomi C. Saïdo, and Kei M. Igarashi. 2020. “Disrupted Place Cell Remapping and Impaired Grid Cells in a Knockin Model of Alzheimer’s Disease.” *Neuron*, July.  
<https://doi.org/10.1016/j.neuron.2020.06.023>.
- Kamondi, Anita, László Acsády, Xiao-Jing Wang, and György Buzsáki. 1998. “Theta Oscillations in Somata and Dendrites of Hippocampal Pyramidal Cells in Vivo: Activity-Dependent Phase-Precession of Action Potentials.” *Hippocampus* 8 (3): 244–61.  
[https://doi.org/10.1002/\(SICI\)1098-1063\(1998\)8:3<244::AID-HIPO7>3.0.CO;2-J](https://doi.org/10.1002/(SICI)1098-1063(1998)8:3<244::AID-HIPO7>3.0.CO;2-J).
- Karalis, Nikolaos, and Anton Sirota. 2018. “Breathing Coordinates Limbic Network Dynamics Underlying Memory Consolidation.” *BioRxiv*, August, 392530. <https://doi.org/10.1101/392530>.
- Kelly, Peter H., L. Bondolfi, D. Hunziker, H. P. Schlecht, K. Carver, E. Maguire, D. Abramowski, et al. 2003. “Progressive Age-Related Impairment of Cognitive Behavior

- in APP23 Transgenic Mice.” *Neurobiology of Aging* 24 (2): 365–78.  
[https://doi.org/10.1016/S0197-4580\(02\)00098-2](https://doi.org/10.1016/S0197-4580(02)00098-2).
- Klausberger, Thomas, Peter J. Magill, László F. Márton, J. David B. Roberts, Philip M. Cobden, György Buzsáki, and Peter Somogyi. 2003. “Brain-State- and Cell-Type-Specific Firing of Hippocampal Interneurons in Vivo.” *Nature* 421 (6925): 844–48.  
<https://doi.org/10.1038/nature01374>.
- Klinzing, Jens G., Niels Niethard, and Jan Born. 2019. “Mechanisms of Systems Memory Consolidation during Sleep.” *Nature Neuroscience*. Nature Publishing Group.  
<https://doi.org/10.1038/s41593-019-0467-3>.
- Kloosterman, Fabian, Theo van Haeften, Menno P. Witter, and Fernando H. Lopes da Silva. 2003. “Electrophysiological Characterization of Interlaminar Entorhinal Connections: An Essential Link for Re-Entrance in the Hippocampal-Entorhinal System.” *European Journal of Neuroscience* 18 (11): 3037–52. <https://doi.org/10.1111/j.1460-9568.2003.03046.x>.
- Kosel, Filip, Paula Torres Munoz, J. Renee Yang, Aimee A. Wong, and Tamara B. Franklin. 2019. “Age-Related Changes in Social Behaviours in the 5xFAD Mouse Model of Alzheimer’s Disease.” *Behavioural Brain Research* 362 (April): 160–72. <https://doi.org/10.1016/j.bbr.2019.01.029>.
- Kramis, R., C. H. Vanderwolf, and B. H. Bland. 1975. “Two Types of Hippocampal Rhythmical Slow Activity in Both the Rabbit and the Rat: Relations to Behavior and Effects of Atropine, Diethyl Ether, Urethane, and Pentobarbital.” *Experimental Neurology* 49 (1): 58–85. [https://doi.org/10.1016/0014-4886\(75\)90195-8](https://doi.org/10.1016/0014-4886(75)90195-8).
- Lane, C. A., J. Hardy, and J. M. Schott. 2018. “Alzheimer’s Disease.” *European Journal of Neurology* 25 (1): 59–70. <https://doi.org/10.1111/ene.13439>.
- Lasztóczy, Bálint, and Thomas Klausberger. 2014. “Layer-Specific GABAergic Control of Distinct Gamma Oscillations in the CA1 Hippocampus.” *Neuron* 81 (5): 1126–39.  
<https://doi.org/10.1016/J.NEURON.2014.01.021>.
- Lasztóczy, Bálint, and Thomas Klausberger. 2016. “Hippocampal Place Cells Couple to Three Different Gamma Oscillations during Place Field Traversal.” *Neuron* 91 (1): 34–40.  
<https://doi.org/10.1016/j.neuron.2016.05.036>.
- Lithfous, Ségolène, André Dufour, and Olivier Després. 2013. “Spatial Navigation in Normal Aging and the Prodromal Stage of Alzheimer’s Disease: Insights from Imaging and Behavioral Studies.” *Ageing Research Reviews*. Elsevier.  
<https://doi.org/10.1016/j.arr.2012.04.007>.
- Lockmann, André L.V., Diego A. Laplagne, Richardson N. Leão, and Adriano B.L. Tort. 2016. “A Respiration-Coupled Rhythm in the Rat Hippocampus Independent of Theta

- and Slow Oscillations.” *Journal of Neuroscience* 36 (19): 5338–52.  
<https://doi.org/10.1523/JNEUROSCI.3452-15.2016>.
- Lorente de Nò, R. 1934. “Studies on the Structure of the Cerebral Cortex II. Continuation of the Study of the Ammonic System.” *Journal Für Psychologie Und Neurologie* 46: 113–77.
- MacLean, P. D. 1949. “Psychosomatic Disease and the Visceral Brain; Recent Developments Bearing on the Papez Theory of Emotion.” *Psychosomatic Medicine* 11 (6): 338–53.  
<https://doi.org/10.1097/00006842-194911000-00003>.
- Masuda, Akira, Yuki Kobayashi, Naomi Kogo, Takashi Saito, Takaomi C. Saïdo, and Shigeyoshi Itohara. 2016. “Cognitive Deficits in Single App Knock-in Mouse Models.” *Neurobiology of Learning and Memory* 135 (November): 73–82. <https://doi.org/10.1016/j.nlm.2016.07.001>.
- Mathis, Alexander, Pranav Mamidanna, Kevin M. Cury, Taiga Abe, Venkatesh N. Murthy, Mackenzie Weygandt Mathis, and Matthias Bethge. 2018. “DeepLabCut: Markerless Pose Estimation of User-Defined Body Parts with Deep Learning.” *Nature Neuroscience* 21 (9): 1281–89. <https://doi.org/10.1038/s41593-018-0209-y>.
- McFarland, Willard L., Herman Teitelbaum, and Elizabeth K. Hedges. 1975. “Relationship between Hippocampal Theta Activity and Running Speed in the Rat.” *Journal of Comparative and Physiological Psychology* 88 (1): 324–28.  
<https://doi.org/10.1037/h0076177>.
- Mizuseki, Kenji, Anton Sirota, Eva Pastalkova, and György Buzsáki. 2009. “Theta Oscillations Provide Temporal Windows for Local Circuit Computation in the Entorhinal-Hippocampal Loop.” *Neuron* 64 (2): 267–80.  
<https://doi.org/10.1016/j.neuron.2009.08.037>.
- Montgomery, Sean M, and György Buzsáki. 2007. “Gamma Oscillations Dynamically Couple Hippocampal CA3 and CA1 Regions during Memory Task Performance.” *Proceedings of the National Academy of Sciences of the United States of America* 104 (36): 14495–500. <https://doi.org/10.1073/pnas.0701826104>.
- Montgomery, Sean M, Anton Sirota, and György Buzsáki. 2008. “Theta and Gamma Coordination of Hippocampal Networks during Waking and Rapid Eye Movement Sleep.” *The Journal of Neuroscience : The Official Journal of the Society for Neuroscience* 28 (26): 6731–41. <https://doi.org/10.1523/JNEUROSCI.1227-08.2008>.
- Müller, Christina, and Stefan Remy. 2018. “Septo–Hippocampal Interaction.” *Cell and Tissue Research*. Springer Verlag. <https://doi.org/10.1007/s00441-017-2745-2>.
- Murphy, M. Paul, and Harry Levine. 2010. “Alzheimer’s Disease and the Amyloid- $\beta$  Peptide.” *Journal of Alzheimer’s Disease*. IOS Press. <https://doi.org/10.3233/JAD-2010-1221>.

- Nakazono, Tomoaki, Travis N Lam, Ayushi Y Patel, Masashi Kitazawa, Takashi Saito, Takaomi C Saïdo, and Kei M Igarashi. 2017. "Impaired In Vivo Gamma Oscillations in the Medial Entorhinal Cortex of Knock-in Alzheimer Model." *Frontiers in Systems Neuroscience* 11 (June): 48. <https://doi.org/10.3389/fnsys.2017.00048>.
- Nath, Tanmay, Alexander Mathis, An Chi Chen, Amir Patel, Matthias Bethge, and Mackenzie Weygandt Mathis. 2019. "Using DeepLabCut for 3D Markerless Pose Estimation across Species and Behaviors." *Nature Protocols* 14 (7): 2152–76. <https://doi.org/10.1038/s41596-019-0176-0>.
- Nicole, O, S Hadzibegovic, J Gajda, B Bontempi - . n.d. "Soluble Amyloid Beta Oligomers Block the Learning-Induced Increase in Hippocampal Sharp Wave-Ripple Rate and Impair Spatial Memory Formation." *Scientific Reports*, 2016 <https://www.nature.com/articles/srep22728>.
- O'Keefe, J; Nadel, L. 1978. "The Hippocampus as a Cognitive Map." *Oxford University Press*.
- O'Keefe, J., and J. Dostrovsky. 1971. "The Hippocampus as a Spatial Map. Preliminary Evidence from Unit Activity in the Freely-Moving Rat." *Brain Research* 34 (1): 171–75. [https://doi.org/10.1016/0006-8993\(71\)90358-1](https://doi.org/10.1016/0006-8993(71)90358-1).
- Oakley, Holly, Sarah L. Cole, Sreemathi Logan, Erika Maus, Pei Shao, Jeffery Craft, Angela Guillozet-Bongaarts, et al. 2006. "Intraneuronal  $\beta$ -Amyloid Aggregates, Neurodegeneration, and Neuron Loss in Transgenic Mice with Five Familial Alzheimer's Disease Mutations: Potential Factors in Amyloid Plaque Formation." *Journal of Neuroscience* 26 (40): 10129–40. <https://doi.org/10.1523/JNEUROSCI.1202-06.2006>.
- Onishi, Joji, Yusuke Suzuki, Kenichi Yoshiko, Shin Hibino, and Akihisa Iguchi. 2005. "Predictive Model for Assessing Cognitive Impairment by Quantitative Electroencephalography." *Cognitive and Behavioral Neurology : Official Journal of the Society for Behavioral and Cognitive Neurology* 18 (3): 179–84. <https://doi.org/10.1097/01.wnn.0000178227.54315.38>.
- Pace-Schott, Edward F., and J. Allan Hobson. 2002. "The Neurobiology of Sleep: Genetics, Cellular Physiology and Subcortical Networks." *Nature Reviews Neuroscience*. European Association for Cardio-Thoracic Surgery. <https://doi.org/10.1038/nrn895>.
- Pachitariu, Marius, Nicholas A. Steinmetz, Shabnam N. Kadir, Matteo Carandini, and Kenneth D. Harris. 2016. "Fast and Accurate Spike Sorting of High-Channel Count Probes with KiloSort."
- Pachitariu, Marius, Nicholas Steinmetz, Shabnam Kadir, Matteo Carandini, and Harris Kenneth D. 2016. "Kilosort: Realtime Spike-Sorting for Extracellular Electrophysiology with Hundreds of Channels." *BioRxiv*, June, 061481. <https://doi.org/10.1101/061481>.

- Papez, J. W. 1936. "A Proposed Mechanism of Emotions." *Archives of Neurology & Psychiatry* 38 (March 5): 725–743.
- Petersen, Peter Christian, and György Buzsáki. 2020. "Cooling of Medial Septum Reveals Theta Phase Lag Coordination of Hippocampal Cell Assemblies." *Neuron* 107 (4): 731–744.e3. <https://doi.org/10.1016/j.neuron.2020.05.023>.
- Prichep, L.S., E.R. John, S.H. Ferris, L. Rausch, Z. Fang, R. Cancro, C. Torossian, and B. Reisberg. 2006. "Prediction of Longitudinal Cognitive Decline in Normal Elderly with Subjective Complaints Using Electrophysiological Imaging." *Neurobiology of Aging* 27 (3): 471–81. <https://doi.org/10.1016/j.neurobiolaging.2005.07.021>.
- Prichep, L.S., E.R. John, S.H. Ferris, B. Reisberg, M. Almas, K. Alper, and R. Cancro. 1994. "Quantitative EEG Correlates of Cognitive Deterioration in the Elderly." *Neurobiology of Aging* 15 (1): 85–90. [https://doi.org/10.1016/0197-4580\(94\)90147-3](https://doi.org/10.1016/0197-4580(94)90147-3).
- Quyen, Michel Le Van, Richard Staba, Anatol Bragin, Clayton Dickson, Mario Valderrama, Itzhak Fried, and Jerome Engel. 2010. "Large-Scale Microelectrode Recordings of High-Frequency Gamma Oscillations in Human Cortex during Sleep." *Journal of Neuroscience* 30 (23): 7770–82. <https://doi.org/10.1523/JNEUROSCI.5049-09.2010>.
- Rajji, Tarek K., Reza Zomorodi, Mera S. Barr, Daniel M. Blumberger, Benoit H. Mulsant, and Zafiris J. Daskalakis. 2017. "Ordering Information in Working Memory and Modulation of Gamma by Theta Oscillations in Humans." *Cerebral Cortex (New York, N.Y. : 1991)* 27 (2): 1482–90. <https://doi.org/10.1093/cercor/bhv326>.
- Ravassard, Pascal, Ashley Kees, Bernard Willers, David Ho, Daniel Aharoni, Jesse Cushman, Zahra M. Aghajan, and Mayank R. Mehta. 2013. "Multisensory Control of Hippocampal Spatiotemporal Selectivity." *Science* 340 (6138): 1342–46. <https://doi.org/10.1126/science.1232655>.
- Saito, Takashi, Yukio Matsuba, Naomi Mihira, Jiro Takano, Per Nilsson, Shigeyoshi Itoharu, Nobuhisa Iwata, and Takaomi C Saido. 2014. "Single App Knock-in Mouse Models of Alzheimer's Disease." *Nature Neuroscience* 17 (5): 661–63. <https://doi.org/10.1038/nn.3697>.
- Saper, Clifford B., Patrick M. Fuller, Nigel P. Pedersen, Jun Lu, and Thomas E. Scammell. 2010. "Sleep State Switching." *Neuron*. *Neuron*. <https://doi.org/10.1016/j.neuron.2010.11.032>.
- Schaffer, Karl. 1892. "Beitrag Zur Histologie Der Ammonshornformation." *Archiv Für Mikroskopische Anatomie* 39 (1): 611–32. <https://doi.org/10.1007/BF02961541>.
- Schomburg, Erik W., Antonio Fernández-Ruiz, Kenji Mizuseki, Antal Berényi, Costas A. Anastassiou, Christof Koch, and György Buzsáki. 2014. "Theta Phase Segregation of Input-Specific Gamma Patterns in Entorhinal-Hippocampal Networks." *Neuron* 84 (2): 470. <https://doi.org/10.1016/J.NEURON.2014.08.051>.

- Scoville, W. B., and B. Milner. 1957. "Loss of Recent Memory after Bilateral Hippocampal Lesions." *Journal of Neurology, Neurosurgery, and Psychiatry* 20 (1): 11–21. <https://doi.org/10.1136/jnnp.20.1.11>.
- Selkoe, Dennis J. 1991. "The Molecular Pathology of Alzheimer's Disease." *Neuron*. Neuron. [https://doi.org/10.1016/0896-6273\(91\)90052-2](https://doi.org/10.1016/0896-6273(91)90052-2).
- Sirota, Anton, and György Buzsáki. 2005. "Interaction between Neocortical and Hippocampal Networks via Slow Oscillations." *Thalamus and Related Systems* 3 (4): 245–59. <https://doi.org/10.1017/S1472928807000258>.
- Sirota, Anton, Jozsef Csicsvari, Derek Buhl, and György Buzsáki. 2003. "Communication between Neocortex and Hippocampus during Sleep in Rodents." *Proceedings of the National Academy of Sciences of the United States of America* 100 (4): 2065–69. <https://doi.org/10.1073/pnas.0437938100>.
- Sirota, Anton, Sean Montgomery, Shigeyoshi Fujisawa, Yoshikazu Isomura, Michael Zugaro, and György Buzsáki. 2008. "Entrainment of Neocortical Neurons and Gamma Oscillations by the Hippocampal Theta Rhythm." *Neuron* 60 (4): 683–97. <https://doi.org/10.1016/j.neuron.2008.09.014>.
- Siwek, Magdalena Elisabeth, Ralf Müller, Christina Henseler, Astrid Trog, Andreas Lundt, Carola Wormuth, Karl Broich, Dan Ehninger, Marco Weiergräber, and Anna Papazoglou. 2015. "Altered Theta Oscillations and Aberrant Cortical Excitatory Activity in the 5XFAD Model of Alzheimer's Disease." *Neural Plasticity* 2015. <https://doi.org/10.1155/2015/781731>.
- Stark, Eran, Lisa Roux, Ronny Eichler, Yuta Senzai, Sebastien Royer, and György Buzsáki. 2014. "Pyramidal Cell-Interneuron Interactions Underlie Hippocampal Ripple Oscillations." *Neuron* 83 (2): 467–80. <https://doi.org/10.1016/j.neuron.2014.06.023>.
- Steriade, M., P. Gloor, R. R. Llinás, F. H. Lopes da Silva, and M. M. Mesulam. 1990. "Basic Mechanisms of Cerebral Rhythmic Activities." *Electroencephalography and Clinical Neurophysiology* 76 (6): 481–508. [https://doi.org/10.1016/0013-4694\(90\)90001-Z](https://doi.org/10.1016/0013-4694(90)90001-Z).
- Sun, Yanjun, Amanda Q. Nguyen, Joseph P. Nguyen, Luc Le, Dieter Saur, Jiwon Choi, Edward M. Callaway, and Xiangmin Xu. 2014. "Cell-Type-Specific Circuit Connectivity of Hippocampal CA1 Revealed through Cre-Dependent Rabies Tracing." *Cell Reports* 7 (1): 269–80. <https://doi.org/10.1016/j.celrep.2014.02.030>.
- Tolman, Edward C. 1948. "Cognitive Maps in Rats and Men." *Psychological Review* 55 (4): 189–208. <https://doi.org/10.1037/h0061626>.
- Varga, Viktor, Balázs Hangya, Kinga Kránitz, Anikó Ludányi, Rita Zemankovics, István Katona, Ryuichi Shigemoto, Tamás F. Freund, and Zsolt Borhegyi. 2008. "The Presence of Pacemaker HCN Channels Identifies Theta Rhythmic GABAergic Neurons in the

- Medial Septum.” *Journal of Physiology* 586 (16): 3893–3915.  
<https://doi.org/10.1113/jphysiol.2008.155242>.
- Vecchio, Robert A. Del, Lisa H. Gold, Steve J. Novick, Gwen Wong, and Lynn A. Hyde. 2004. “Increased Seizure Threshold and Severity in Young Transgenic CRND8 Mice.” *Neuroscience Letters* 367 (2): 164–67. <https://doi.org/10.1016/j.neulet.2004.05.107>.
- Vinck, Martin, Marijn van Wingerden, Thilo Womelsdorf, Pascal Fries, and Cyriel M.A. Pennartz. 2010. “The Pairwise Phase Consistency: A Bias-Free Measure of Rhythmic Neuronal Synchronization.” *NeuroImage* 51 (1): 112–22.  
<https://doi.org/10.1016/j.neuroimage.2010.01.073>.
- Wiegand, Jean Paul L., Daniel T. Gray, Lesley A. Schimanski, Peter Lipa, C. A. Barnes, and Stephen L. Cowen. 2016. “Age Is Associated with Reduced Sharp-Wave Ripple Frequency and Altered Patterns of Neuronal Variability.” *Journal of Neuroscience* 36 (20): 5650–60. <https://doi.org/10.1523/JNEUROSCI.3069-15.2016>.
- Wilson, Matthew A., and Bruce L. McNaughton. 1993. “Dynamics of the Hippocampal Ensemble Code for Space.” *Science* 261 (5124): 1055–58.  
<https://doi.org/10.1126/science.8351520>.
- Wilson, Matthew A., and Bruce L. McNaughton. 1994. “Reactivation of Hippocampal Ensemble Memories during Sleep.” *Science* 265 (5172): 676–79. <https://doi.org/10.1126/science.8036517>.
- Xiao, Nai An, Jing Zhang, Meng Zhou, Zhen Wei, Xi Lin Wu, Xiao Man Dai, Yuan Gui Zhu, and Xiao Chun Chen. 2015. “Reduction of Glucose Metabolism in Olfactory Bulb Is an Earlier Alzheimer’s Disease-Related Biomarker in 5XFAD Mice.” *Chinese Medical Journal* 128 (16): 2220–27. <https://doi.org/10.4103/0366-6999.162507>.
- Yanovsky, Yevgenij, Mareva Ciatipis, Andreas Draguhn, Adriano B.L. Tort, and Jurij Brankačk. 2014. “Slow Oscillations in the Mouse Hippocampus Entrained by Nasal Respiration.” *Journal of Neuroscience* 34 (17): 5949–64.  
<https://doi.org/10.1523/JNEUROSCI.5287-13.2014>.
- Zelano, Christina, Heidi Jiang, Guangyu Zhou, Nikita Arora, Stephan Schuele, Joshua Rosenow, and Jay A. Gottfried. 2016. “Nasal Respiration Entrain Human Limbic Oscillations and Modulates Cognitive Function.” *Journal of Neuroscience* 36 (49): 12448–67. <https://doi.org/10.1523/JNEUROSCI.2586-16.2016>.